Razvoj funkcionalnih obloga za rane s terapijskim (nano)sustavima kitozana i melatonina

Duvnjak Romić, Marieta

Doctoral thesis / Disertacija

2019

Degree Grantor / Ustanova koja je dodijelila akademski / stručni stupanj: **University of Zagreb, Faculty of Pharmacy and Biochemistry / Sveučilište u Zagrebu, Farmaceutsko-biokemijski fakultet**

Permanent link / Trajna poveznica: https://urn.nsk.hr/urn:nbn:hr:163:242111

University of Zagreb

Faculty of Pharmacy and Biochemistry

Marieta Duvnjak Romić

DEVELOPMENT OF FUNCTIONAL WOUND-DRESSINGS WITH CHITOSAN AND MELATONIN THERAPEUTIC (NANO)SYSTEMS

DOCTORAL DISSERTATION

Zagreb, 2019

University of Zagreb

Faculty of Pharmacy and Biochemistry

Marieta Duvnjak Romić

DEVELOPMENT OF FUNCTIONAL WOUND-DRESSINGS WITH CHITOSAN AND MELATONIN THERAPEUTIC (NANO)SYSTEMS

DOCTORAL DISSERTATION

Supervisor: Associate Prof. Anita Hafner, PhD

Zagreb, 2019

Sveučilište u Zagrebu

Farmaceutsko-biokemijski fakultet

Marieta Duvnjak Romić

RAZVOJ FUNKCIONALNIH OBLOGA ZA RANE S TERAPIJSKIM (NANO)SUSTAVIMA KITOZANA I MELATONINA

DOKTORSKI RAD

Mentor: dr. sc. Anita Hafner, izv. prof.

Zagreb, 2019

The doctoral dissertation was submitted to the Faculty Council of the Faculty of Pharmacy and Biochemistry, University of Zagreb in order to acquire a PhD degree in the area of Biomedicine and Health, the field of Pharmacy, the branch of Pharmacy.

The work presented in this doctoral dissertation was performed at the PLIVA Croatia Ltd. and Faculty of Pharmacy and Biochemistry, University of Zagreb, under supervision of Associate Prof. Anita Hafner, PhD. The research was supported by the projects “Development of functional wound dressings with drug delivery nanosystems” (founded by University of Zagreb) and “Melatonin-loaded chitosan (nano)systems” (industrial partner PLIVA Croatia Ltd.).

ZAHVALE / ACKNOWLEDGEMENTS

Prije svega, zahvaljujem svojoj mentorici za stručno usmjeravanje, vodstvo i podršku koji su započeli još u mojim studentskim danima. Draga Anita, neizmjerno vam hvala za svo razumijevanje, nedjeljne kolače, kasnovečernje razgovore, slavljeničke osmijehe i bodrenje kada stvari nisu išle prema planu. Iskreno se nadam da sam bila prva i posljednja doktorandica s kojom ste radili u svako doba, osim uredovnog radnog vremena! ☺

Hvala profesorici Jeleni što mi je u jesen 2010. otvorila vrata znanosti i farmaceutske tehnologije, te uvijek bila potpora u pozadini.

Jasmini i Ivanu, kao i ostalim zaposlenicima Tehnologije, veliko hvala za savjete, pomoć i osmijehe kojima su me uvijek dočekali kada bih dolazila u posjetu.

Zahvaljujem Maji za neizostavan doprinos ovoj disertaciji i svu podršku tijekom godina.

Neizmjerno hvala Biserki što mi je pružila priliku, gurala me i pustila da rastem. Draga Biserka, vi ste bili moja poslovna „mama“, te iako su vam zamjerali čvrstoću i strogoću, mene ste odgojili i pripremili za svijet i na tome ću vam zauvijek biti zahvalna! ☺

Jedinoj osobi koja je znala kako je to raditi doktorat uz posao, Andrei, zahvaljujem za sva popodneva u Plivi i Milkysu, te za znanje o fizikalnoj karakterizaciji koje je svima nesebično dijelila.

Hvala Dunji za formulatorske konzultacije i vikend druženja u praznoj zgradi!

Maji Radić hvala što me upoznala sa svijetom stanica i inkubatora.

Posebno hvala Andreju i Mariu za svu pomoć, čišćenje skurenog DSC-a i skupljanje sljepljenih čašica po labosu. I ta vremena su završila!

Dragi hvala za statistički značajan doprinos ovoj disertaciji, kao i za mnoge statističke i životne razgovore koje smo vodili u kratkom vremenu zajedničkog rada.

Mom bivšem IVIVC-u (Lani, Antoneli i Nikoli) veliko hvala za razumijevanje, filozofske rasprave, maštovite čestitke te zajedničke suze i osmijehe. Posebno hvala Marini za kasnopopodnevna međusobna bodrenja i veliku pomoć pri završnim pripremama.

Bivšim kolegama iz R&D-a zahvaljujem na pruženoj pomoći i razumijevanju tijekom eksperimentalne izrade ovog rada.

Veliko hvala mojim roditeljima što su mi omogućili školovanje te pružali konstantnu potporu. Zrini hvala jer je tu, zbog nje moram biti najbolja moguća verzija sebe.

Hvala mojoj mirnoj luci na bezuvjetnoj podršci, bezgraničnom strpljenju i nepokolebljivoj vjeri. Eto, još sam ja i škole završila! ☺

Adeunt etiam optima.

SUMMARY

Wound healing is a dynamic well-coordinated biological process involving complex interactions among cells, extracellular matrix components and signalling compounds, resulting in wound closure. Healing process is usually divided into four overlapping phases – haemostasis, inflammation, proliferation and remodelling. Many internal and external factors, with infection being the most common one, can disrupt the healing cascade and subsequently lead to chronic and nonhealing states. Accompanied with growing bacterial resistance, design of functional wound dressings that provide adequate conditions for healing in terms of moist environment, gas exchange, protection from external contamination and drug delivery, represents a great imperative and challenge. In this thesis, novel chitosan-based wound dressing in the form of dry powder was developed by spray drying technology and evaluated and compared with complementary microparticulate dressings. Three variants of melatonin loaded wound dressings were evaluated - chitosan, chitosan/Pluronic® F127 and nanostructured lipid carriers (NLC) enriched chitosan/Pluronic® F127 microspheres. Dressings were designed in form of dry powder that swells in contact with wound exudate, forming an *in situ* hydrogel. Therefore, dressings were characterized in terms of physico-chemical properties, *in vitro* drug release, moisture related properties, antibacterial efficacy, *in vitro* biocompatibility with skin cell lines, *in vitro* healing potential and long-term stability in dry state. Melatonin loaded NLC enriched chitosan/Pluronic® F127 microspheres were optimized employing definitive screening design. NLC enriched microspheres showed improved flowability features and prolonged drug release when exposed to slightly acidic conditions, as well as lower fluid uptake capacity, water vapour transition and evaporation rate. Melatonin loaded chitosan/Pluronic® F127 microspheres were shown to be suitable for application as dressing for wounds that produce high amounts of exudate, while NLC enriched microspheres were more appropriate for application to moderately exuding wounds. Tested systems showed antimicrobial activity and biofilm inhibition/eradication potential against *S. aureus* ATCC and *S. aureus* MRSA strains. Melatonin loaded NLC enriched and NLC free chitosan/Pluronic® F127 microspheres were shown as biocompatible with dermal keratinocytes and fibroblasts *in vitro*, with respectable potential to promote wound healing process. Powders in dry state demonstrated good long-term stability. Conclusively, proposed *in situ* forming dressings showed the complementary potential to improve healing of different types of chronic wounds by maintaining favourable moist environment, while providing antibacterial shelter.

KEYWORDS: melatonin, chitosan, microspheres, spray drying, NLC, wound healing

SAŽETAK

Uvod: Cijeljenje rane je dinamičan biološki proces koji uključuje interakcije stanica, izvanstaničnog matriksa i signalnih molekula. Proces cijeljenja sastoji se od četiri faze: 1. hemostaza koja završava koagulacijom uz stvaranje fibrina; 2. upalna faza tijekom koje se formiraju granulociti uz odstranjenje bakterija i stranog sadržaja; 3. proliferativna faza u kojoj dolazi do sinteze kolagena, angiogeneze i reepitelizacije; 4. maturacija i remodeliranje oštećenog tkiva. Sprječavanje bakterijske infekcije i njenog širenja preduvjet je za cijeljenje rane bez komplikacija i ožiljaka. Rezistencija bakterija na antibiotike i razvoj biofilma rastući su problemi današnjice i prepreka antimikrobnoj terapiji inficiranih rana. Stoga, razvoj inovativnih, funkcionalnih obloga za rane koje pružaju odgovarajuće uvjete vlage, zaštitu od vanjskih faktora te omogućuju kontrolirano oslobađanje djelatne tvari u područje rane, jedan je od imperativa u istraživanju.

Melatonin je hormon epifize s mnogim fiziološkim funkcijama, a istražuje se i njegovo antibakterijsko djelovanje te promotivni učinak na cijeljenje rane. Kitozan je biokompatibilni i biorazgradljivi prirodni poliaminosaharid s utvrđenim antimikrobnim učinkom, dobro poznat i široko korišten kao konstituens obloga koje potiču cijeljenje rane. Cilj ovog doktorskog rada je razvoj funkcionalne obloge za rane koja uključuje inovativni terapijski (nano)sustav s kitozanom i melatoninom, u obliku suhog praška. Uz kitozan i melatonin, u sastav terapijskog sustava uvršten je i Pluronic® F127 (poloksamer) s ciljem optimiranja ponašanja sustava u kontaktu s eksudatom rane, te je istražen utjecaj nanostrukturiranih lipidnih nosača na fizikalno-kemijske i funkcionalne karakteristike finalne obloge. S tim ciljem pripravljena su tri različita terapijska sustava: kitozanske mikrosfere, kitozansko-poloksamerske mikrosfere te kitozansko-poloksamerske mikrosfere s uklopljenim nanostrukturiranim lipidnim nosačima. Terapijski sustavi su karakterizirani i uspoređeni s obzirom na fizikalno-kemijska te specifična svojstva bitna za način i mjesto primjene. Ispitan je antibakterijski/antibiofilm učinak te učinak na cijeljenje rane *in vitro*.

Metode: Kitozansko-poloksamerske mikrosfere s uklopljenim nanostrukturiranim lipidnim nosačima i melatoninom razvijene su i optimirane koristeći statistički dizajn eksperimenta. Nanostrukturirani lipidni nosači pripravljeni su tehnikom vruće homogenizacije, dok su finalne mikrosfere pripravljene postupkom sušenja raspršivanja. Uz pomoću definitivnog pretražnog dizajna, u jednom koraku optimirani su formulacijski i procesni parametri oba sustava - nanostrukturiranih lipidnih nosača i mikrosfera. Ispitani su i optimirani sljedeći parametri:

trajanje homogenizacije, udio tekućeg lipida, udio lipida u nanosuspenziji, udio lipida u mikrosferama, brzina protoka raspršivanog sustava te ulazna temperatura u procesu sušenja. Utjecaj pojedinih parametara i njihovih interakcija evaluiran je s obzirom na iskorištenje procesa, sadržaj vlage, srednju veličinu čestica te zeta potencijal. Komplementarne mikrosfere bez nanostrukturiranih lipidnih nosača (kitozanske i kitozansko-poloksamerske mikrosfere) pripravljene su već poznatim procesom sušenja raspršivanjem. Sva tri sustava karakteririrana su s obzirom na kristaličnost i termalna svojstva (XRPD, DSC), svojstva tečenja (Hausnerov omjer), apsorpciju eksudata rane (bubrenje/apsorpcija simuliranog eksudata rane), oslobađanje uklopljenog melatonina (*in vitro* difuzija), prijenos i gubitak vodene pare (izbubrena obloga izložena vlažnim i suhim uvjetima). Biokompatibilnost mikrosfera ispitana je na humanim staničnim linijama keratinocita (HaCaT) i fibroblasta (BJ/ MJ90hTERT) u vidu ispitivanja viabilnosti stanica (MTT test) te integriteta staničnih membrana (LDH test). Također, metodom dilucije ispitan je antibakterijski učinak na rezistentne bakterijske sojeve (*Staphylococcus aureus* ATCC i MRSA sojeve) te učinak na inhibiciju nastajanja/razaranje biofilma. Cijeljenje rane *in vitro* evaluirano je pomoću „*scratch*“ testa na MJ90hTERT stanicama fibroblasta. Sva ispitivanja provedena su pri dvije različite pH vrijednosti – pH 7,4 (fiziološki pH), te pH 6,3 koji je izmjeren u bakterijskom bujonu. Ispitana je i stabilnost pripravljenih praškastih sustava tijekom 6 mjeseci pri dva uvjeta - 5 ± 3 °C i 25 ± 2 °C/60 ± 5% RH. Tijekom tog perioda, praškaste mikrosfere karakterizirane su s obzirom na veličinu čestica, zeta potencijal, sadržaj vlage, termalna svojstva te sadržaj lijeka.

Rezultati: Statistički dizajn eksperimenta, primijenjen u razvoju i optimiranju procesnih i formulacijskim parametara priprave kitozansko-poloksamerskih mikrosfera s uklopljenim nanostrukturiranim lipidnim nosačima i melatoninom, rezultirao je sljedećim optimalnim uvjetima priprave: 20% tekućeg lipida (Miglyol 812N) u nanočesticama, 5% lipida (Miglyol 812N i Compritol® 888ATO) u finalnoj nanosuspenziji, 20 min homogenizacije, 21,6% lipidnih nosača u mikrosferama, protok raspršivanog sustava od 1,8 mL/min te ulazna temperatura u procesu sušenja od 110°C.

Sva tri pripravljena sustava s melatoninom - kitozanske mikrosfere, kitozansko-poloksamerske mikrosfere te kitozansko-poloksamerske mikrosfere s uklopljenim nanostrukturiranim lipidnim nosačima, karakterizirana su potpunim uklapanjem melatonina. Proces sušenja raspršivanjem rezultirao je djelomičnom amorfizacijom melatonina. Udio amorfnog melatonina bio je veći u mikrosferama u čijoj pripravi je korišten poloksamer. Snižena temperatura tališta čvrstog lipida u mikrosferama s nanostrukturiranim lipidnim nosačima potvrdila je prisutnost nano sustava u

mikrosferama i nakon postupka sušenja raspršivanjem. Sustav obogaćen lipidima karakteriziran je poboljšanim svojstvima tečenja, te značajno manjom apsorpcijom tekućine tijekom procesa bubrenja. Značajna razlika u količini apsorbirane tekućine između kitozanskih i kitozansko-poloksamerskih mikrosfera uočena je pri pH 6,3, dok u neutralnom pH nije bilo razlike među ispitanim uzorcima.

Uspostavljanje vlažnog okruženja jedan je od osnovnih preduvjeta za uspješno cijeljenje. Stoga je svim uzorcima nakon formiranja hidrogela (bubrenja) određena brzina prijenosa vodene pare. Iako su većinom u optimalnom rasponu, kitozanski hidrogel je pokazao nešto viši prijenos vodene pare od optimalnog. Kako bi se okarakteriziralo ponašanje hidrogelova u kontaktu s ranom koje ne proizvodi veliku količinu eksudata, izbubreni uzorci su izloženi suhoj klimi te je utvrđeno da uzorci bez nanostrukturiranih lipidnih nosača znatno brže gube vlagu. S obzirom na uočena svojstva vezana uz apsorpciju/zadržavanje vlage, zaključeno je da su kitozanske i kitozansko-poloksamerske mikrosfere prikladnije za primjenu na ranu s velikom količinom eksudata.

Oslobađanje melatonina is mikrosfera bilo je u skladu s rezultatima bubrenja – u blago kiselom mediju bubrenje mikrosfera kontrolira difuziju kao glavni mehanizam oslobađanja, dok je u kasnijim vremenima uočena retradacija profila oslobađanja kod uzorka obogaćenog nanostrukturiranim lipidnim nosačima, budući da je melatonin djelomično ukopljen i u lipidnu fazu. U neutralnim uvjetima, zbog izostanka značajnog efekta bubrenja i stvaranja difuzijskog sloja, oslobađanje melatonina manje je kontrolirano, te nema značajne razlike u profilima oslobađanja između uzoraka.

Sva tri sustava karakterizirana su antibakterijskim učinkom protiv *S. aureus* ATCC i MRSA sojeva te inhibirajućim utjecajem na formiranje biofilma, dok su se kitozansko-poloksamerske mikrosfere pokazale najpotentnijima. Kitozanske mikrosfere u ispitivanim koncentracijama pokazale su manju učinkovitost jer nisu u potpunosti razorile već formirani biofilm, dok su preostala dva tipa mikrosfera učinkovitija, pokazujući sposobnost razaranja biofilma u istovjetnim koncentracijama. S obzirom na obim bubrenja mikrosfera, izračunate su teorijske koncentracije sastavnica u rani nakon primjene, te je utvrđeno da su one veće od onih potrebnih za antimikrobno djelovanje.

Suspenzije mikrosfera, u koncentracijama pri kojima je postignut antibakterijski učinak, aplicirane su na humane stanice keratinocita i fibroblasta kako bi se ispitala biokompatibilnost mikrosfera. Rezultati ispitivanja viabilnosti i integriteta staničnih membrana prije i nakon

izlaganja mikrosferama bili su istovjetni, nedvojbeno potvrđujući biokompatibilnost ispitivanih uzoraka.

Budući da su kitozansko-poloksamerske mikrosfere sa i bez nanostrukturiranih lipidnih nosača pokazali superiorna i komplementarna svojstva u smislu fizikalno-kemijskih karakteristika, prijenosa vodene pare i antibakterijskog djelovanja, evaluiran je njihov utjecaj na cijeljenje rane *in vitro* pomoću „*scratch*“ testa na stanicama fibroblasta. Za oba tipa mikrosfera zabilježeni su blago bolji rezultati u odnosu na kontrolu, dok su mikrosfere obogaćene nanostrukturiranim lipidnim nosačima značajno ubrzale „cijeljenje“ u odnosu na kontrolni uzorak, pri obje ispitane pH vrijednosti medija.

Studija stabilnosti suhih prašaka čuvanih u hermetički zatvorenim plastičnim epruvetama zaštićenim od svjetlosti ispitana je kroz period od 6 mjeseci. U danom periodu, nisu uočene značajne promjene u veličini čestica i zeta potencijalu, dok je za kitozansko-poloksamerske mikrosfere uočeno povećanje sadržaja vlage, pri oba uvjeta čuvanja. Evaluacija termalnih svojstava pokazala je povećanje udjela kristaličnog melatonina u kitozansko-poloksamerskim mikrosferama skladištenim pri 5 ± 3 °C. U isto vrijeme, za kitozansko-poloksamerske mikrosfere obogaćene nanostrukturiranim lipidnim nosačima taj efekt nije uočen, no u uzorcima skladištenim pri sobnim uvjetima (25 ± 2 °C/60 ± 5% RH) s vremenom je došlo do povećanja temperature taljenja čvrstog lipida što je znak narušavanja stabilnosti lipidne faze mikrosfera. Stoga je temperatura od 5 ± 3 °C odabrana kao uvjet čuvanja kitozansko-poloksamerskih mikrosfera, dok temperatura i relativna vlažnost redom od 25 ± 2 °C i 60 ± 5% RH predstavljaju prikladne uvjete čuvanja lipidima obogaćenih mikrosfera.

Zaključak: Kitozansko-poloksamerske mikrosfere obogaćene nanostrukturiranim lipidnim nosačima s melatoninom pripravljene tehnikom sušenja raspršivanjem, uspješno su razvijene i optimirane uz pomoć statističkog dizajna eksperimenta. Razvijene mikrosfere karakterizirane su malom i ujednačenom veličinom čestica, pozitivnim zeta potencijalom, relativno niskim sadržajem vlage, potpunim uklapanjem melatonina te visokim iskorištenjem samog procesa priprave. U svrhu razvoja i ispitivanja praškastih mikrosfera kao funkcionalnih obloga za rane koje bubre u kontaktu s eksudatom rane, pripravljena su tri različita terapijska sustava: kitozanske mikrosfere, kitozansko-poloksamerske mikrosfere te kitozansko-poloksamerske mikrosfere s uklopljenim nanostrukturiranim lipidnim nosačima. U usporedbi s kitozanskim i kitozansko-poloksamerskim mikrosferama, lipidom obogaćeni sustav karakteriziran je poboljšanim svojstvima tečenja te produljenim oslobađanjem pri blago kiselim uvjetima.

Mikrosfere bez lipida pokazale su značajno veći kapacitet bubrenja, prijenos te gubitak vodene pare. Sva tri tipa mikrosfera biokompatibilna su sa stanicama keratinocita i fobroblasta te su karakterizirana antimikrobnim i antibiofilm učinkom. Mikrosfere obogaćene naostrukturiranim lipidnim nosačima značajno su ubrzale cijeljenje rane *in vitro*. Mikrosfere u obliku suhog praška stabilne su tijekom perioda od 6 mjeseci pri odgovarajućim uvjetima čuvanja. Dodatak lipidnih nanosustava u mikrosfere značajno je promijenio njihova svojstva bitna za način primjene, čime je osigurana komplementarnost razvijenih terapijskih sustava, odnosno mogućnost izbora najprikladnije praškaste obloge ovisno o tipu rane.

KLJUČNE RIJEČI: melatonin, kitozan, mikrosfere, sušenje raspršivanjem, nanostrukturirani lipidni nosači, cijeljenje rana

Table of Contents

1. INTRODUCTION

1.1 Wounds and wound healing

Wounds are defined as a break in the physical and functional continuity of the surface epithelium or underlying connective tissue. Disruption can be caused by thermal (e.g. steam or fire), chemical (e.g. acids or alkalis), mechanical (e.g. crash or cut) trauma or as a result of a disease (e.g. diabetic ulcer or carcinoma).

Wound healing is a dynamic, complex and well-coordinated process, usually divided into four overlapping phases (Figure 1 A-C). First phase, haemostasis (Figure 1 A) occurs immediately after injury and is characterized by vasoconstriction, followed by platelet aggregation and leucocyte migration. In this phase, cascade release, activation and attraction of cytokines and inflammatory cells happens. After the bleeding is stopped, neutrophils release chemoattractive agents in the early inflammation phase to kill bacteria and cleanse wound bed. Late inflammation phase last up to several days and includes differentiation of monocytes to macrophages which phagocytose and remove foreign matter, dead cells and bacteria. Macrophages also secret the cytokines and growth factors which enable healing progression to next phase. Proliferation (Figure 1 B) is the third phase of the healing process where fibroblast proliferation and extra cellular matrix deposition dominates. New blood vessels and granulation tissue are formed, followed by keratinocytes re-epithelization. Tissue remodelling (Figure 1 C) is the final phase of the healing process and can last up to several months/years. Further epithelialization, wound contraction and extracellular matrix remodelling occur, with progressive increase in the tensile strength of new tissue (Kim et al., 2018; Thiruvoth et al., 2015).

1.1.1 Chronic wounds

As wound healing is very complex, any interruption or disbalance in the healing cascade can lead to failed progression of the process. Factors that influence healing are age, genetics, chronic medical conditions, immunosuppression and malnutrition. Wound Healing Society has classified majority of nonhealing wounds based on their aetiology in four categories: pressure, venous, diabetic and arterial insufficiency ulcers (Kirsner, 2016). However, incidence of nonhealing wounds developed as a sequel from other aetiologies, like trauma, autoimmune diseases and skin tumours, are becoming more often with total chronic wound prevalence up to 6% (Phillips et al., 2016).

Nonhealing wounds are the most often trapped in the inflammation phase (Figure 1 D), where macrophages release pro-inflammatory cytokines at increased concentrations, which

leads to high presence of proteases and free radicals. Disrupted balance consequently leads to defect in cell differentiation and proliferation with degradation of growth factors and extracellular matrix. Recent findings have shown that non-healing wound bed contains increased concentration of free iron, most probably due to release from pro-inflammatory macrophages, damaged erythrocytes or other pathological activities (Wlaschek et al., 2019). Considering the fact that iron is essential for bacterial replication and infection expansion (Skaar, 2010), persistent inflammation makes wound bed susceptible to critical microbial colonization and biofilm formation, closing the deleterious inflammation cycle (Kim et al., 2018; Morton and Phillips, 2016).

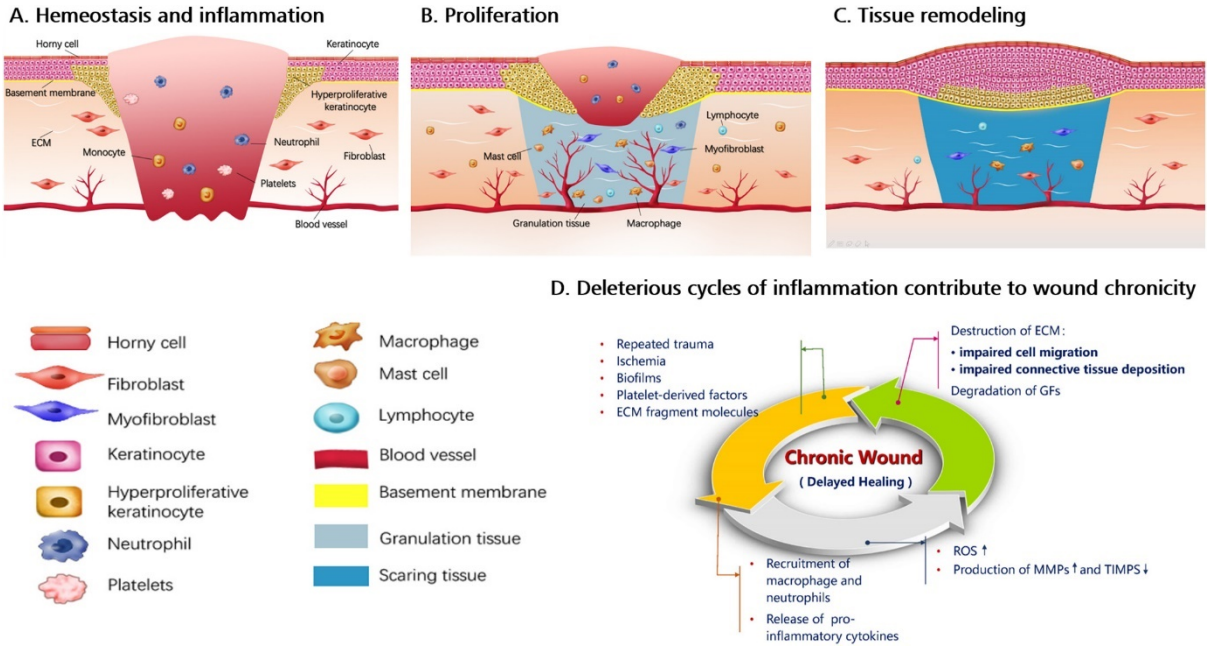

Figure 1. Phases of wound healing – haemostasis and inflammation (A), proliferation (B) and remodelling (C). Scheme showing destructive inflammation cycles present in chronic wounds (D) (reprinted from Kim et al., 2019, with permission from Elsevier).

Gram-positive microorganisms, mainly *Staphylococcus aureus* (*S. aureus*) and *Streptococcus pyogenes*, play a major role in the first stage of bacterial wound infection, while gram-negative species like *Pseudomonas aeruginosa* (*P. aeruginosa)* and *Escherichia coli* are found only at the late stage of the infection (Simões et al., 2018). Both, *S. aureus* and *P. aeruginosa* are known to form biofilms in the wound bed, additionally interacting with and altering immune response to further prolong inflammation phase. It was shown that *P. aeruginosa* uses host's necrotic tissue as scaffold for biofilm progression, while *S. aureus*

attracts macrophages and downregulate their microbicidal activity (Wu et al., 2019). With growing antimicrobial resistance and over 60% biofilm incidence in wounds requiring debridement, effective antibacterial treatment represent crucial step in treatment of chronic wounds.

1.2 Drug delivery systems for wound healing application

Because of complex healing process and diverse aetiology of chronic wounds, almost two decades ago, a TIME framework was set up for the treatment of nonhealing wounds. TIME is an acronym for critical points in wound assessment: tissue and debridement (T), inflammation and infection (I), moisture balance (M) and edge management (E) (Leaper et al., 2012). Prerequisite for effective drug delivery in the nonhealing wound bed is debridement and cleaning of necrotic and nonviable tissue. As chronic wounds are characterized by persistent inflammation and bacterial infection, early recognition of infection and biofilm formation is needed to establish appropriate therapy. Next, moisture balance regulation of excessive wound exudate or dry conditions in the wound bed is necessary for optimal healing progression. Finally, wound closure starts from the edge, therefore epidermal advancement is the final step allowing successful closure.

1.2.1 Wound dressings

To facilitate healing, local wound therapy should be able to regulate temperature and moisture in the wound bed, allow exchange on the air while providing a shelter for microbial penetration, promote reepithelization and protect peri wound skin. Although traditional wounds therapies like gauze or cotton coverage, that don’t provide moisture control and bacterial protection, are obsolete, therapies that would provide all required characteristic are still in the focus of research. Wound dressings are most widely investigated systems that allow facilitation of healing process. Additionally, they allow protection and controlled release of incorporated drug/delivery system, thus synergistically promote wound healing. Antibiotics, growth factors, nucleic acids and different peptides are the most commonly investigated healing agents (Kaplani et al., 2018). Dressings are usually polymer-based and formulated as films, foams, hydrocolloids or hydrogels (Powers et al., 2016; Vowden and Vowden, 2017).

Film dressings are made of thin and transparent polyurethane, semipermeable to water and gasses. They are not appropriate for treating wounds with high levels of exudate since they are non-absorbent. Main disadvantage is their adhesiveness to the tissue, which could cause are

injuries and disruptions during dressing removal/exchange (Vowden and Vowden, 2017). Foam dressings are usually also made from polyurethane, or/with addition of other polymers like carboxy-methil-cellulose (CMC, Aquacel®) or polyethylene glycol (PEG). Foams have very good exudate absorption capacity, can be loaded with healing agents and can be easily removed (Powers et al., 2016). Hydrocolloids are often composed of starch, gelatin or CMC that swell in contact with wound exudate. They are non-adherent highly absorbent materials, but also lacking mechanical stiffness. Therefore, they are usually manufactured with supporting film layer that can also be impermeable for water and air and produce odour in the wound bed (Saghazadeh et al., 2018).

Hydrogels, three-dimensional swollen polymeric networks, are dressings suited for the majority wound types. They are made of natural (e.g. chitosan, alginate and collagen) or synthetic polymers (e.g. PEG and polyvinyl alcohol, Pluronic®). Natural polymers can often act as antibacterial agents/healing promotors, however compared to synthetic ones, have weak mechanical strength, often requiring secondary cover. Hydrogels have high absorbing capacity, but can also hydrate wound bed in case of dry environment. They are non-adhesive and semipermeable to water and gas and serve as a good carrier for different types of antimicrobial and wound healing agents (Gupta et al., 2019). Hydrogel dressings can also be designed in form of dry powder or film. Dry material swells when exposed to wet wound bed, forming hydrogel *in situ*. This type of delivery system is extremely patient compliant, as it is easy to handle and can easily be tailored to fit irregular shaped wound bed. Moreover, polymer dressing and incorporated healing agent have better long-term stability properties compared to solvated state (Liu et al., 2016).

1.2.2 Nanopharmaceuticals

Nanotechnology-based delivery systems are widely investigated in all fields of pharmaceutical research. Potent activity due to high surface to volume ratio, controlled drug release and intracellular delivery with improved bioavailability are among the most important advantages of nanosized delivery systems. Inorganic, polymer or lipid-based nanoparticles are frequently studied for wound healing application (Ashtikar and Wacker, 2018).

Silver ions, commonly used inorganic system, have well known antibacterial effect (Rai et al., 2009), with slow releasing silver nanocrystal products already on the market (Actiocoat^{TM}, Polymem® silver). Also, cerium oxide and silicon based nanoparticles showed proliferative and targeted delivery potential (Chigurupati et al., 2013; Turner et al., 2016).

Polymeric nanoparticles are extensively investigated in many therapeutic areas due to their adjustable physico-chemical properties and drug release rate. Poly(lactic-co-glycolic acid) (PLGA) is the most frequently evaluated synthetic polymer for medical application. Additionally, it was shown that PLGA degradants can act as healing promotors (Chereddy et al., 2016; Porporato et al., 2012).

Lipid nanoparticles provide close and prolonged contact with the tissue due to similar lipidic composition (Xiang et al., 2011). Liposomes and multilammelar liposomes have been systematically evaluated due to ability to encapsulate hydrophobic and hydrophilic drugs (Pierre et al., 1997). Despite the efforts to stabilize lipid layer, liposomes show rapid drug release and instability. For wound healing application, nanoparticles comprising solid lipids have been investigated. Solid lipid nanoparticles (SLN) show better stability and prolonged drug release in wound healing applications (Fumakia and Ho, 2016; Gad et al., 2019). However, on long-term scale, expulsion of the drug occurs due to change of crystalline state within the particles.

NLCs

Nanostructured lipid carriers (NLCs), have been developed as second generation of solid lipid-nanocarriers. Solid lipid nanoparticles (SLN) were the first generation, constituted of the lipid with high melting temperature. Compared to other lipid systems, SLNs showed improved stability and higher drug loading potential. However, expulsion of the drug due to recrystallization of the solid lipid occurs with time. To overcome this issue, deliver system containing mixture of two lipids – solid and liquid was developed. Due to presence of liquid lipid, NLCs have no/less crystalline matrix, which provides further increase in drug loading capacity and prolonged stability (Jain et al., 2017). In line with their name, solid lipids used for the preparation of NLCs have high melting temperature, making them solid at room temperature (e.g. glyceryl palmitostearate, T_m~55°C, glyceryl dibehenate, T_m~70°C). For liquid lipid phase, caprylic/capric triglycerides and lauroyl polyoxylglycerides are most commonly used. Final choice of lipid composition and lipid components ratio is based on their HLB value and drug solubilization potential (Beloqui et al., 2016).

Although primary intended as delivery system for oral administration, NLCs are widely developed for dermal application, with cosmetic products available on the market for more than 10 years (Pardeike et al., 2009). In addition to effective drug delivery, lipids in NLCs hydrate skin by formation of occlusive layer, making them attractive for dermal application (Khurana et al., 2013). Recent research in the area of wound healing treatments support the idea of

incorporation of NLCs in wound dressings as delivery systems for peptides, small molecules and oils (Gainza et al., 2014; Garcia-Orue et al., 2016; Ghodrati et al., 2019; Saporito et al., 2017), as well as agent for dressing's mechanical improvement (Garcia-Orue et al., 2019).

NLCs preparation

The most common preparation methods are based on hot or cold homogenization and hot emulsification-ultrasonication. Both follow the same principle: solid and liquid lipids are mixed (typically in ratio 70/30 - 99.9/0.1) and heated above the melting point. Drug is then dissolved or dispersed in the lipid melt and the mixture is introduced in hot aqueous phase with surfactant in concentration of 1.5-5%. Lipid emulsion particle size reduction is achieved by applying high pressure (high pressure homogenization) or by ultrasound (ultrasonication). By cooling nanoemulsion below melting point, formation of solid nanoparticles occurs. Although relatively simple and short, each method has some disadvantages. Hot homogenization is not suitable for thermolabile substances, cold homogenization often provides particles with wide size distribution, while ultrasonication may results with metal contamination if long sonication is required (Beloqui et al., 2016; Salvi and Pawar, 2019).

Another approach for preparation of NLCs comprises solvent-based methods where lipid phase is dissolved in water miscible (solvent diffusion) or immiscible (solvent emulsification evaporation) organic phase. After organic phase with lipids is mixed with aqueous surfactant phase, evaporation step is performed which leads to NLC formation. As evaporation step is critical and often not complete, solvent based methods are less common for preparation of NLCs (Salvi and Pawar, 2019).

1.2.3 Microparticles

Although microparticles are "older" delivery systems compared to nanopharmaceuticals they have some advantages, as lower toxicity, better controlled drug release and simpler preparation and characterization (Ranjan et al., 2016). Similar to nanoparticles, PLGA is the is the most frequently used synthetic polymer used for preparation of microparticles (Chereddy et al., 2016; Dong et al., 2008; Wang et al., 2015). However, vast majority of microparticulate drug delivery systems is natural or synthetic polymer-based. Natural polymers are biocompatible and biodegradable, however, drawback in the general usage is batch to batch variability and susceptibility to cross-contamination. Chitosan is a well-known wound material with antimicrobial activity and positive influence on different phases of healing process (Dai et al., 2011). Alginate is another widely used polymer, obtained from the seaweed. As chitosan

and alginate are prone to swelling, they usually serve as exudate absorber, forming a hydrogel dressing with encapsulated antimicrobial or healing agent (Gainza et al., 2013; Liu et al., 2017).

Along with the variety of microparticle carriers and types and characteristics of polymer they are based on, diverge the methods for their production. In general, three different approaches can be distinguished – emulsification, crosslinking and droplet formation/evaporation. Briefly, emulsification/solvent evaporation is the process in which polymer and drug are dissolved/dispersed in the oil/solvent phase which is introduced in aqueous phase containing surfactant. Mixture is then submitted to solvent extraction/evaporation/coacervation, which leads to shrinkage and the formation of solid polymeric particles. In crosslinking/ionotropic gelation, polymer and drug are dissolved in one phase, which is then introduced in the crosslinker (agent with opposite charge) solution. Microparticles, formed spontaneously by ionic interaction, are mixed, washed and dried. Spray dryer, microfluidics or printers are used to scatter polymer/drug solution/dispersion into small droplets which are submitted to drying/evaporation leading to the formation of microparticles.

Spray drying

Spray drying is technique widely used in food and pharmaceutical industry. It provides dry powder formation from solution, emulsion or dispersion in one step. Spray drying in especially interesting because it allows formation of amorphous solid dispersions for all types of agents, small and macromolecules (Davis and Walker, 2018). Process starts with atomization of liquid feed into droplets which are then dried in the heated gas stream, resulting in solid spheres that are finally separated from the gas by specially designed cyclone (Figure 2). The whole process of particle formation lasts up to several seconds, making it suitable even for thermosensitive molecules.

Atomization is the first step that determines size of future particles. Depending of the type of the atomizer, droplets can be obtained by applying pressure, centrifugal, kinetic or ultrasonic energy. Most commonly used are pneumatic two-fluid nozzles, which atomize the feed by frictional forces of compressed gas. Droplets are then introduced to drying chamber with hot gas. Depending on the feed liquid composition, drying can be achieved by air or nitrogen; in co-current, counter-current of mixed flow. In co-current flow setup, droplets and hot gas are introduced from the same side (top) of drying chamber, making it the least efficacious, but at the same time the only one suitable for drying of thermolabile substances. During the flow of droplets through the chamber, drying process occurs as a result of heat transfer and moisture evaporation. Drying step is critical for determination of type and

morphology of particles that are formed (e.g. hollow, dense, encapsulated, porous). Dried particles are finally separated from the gas by centrifugal force in cyclone separator and collected in a chamber (Santos et al., 2018).

Spray dryer setup, formulation design and process optimization, allow tailored production of spheres with desired characteristics, such as microcapsules, matrix, core-shell or porous microspheres as well as nanoparticles. Feed viscosity and surface tension, defined by composition and concentration of the dissolved/dispersed components and the type of solvent, dictate type of solid particle that will be formed. Furthermore, process parameters, like feed flow rate, atomization pressure, gas flow rate, inlet and outlet temperature and dryer geometry must be closely investigated and tuned to obtain final powder with desired characteristics (Singh and Van den Mooter, 2016; Ziaee et al., 2019).

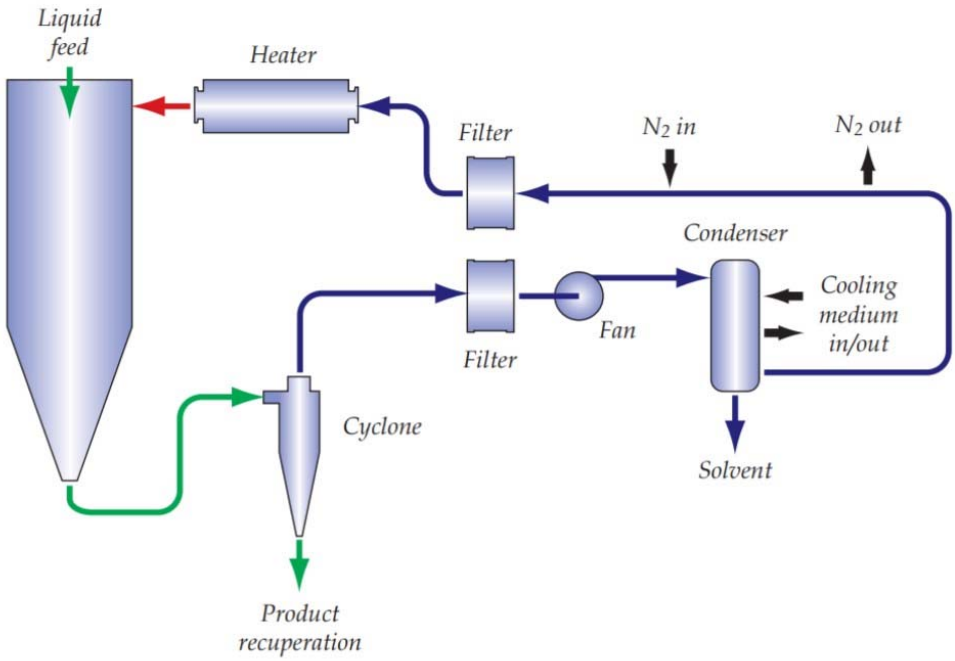

Figure 2. Spray dryer scheme (reprinted from Spray Dryer 4M8-Trix brochure, with permission from ProCepT).

1.2.4 Wound dressing characterization

Moist-related properties

The concept of moist wound healing (George D. Winter, 1962) transformed clinical approach of wound treatment and started the new era in dressing development. To provide optimal moist healing environment, exudate absorption, water vapour transmission and dehydration properties of the dressing must be fine-tuned. Kinetics and capacity of exudate

absorption is especially important for treatment of highly exuding wounds (e.g. leg ulcers, burns) and when dressing is applied in the solid form (e.g. powder, film) (Davies, 2012). Dressing exudate absorption (swelling) heavily depends on type of fluid employed for testing (e.g. simple buffer or simulated wound fluid (SWF), experimental conditions, dressing type and dressing composition, therefore definition of optimal swelling ranges and comparison between results is challenging. Salmerón-González et al. evaluated swelling of top selling wound dressings in the USA in terms of change in dressing volume (Salmerón-González et al., 2018). They found that polyurethane foams have the highest exudate absorbing capacity. On the other hand, Hasatsari et al. evaluated marketed products in Thailand and observed differences from 200-fold increase in mass for composite hydrocolloid dressing to almost 2000-fold increase for alginate dressing (Hasatsri et al., 2018). When reviewing swelling behaviour of dressings in the early development, wide absorption ranges with lower overall swelling capacities are also reported. Uptake of 90% of the mass of collagen-hyaluronic hydrogel was recently reported (Ying et al., 2019), while Akauru and Isiuku reported uptake of 120% of the mass for non-crosslinked chitosan hydrogels and around 40% for glutaraldehyde-crosslinked ones (Akakuru and Isiuku, 2017).

Water retention capacity characterizes swellable dressing behaviour in dry conditions. Evaluation of kinetics and extent of water loss is especially important when dressing is applied to dry wounds. Water loss again depends on type and composition of the dressing. Generally, dressings with high absorption capacity tend to lose absorbed water faster mainly due to lack of strong interaction between (polymer) chains (Lee et al., 2016). To overcome this issue, physically and chemically crosslinked wound dressing are being investigated (Gupta et al., 2019). Another possibility to modify moisture related properties is composition modification with hydrophobic components to increase occlusion effect (e.g. oils, lipids and hydrophobic polymers) (Yari et al., 2014).

Rate of water vapour transmission (WVTR) is a key feature for both, swellable and non-swellable dressings, since it provides information about dressings capability to maintain moist environment in the open wound bed. WVTR in range of 2000-2500 g/m^2/day provides adequate level of moisture without risking dehydration of the wound bed (Queen et al., 1987). To determine WVTR, humidity difference is usually formed between two sides of the dressing and vapour permeating is monitored by change of weight during time (British Standards Institution, 2002). Dressings with high absorbing capacity often have WVTR in the upper part of the optimal range, which makes them suitable for application to highly exuding wounds (Gupta et

al., 2019). For dry wounds, opposite applies. Xu et al. prepared a set of polyurethane membranes with different porosities to evaluate the influence of WVTR on the healing *in vivo* (Xu et al., 2016). They confirmed the significance of optimal WVTR for successful healing, nonrelated to the composition of the dressing, by showing accelerated wound closure for membranes having WVTR within the optimal range (Xu et al., 2016). Chitosan based dressings usually have extensively high WVTR, due to inherent absorbing properties. If dressing is formulated with chitosan derivates (Lu et al., 2010), chitosan crosslinked with other polymers (Kim et al., 2007; Sung et al., 2010), or in the form of nanoparticles (Archana et al., 2013), reported WVTRs are optimal for the treatment of highly exuding wounds. However, when formulated as a film, chitosan-based dressings can also show increased water retention capacity, due to dense film structure (Güneş and Tıhmınlıoğlu, 2017; Kouchak et al., 2015).

Biocompatibility and Healing potential

First step in biocompatibility screening of wound dressing in the early phase of its development comprises *in vitro* cytotoxicity assessment. Initial biocompatibility is evaluated with relatively simple *in vitro* tools like cell tests. Cell assays are generally reliable, short, sensitive and well-established for toxicity assessment for different indications. Cell assay tests as 2,3,5-triphenyltetrazolium chloride (TTC) and 3-(4,5-dimethylthiazol-2-yl)-2,5-diphenyltetrazolium bromide (MTT) assay are performed to assess the metabolic activity of cells. Both assays are easily quantified spectrophotometrically due to colour change. In viable cells, white TTC is converted by dehydrogenase activity to a red formazan product, while MTT is a yellow dye that gets converted into purple formazan by mitochondria. Lactate dehydrogenase (LDH) leakage assay provides insight into integrity of cell membranes upon the treatment, as LDH is normally present in the cytosol of all cell types. Cell assays always include non-treated cells as negative, and already known treatment that induces/exerts cytotoxic effect as positive control (da Costa et al., 1999). In case of wound dressings, keratinocytes and fibroblasts are the skin cells lines most relevant for cytotoxic evaluation.

When dressing is proven as biocompatible, the healing potential is the next point to be assessed. Due to complexity of the healing process, characterisation of healing potential is challenging to evaluate. Cellular migration/proliferation is occurring at all stages of healing process and is considered critical for evaluation of healing rates (Braiman-Wiksman et al., 2007; Wiegand and Hipler, 2009). *In vitro* scratch assay is the most commonly used test for evaluation of cell migration/proliferation. With this simple and inexpensive test, the “wound” is mimicked by creating an artificial gap in the confluent layer of cells and the “healing“ is

reflected by visual observation of cell migration in time. As cellular proliferation and migration are coextensive and challenging to distinguish, cells are usually incubated in serum-free medium to supress the proliferation phase. *In vitro* migration patterns of different cells well correspond to behaviour *in vivo* (Liang et al., 2007). For assessment of wound healing potential, scratch assay is usually performed on fibroblast (Fronza et al., 2009; Pérez-Díaz et al., 2016; Premarathna et al., 2019; Wiegand et al., 2019) and keratinocyte (Chigurupati et al., 2013; Teo et al., 2017) cell lines. Main limitation of the scratch test lies in the fact that it screens the effect of the wound healing dressing on a single type of cells, not capturing coordinated interactions between different cell types and processes. However, scratch assay is still the most widely used method for initial assessment of dressing wound healing potential.

1.3 Wound healing agents

1.3.1 Melatonin

Melatonin (N-acetyl-5-methoxytryptamine), evolutionary one of the oldest molecules with hormonal properties, is found in bacteria, eukaryotes, plants, fungi and animal species. This methoxyindol is synthesised from tryptophan through serotonin and secreted by the pineal gland. It is also largely synthesised by other organs such as gastrointestinal tract, retina and lens, liver and kidney, lung, brain and skin (Slominski et al., 2018). It exerts the activity through G-protein membrane receptors (MT1 and MT2) and potential nuclear receptor (Fischer et al., 2008; Slominski et al., 2016).

Along with the best-known activity as a regulator of circadian and seasonal biorhythm, melatonin exerts pleiotropic functions as a neurotransmitter, cytokine and signalling modifier. Melatonin is a high-potent antioxidant, as it directly scavenges hydroxyl and peroxyl radicals and stimulates antioxidative enzymes such as superoxide dismutase, glutathione peroxidase and reductase (Anisimov et al., 2006). Moreover melatonin has been investigated as an immunomodulator (Calvo et al., 2013), anti-cancer (Reiter et al., 2017) and DNA-repair agent (Majidinia et al., 2017) and a nervous (Yu et al., 2017) and cardiovascular system regulator (Pechanova et al., 2014).

As chronic wounds exhibit high levels of reactive oxygen species, melatonin is widely explored as healing promotor. Although some studies had reported controversy effect of melatonin on wound healing (Bulbuller et al., 2005; Drobnik, 2012; Nursal et al., 2002; Soybir et al., 2003), more recent data support the idea of melatonin as healing agent (Slominski et al.,

2018). It was shown that melatonin promoted disposition of collagen in fibroblast and myofibroblast culture *in vitro* (Drobnik et al., 2013) and regulated keratinocyte activity in diabetic wound model by extracellular signalling pathway (Song et al., 2016).

In vivo studies had shown that locally applied melatonin accelerated closure of full-thickness incisional wound model (Pugazhenthi et al., 2008), promoted bone formation (Yousuf et al., 2013), corneal wound healing (Crooke et al., 2015), as well as burn wounds regeneration (Murali et al., 2016). Moreover, applied as antioxidant in burn patients, melatonin significantly reduced endothelial dysfunction (Sahib et al., 2009).

Potential antimicrobial effect of melatonin has been reported in the literature, owing to its metal chelating activity (Srinivasan et al., 2012; Tekbas et al., 2008). Similar to radical scavenging, melatonin is very effective intracellular metal chelator (Gulcin et al., 2003). Considering high level or free iron present in the chronic wounds (Wlaschek et al., 2019), melatonin has high potential to act as a nonspecific antimicrobial agent.

1.3.2 Chitosan

Chitosan is a copolymer consisting of N-acetyl-glucosamine (β-(1,4)-2-acetamido-2-deoksi-β-D-glucose) and glucosamine (2-amino-2-deoksi-β-D-glucose) units. It is obtained by deacetylation of natural polysacharide chitin (poly(β-(1→4)-N-acetyl-D-glucosamine)). Chitin is exoskeleton component of crustaceans and insects, also present as proteoglycan in the extracellular matrix. Chitosan is soluble in acidic conditions due to protonation of the primary amino groups (pKa ~6.5). Molecular weight (typically 300-1000 kDa) and degree of deacetylation (i.e. number of free amino groups in the polymer chain; typically 60-100%) are two main parameters influencing chitosan's solubility, degradation kinetics and biological activity (Dash et al., 2011).

Considering its natural origin, chitosan is biocompatible and biodegradable polymer, widely used in the cosmetics, food and pharmaceutical industry (Bagheri-Khoulenjani et al., 2009; Sinha et al., 2004). It is also very well known as wound healing material with commercial dressings already available on the market (e.g. ChitoSam®, Chitoflex®, Axiostat®) (Hamedi et al., 2018). The exact mechanism how chitosan promotes wound healing is not clear yet (Patrulea et al., 2015), however, beneficial influence in all stages of wound healing had been demonstrated, from promotion of neutrophil concentration (Park et al., 2009), fibroblast proliferation and collagen deposition by degraded chitosan monomers (Ribeiro et al., 2009), to controlled scar formation (Baxter et al., 2013).

Owing to its positively charged amino groups, chitosan has a strong antimicrobial activity (Perinelli et al., 2018). It is hypothesised that chitosan acts via three different modes, including increasing bacterial wall permeability due to electrostatic binding to negatively charged wall membranes; interaction with microbial DNA and metal chelation with consequent reduced metalloproteins activity (Goy et al., 2009). Antimicrobial effect strongly depends on the molecular weight and deacetylation degree, as well as on environmental factors like microbial species, pH and temperature (Ma et al., 2017). In addition to variety of microorganisms susceptible to chitosan action (Ma et al., 2017; Perinelli et al., 2018), successful *P. aeruginosa* and *Staphylococcus* species biofilm elimination potential has been recently reported (Felipe et al., 2019; Liu et al., 2019). As protonation of amino groups is crucial for chitosan's biological activity, polymeric derivates with improved water solubility are widely explored. Trimethylation, crosslinking, coupling with carboxymethyl groups and peptides are the most common ones, showing potential in wound healing application (Ahmed and Ikram, 2016; Hamedi et al., 2018).

When formulated as wound dressing, chitosan and it's derivates are commonly used as functional drug carriers in form of micro or nanoparticulate based systems that absorb wound exudate, maintain moist environment, retain temperature and provide bacterial protection. Usually, dressings are formulated as hydrogels, films, sponges or powders (Patrulea et al., 2015).

2. Melatonin-loaded chitosan/Pluronic® F127 microspheres as *in situ* forming hydrogel: An innovative antimicrobial wound dressing

European Journal of Pharmaceutics and Biopharmaceutics 107 (2016) 67–79

Contents lists available at ScienceDirect

European Journal of Pharmaceutics and Biopharmaceutics

journal homepage: www.elsevier.com/locate/ejpb

Research paper

Melatonin-loaded chitosan/Pluronic® F127 microspheres as in situ forming hydrogel: An innovative antimicrobial wound dressing

Marieta Duvnjak Romić [a], Maja Šegvić Klarić [b], Jasmina Lovrić [c], Ivan Pepić [c], Biserka Cetina-Čižmek [a], Jelena Filipović-Grčić [c], Anita Hafner [c,*]

[a] R&D, PLIVA Croatia Ltd, TEVA Group Member, Prilaz baruna Filipovića 25, 10000 Zagreb, Croatia
[b] University of Zagreb, Faculty of Pharmacy and Biochemistry, Department of Microbiology, Schrottova 39, 10000 Zagreb, Croatia
[c] University of Zagreb, Faculty of Pharmacy and Biochemistry, Department of Pharmaceutical Technology, Domagojeva 2, 10000 Zagreb, Croatia

ARTICLE INFO

Article history:
Received 10 March 2016
Revised 15 June 2016
Accepted in revised form 16 June 2016
Available online 18 June 2016

Keywords:
Melatonin
Microspheres
Chitosan
Wound dressing
Pluronic® F127

ABSTRACT

The aim of this study was to develop melatonin-loaded chitosan based microspheres as dry powder formulation suitable for wound dressing, rapidly forming hydrogel in contact with wound exudate.

Microspheres were produced by spray-drying method. Fractional factorial design was employed to elucidate the effect of formulation and process parameters (feed flow rate, inlet air temperature, chitosan concentration, chitosan/melatonin ratio and chitosan/Pluronic® F127 ratio) on the product characteristics related to process applicability (production yield, entrapment efficiency and product moisture content) and microsphere performance in biological environment (microsphere mean diameter and surface charge). Appropriate formulation and process parameters for the establishment of efficient drying process resulting in fine-tuned chitosan and chitosan/Pluronic® F127 microspheres (efficient melatonin encapsulation, small diameter positive surface charge and low moisture content) were identified. Microspheres were characterized by appropriate flowability and high rate and extent of fluid uptake. Incorporation of Pluronic® F127 in microsphere matrix resulted in high melatonin amorphization and consequent higher melatonin release rate. Entrapment of melatonin in chitosan/Pluronic® F127 microspheres has potentiated chitosan antimicrobial activity against *Staphylococcus aureus* and five clinical isolates *S. aureus* MRSA strains. Microspheres were shown to be biocompatible with skin keratinocytes and fibroblasts at concentrations relevant for antimicrobial activity against planktonic bacteria.

1. Introduction

Wound healing is a dynamic well-ordered biological process involving complex interactions among cells, extracellular matrix components and signalling compounds, resulting in wound closure [1]. If this process is hindered for some local or systemic factors, the risk for persisting wounds colonization by different pathogens is increased. In case of wound infections, healing process cannot progress ending-up in non-healing chronic wounds which can lead to large area of necrosis and even to systemic infection [2,3].

Antibacterial agents are topically administered to enable wound healing process and to prevent the infection spreading. However, significant drawback in antibacterial therapy of wound infections is growing bacterial resistance to conventional antibiotic

Abbreviations: QbD, Quality by Design; HPLC, high performance liquid chromatography; MDSC, modulated differential scanning calorimetry; XRPD, X-ray powder diffraction; SWF, simulated wound fluid; WVTR, water vapour transmission rate; MHB, Mueller-Hinton broth; DMSO, dimethyl sulfoxide; MIC, minimal inhibitory concentrations; NCCLS, National Committee for Clinical Laboratory Standards; TTC, 2,3,5-triphenyl tetrazolium chloride; TSB, tryptic-soy broth; TSBGlc, tryptic-soy broth TSB supplemented with 0.25% D-(+)-glucose; PBS, phosphate buffer saline; MTT, [3-(4,5-dimethylthiazol-2-yl)-2,5 diphenyltetrazolium bromide]; HBSS, Hank's balanced salt solution; HEPES, N-2-hydroxyethylpiperazine-N0-2-ethanesulfonic acid; LDH, lactate dehydrogenase; MBIC, minimum biofilm inhibitory concentrations; MBEC, minimum biofilm eliminating concentrations; CC, chitosan concentration; T, inlet temperature; C/M, chitosan/melatonin ratio; F, feed rate; C/P, chitosan/Pluronic® F127 ratio; MCP, melatonin-loaded chitosan/Pluronic® F127 microspheres; MC, melatonin-loaded chitosan microspheres; CP, chitosan/Pluronic® F127 microspheres; C, chitosan microspheres.

* Corresponding author at: A. Kovacica 1, 10000 Zagreb, Croatia.
E-mail address: ahafner@pharma.hr (A. Hafner).

http://dx.doi.org/10.1016/j.ejpb.2016.06.013
0939-6411/

agents. At the same time, bacterial biofilms, a common cause of recurring infections, are not responsive to conventional antibiotic therapy [4]. Therefore, a nonconventional approach has recently been of tremendous interest in overcoming bacterial resistance [5,6]. Antibacterial micro- and nanoparticles can exhibit different non-specific antibacterial and antibiofilm activities while at the same time they serve as carriers for additional conventional or nonconventional antibiotic agent [6,7].

Melatonin, methoxyindole secreted by the pineal gland, has pleiotropic bioactivities as a neurotransmitter as well as hormone, cytokine and biological-response modifier [8]. Many of its effects which are not related to its primary neurohormonal functions are linked with its anti-inflammatory properties, effective free radical scavenging and stimulation of antioxidant enzymes activity [9]. It has been reported that melatonin may have antibacterial effects and could improve wound healing process. Melatonin showed antibacterial effects against gram-positive and gram-negative bacteria, which has been ascribed to its ability to reduce intracellular substrates availability such as free iron and fatty acids [10,11]. Metal chelating activity of melatonin has been well described in the literature [12]. At the same time, melatonin influences different phases of wound repair such as inflammation, cell proliferation and migration, as well as collagen and glycosaminoglycan accumulation at the wound site [13]. Owing to reactive oxygen species antagonizing, the involvement of melatonin in burns treatment seems to reduce endothelial dysfunction and improve burn outcome in general, which is evidenced by the reduced incidence of wound infection and shortening of healing time [14,15]. Stated supports the idea of antibacterial and wound healing potential of melatonin administered locally by means of functionalized delivery system.

Chitosan is a biocompatible and biodegradable cationic polysaccharide with a wide-spectrum of antibacterial activities [5]. The antimicrobial effect of chitosan is strongly dependent on its molecular weight and degree of deacetylation and at the same time on the intrinsic differences in target bacterial wall structure [5]. Three models of chitosan antibacterial activity have been proposed: (i) interaction between positively charged chitosan molecules and negatively charged microbial cell membranes, resulting in changes in membrane wall permeability; (ii) binding of chitosan with microbial DNA and consequent inhibition of the mRNA and protein synthesis, and (iii) chelation of metals and consequent decrease in the activities of metalloproteins [16]. Among natural polymers, chitosan is known as a wound dressing material enhancing the healing process by different mechanisms [1]. When formulated in a dry powder, it can rapidly absorb wound exudate forming non-occlusive hydrogel, thus promoting wound desiccation and limiting bacterial proliferation.

The aim of the present work was to verify the idea of melatonin-loaded chitosan based delivery system development, suitable for application in wounds, and to investigate its antibacterial and wound healing potential. Except for chitosan and melatonin, polyoxyethylated non-ionic surfactant Pluronic® F127 was considered as a constitutive material of delivery system as it is expected to play a significant role in fine tuning of delivery system characteristics. In addition, Pluronic® F127 was reported to enhance the rate of wound healing process [17,18].

Melatonin-loaded chitosan based microspheres were produced by spray-drying. Fractional factorial design was employed to elucidate the effect of formulation and process parameters (feed flow rate, inlet air temperature, chitosan concentration, chitosan/melatonin ratio and chitosan/Pluronic® F127 ratio) on the product characteristics related to process applicability (production yield, entrapment efficiency and product moisture content) and microsphere performance in biological environment (microsphere mean diameter and surface charge). This rational approach is advantageous due to time and material savings [19]. Selected samples were characterized in terms of flow properties, swelling, moisture transmission and melatonin release behaviour. The final aim was the evaluation of *in vitro* biocompatibility and antibacterial efficacy of melatonin-loaded chitosan based microspheres, envisioned to be administered as a powder dressing in the wound treatment.

2. Materials and methods

2.1. Materials

Low-viscosity chitosan was purchased from Sigma-Aldrich (⩾75% deacetylated powder, Japan); Pluronic® F127 from BASF (Germany) and melatonin was purchased from Sigma-Aldrich (China). Mupirocin calcium dihydrate was donated by Pliva Croatia (Croatia). Müller-Hinton broth (MHB) and Tryptic soy broth (TSB) were obtained from Merck (Germany). 2,3,5-triphenyltetrazolium chloride (TTC), 3-(4,5-dimethylthiazol-2-yl)-2,5-diphenyltetrazolium bromide (MTT) and DMSO were purchased from Sigma (St. Louis, MO, USA). All other chemicals or solvents used in study were of analytical grade and purchased from Kemika (Croatia) and Sigma-Aldrich.

2.2. Experimental design

Quality by Design (QbD) principles were explored to understand critical process conditions and to optimize formulation parameters in order to evaluate their possible interactions. The influence of five factors at two levels was studied with a 2^{5-1} fractional factorial design. Investigated parameters were feed flow rate, inlet air temperature, feed concentration, polymer/drug ratio and concentration of Pluronic® F127 (Table 1). Preliminary experiments were performed to determine appropriate values for both low and high settings of parameters.

Production yield, particle size, moisture content, zeta potential and entrapment efficiency were investigated as responses. All experiments were triplicated and run in randomized order. The analyses of obtained characterization data were run using Analysis of Variance and fitted with regression. Design of experiments and data analyses were performed with the statistical software JMP® 10.0.2. (SAS Institute, Cary, North Carolina, USA).

2.3. Preparation of microspheres

Chitosan was solubilized in 0.5% acetic acid solution at concentration of 4 or 8 g/l. Chitosan solution was then mixed with ethanolic solution of melatonin or ethanolic solution of melatonin and Pluronic® F127 at constant volume ratio of 4/1. Concentrations of melatonin and Pluronic® F127 in ethanolic solutions were set up to provide defined chitosan to melatonin (5/1 and 2/1; Table 1) and chitosan to Pluronic® F127 (5/1; Table 1) weight ratios in the prepared solution mixtures. Melatonin-loaded microspheres were prepared by spray-drying of solution mixtures, using a Mini Spray Dryer Büchi 190 (Flawil, Switzerland) with a standard 0.7 mm noz-

Table 1
Parameters considered in the experimental design and their levels.

Parameter	High (+1)	Low (−1)
1 – Chitosan concentration (CC)	8 g/L	4 g/L
2 – Inlet temperature (T)	175 °C	145 °C
3 – Chitosan/Melatonin ratio (C/M)	5/1	2/1
4 – Feed rate (F)	7.69 ml/min	2.59 ml/min
5 – Chitosan/Pluronic® F127 ratio (C/P)	5/1	–

zle and compressed air flow rate of 700 Nlh^{-1}. The other process parameters were set according to the requirements of the individual runs as set in the fractional factorial design studies listed in Table 2. Corresponding melatonin-free (empty) microspheres were prepared following the same procedure as for melatonin-loaded microspheres, omitting melatonin and served as control when appropriate. All experiments were performed in triplicate.

The process yield was calculated as the ratio between the weight of the obtained microspheres and the sum of the weights of all dry components introduced into the process.

2.4. Particle size, zeta potential and drug loading

A microscopic imaging analysis technique for determination of microspheres size distribution was applied. Microsphere size and distribution were determined with an Olympus BH-2 microscope, equipped with a camera (CCD Camera ICD-42E; Ikegami Tsushinki Co., Tokyo, Japan) and computer-controlled image analysis system (Optomax V, Cambridge, UK). In all measurements at least 3000 particles were examined.

The zeta potential of the microspheres was determined by laser Doppler anemometry (Zetasizer 3000HS, Malvern Instruments, UK) at 25 °C. Before measurement, particles were dispersed in 10 mM NaCl and placed in an electrophoretic cell, where a potential of 150 mV was established. To calculate the zeta potential, the Henry equation has been employed (1):

$$z = \frac{U_e 3\eta}{2\varepsilon f(\kappa\alpha)} \quad (1)$$

where U_e is experimentally determined electrophoretic mobility, ε is the dielectric constant (ε = 78.6), η is the absolute zero-shear viscosity of the medium (η = 0.891 mPa s) and $f(\kappa\alpha)$ is the Henry function ($f(\kappa\alpha)$ = 1.5).

The total amount of melatonin contained in the microspheres was determined by the high performance liquid chromatography (HPLC) assay method. Before the measurement, microspheres were dispersed in 1 M HCl. The dispersion was shortly sonicated, filtered (0.45 μm) and diluted with the mixture of 96% ethanol and purified water in 1:4 ratio. An HPLC system, which consisted of an Agilent 1100 Series instrument (Agilent Technologies, Waldbronn, Germany) equipped with a diode array detector set at 224 nm, was used to perform the assay. The mobile phase, consisted of HPLC grade water and acetonitrile in the ratio of 52/48, was used at a flow rate of 1 mL/min. The column (Kinetex C18 column 50 × 4.6 mm^2, particle size 5 mm, Phenomenex, USA) suited with an in-line filter (KrudKatcher Ultra HPLC, 0.5 μm Depth Filter × 0.004 in., Phenomenex, USA) was operated at 30 °C. The sample injection volume was 10 μL. The elution was isocratic and the run time was 1 min.

2.5. Thermal analyses

Modulated differential scanning calorimetry (MDSC) analyses were carried out in a TA Instrument modulated DSC Q2000 (TA Instruments, New Castle, DE, USA) using aluminium standard pans with about 0.5–1 mg of the sample, under dynamic nitrogen atmosphere (50 mL/min). The samples were heated at 5 °C/min from 20 °C to 220 °C using a modulation of ±1 °C (amplitude) each 60 s (period).

The moisture content in the powder samples was analysed by thermogravimetric analysis using TGA Q5000 (TA Instruments, New Castle, DE, USA). A powder sample weighting approximately 5 mg was heated from 25 to 500 °C at a rate of 10 °C/min under dynamic nitrogen atmosphere of 35 mL/min.

2.6. X-ray powder diffraction analyses

X-ray powder diffraction (XRPD) data were recorded on a Philips X'Pert PRO diffractometer (PAN Analytical, Kassel Waldau, Germany) equipped with an X'Celerator detector (2.022° 2Θ) using Cu-Kα radiation at 45 kV and 40 mA. The scan angle range (2Θ) was 3–40°, the step size (2Θ) was 0.167°, and the time per step was 100 s.

Samples were applied directly into a Phillips' original zero background silicon plate holder with spatula. Diffractograms were analysed using X'Pert Data Collector software.

2.7. Analysis of flow properties of microsphere powders

Bulk and tap density of powders were measured by modifying the pharmacopoeia test, as reported in the literature [2,20]. Approximately 30 mg of microsphere powders was loaded into a bottom-sealed 1 mL plastic syringe (Terumo Europe, Leuven, Belgium) capped with a laboratory film and tapped until no change in the volume of the powder was observed. The bulk and tap densities were calculated from the difference between the net weight of the plastic syringe content divided by the volume in the syringe before and after tapping, respectively. Experiments were performed in triplicate. Hausner ratio was calculated as tapped density/bulk density ratio.

2.8. Wound dressing characterization

2.8.1. Swelling study

Franz diffusion cell apparatus was used to determine the fluid-absorbing capacity of microspheres. The receiver compartment was filled with the simulated wound fluid (SWF) consisting of 50% foetal calf serum (Sigma Aldrich, Milan, Italy) and 50% maximum recovery diluent (Sigma Aldrich, Milan, Italy, composed of 0.1% (w/v) peptone, peptic digest of animal tissue, and 0.9% (w/v) sodium chloride) [21] with pH adjusted to 6.3 and 7.4. SWF was thermostated at 32 °C and 37 °C. A regenerated cellulose membrane (0.45 μm pore size) with 10 mg of microsphere sample was placed between the donor and the receiver compartment. SWF level in graduated part of receiver compartment lowered due to liquid uptake of the microspheres. At set time intervals, receiver compartment was filled with SWF up to the starting level. The liquid uptake of each sample was expressed as a volume of water added per milligram of the microspheres in 120 min swelling process.

2.8.2. Water vapour transmission rate

To determine the water vapour transmission rate (WVTR) the microspheres were swollen in SWF (pH 6.3 and 7.4) until the formation of homogenous hydrogel, as described in the previous section. Hydrogels were mounted on the Teflon® mesh placed on the mouth of cylindrical plastic cups (15 mm diameter) containing 10 mL of water with negligible water vapour transmission, and placed in an oven at 37 °C for 24 h. The weight loss was measured at regular time intervals and weight loss versus time plot was constructed. The WVTR was calculated using the formula (2):

$$WVTR = \frac{slope \times 24}{A} \frac{g}{m^2}/\text{day} \quad (2)$$

where A represents the test area of the sample in m^2. Experiments were done in triplicate with sealed cups as negative and open cup as positive control.

2.8.3. Evaporative water loss

Hydrogels prepared as described above were kept at 37 °C and 35% relative humidity. After regular time intervals, the weight

was noted. The percentage of the weight remaining was calculated by the Eq. (3):

$$\text{Water weight remaining } (\%) = \frac{Wt - Wt\ last}{Wo - Wt\ last} \times 100 \quad (3)$$

where W_0, W_t and $W_{t\ last}$ are initial weight, weight after time "t" and weight after 12 h, respectively. All experiments were performed in triplicate.

2.9. In vitro drug release study

The release profiles of melatonin-loaded microspheres were evaluated using a Franz diffusion cell apparatus, since this model would allow the microspheres to hydrate slowly in humid environment conditions designed to be similar to those encountered at the wound site. A regenerated cellulose membrane with 0.45 μm pore size was inserted between the donor and the receiver compartment. Receiver compartment was filled with the phosphate buffer pH 6.3 or pH 7.4. The microspheres containing 1.5 mg of melatonin were placed on the donor side, fully covering the membrane. The system was thermostated at 32 °C and 37 °C. The receiving medium was continuously stirred (600 rpm) with a magnetic stirrer. At the set time intervals, the samples (1 mL) were withdrawn from the receiver compartment and replaced with the equal volume of the fresh medium. The drug was detected according to the HPLC assay method described above. Aqueous solution of melatonin was used as a control. All release experiments were performed in triplicate.

2.10. Swelling and drug release kinetics

The *in vitro* swelling and drug release kinetics in each medium were evaluated and the ideal kinetic models were estimated using the following equations [22]:

Zero order kinetics;

$$S = k_{S0}t \quad (4)$$

$$C_t/C_\infty = k_{C0}t \quad (5)$$

First order kinetics;

$$log\ S = k_S t \quad (6)$$

$$\log\ C_t/C_\infty = k_C t \quad (7)$$

Second order kinetics;

$$t/S = t\frac{1}{S_\infty} + \frac{1}{W_\infty^2 k_{s2}} \quad (8)$$

Higuchi model;

$$S = k_{SH}\sqrt{t} \quad (9)$$

$$C_t/C_\infty = k_{CH}\sqrt{t} \quad (10)$$

where S, t, S_∞, k_{s0}, k_s, k_{s2} and k_{SH} are volume of absorbed SWF per milligram of chitosan in microspheres, time (min), absorbed SWF at equilibrium and swelling constants of each model, respectively. C_t/C_∞, k_{c0}, k_c and k_{cH} are drug release fractions and drug release constants of each model, respectively. The coefficient of determination (R^2) was used as an indicator of the best fitting, for each of the model considered.

To elucidate the transport mechanisms, the swelling and release curves were fitted to the following Korsmeyer-Peppas equation [23]:

$$S_t/S_\infty = k_{SKP}\ t^{ns} \quad (11)$$

$$C_t/C_\infty = k_{CKP}\ t^{nc} \quad (12)$$

where k_{SKP} and k_{CKP} represent the kinetic constants and n_s and n_c are the diffusion exponents for swelling and drug release, respectively. The diffusion exponents indicate transport mechanism; if $0.1 < n_s$; $n_c < 0.45$, Fickian diffusion is indicated, $0.45 < n_s$; $n_c < 0.89$ indicates non-Fickian diffusion, while n_s; $n_c \geqslant 0.89$ indicates Case-2 release.

2.11. Antimicrobial assay

2.11.1. Sample preparation

The antimicrobial activity of melatonin-loaded microspheres was investigated with respect to melatonin and Pluronic® F127 solutions as well as melatonin-free microspheres. Prior to the experiment microspheres were resuspended in the mixture of degassed sterile water and MHB (1:1, v/v), melatonin was dissolved in MHB with 5% of DMSO, while Pluronic® F127 was dissolved in distilled water obtaining Pluronic® F127 stock solution. All samples were diluted in MHB with respect to the concentration of melatonin. Mupirocin calcium dihydrate was also dissolved and diluted in MHB and served as positive control. Antimicrobial activity of the prepared samples was tested on *Staphylococcus aureus* (ATCC 29213) and five clinical isolates *S. aureus* MRSA strains (MFBF 10674, MFBF 10676, MFBF 10677, MFBF 10679, MFBF 10680) taken from microbial collection of the Department of Microbiology, Faculty of Pharmacy and Biochemistry, University of Zagreb (Croatia). All experiments were performed in four replicates.

2.11.2. Antimicrobial activity against planktonic bacteria

For determination of minimal inhibitory concentrations (MICs) of samples twofold microdilution assay on a 96-well plate using MHB was carried out following NCCLS method [24]. Culture of *S. aureus* in the broth was treated with microspheres, melatonin or Pluronic® F127 solutions at (relevant) melatonin concentration ranging from 0.008 mg/mL to 1 mg/mL; MHB with or without 2.5% DMSO was used as positive (growth) control, while microsphere samples, melatonin and Pluronic® F127 in appropriate dilutions at (relevant) melatonin concentration without *S. aureus* were negative controls; mupirocin as positive control of antimicrobial activity was applied in concentration range from 0.0625 to 128 μg/mL. After 24 h of incubation at 35 ± 2 °C the MIC was assessed by absorbance measurement at 620 nm as described by Tekbas et al. [10]. The MIC was recorded as the lowest concentration of antimicrobial agent that restricted growth to a level <0.05 at 620 nm (iEMS, Labsystems). MICs were confirmed using TTC reagent dissolved in water (20 mg/mL) according to Klančnik et al. [25].

2.11.3. Antimicrobial activity against biofilm

Minimum biofilm inhibitory concentrations (MBIC) and minimum biofilm eliminating concentrations (MBEC) were determined according to the methods described by Kifer et al. [26]. To assess MBIC *staphylococci* were inoculated to TSB supplemented with 0.25% D-(+)-glucose (TSBGIc) to a final concentration of $1–2 \times 10^6$ cfu/mL and incubated for 24 h at 35 ± 2 °C. Microsphere samples, melatonin or Pluronic® F127 solution in twofold dilutions in TSBGIc at (relevant) melatonin concentration ranging from 0.01 mg/mL to 1.35 mg/mL were distributed on a 96-well (50 μL per well) tissue culture plate (Nunclon™ Surface, Nunc). The overnight bacterial cultures were diluted 1:10 in TSBGIc and 50 μL was added to each well. After incubation (24 h at 35 ± 2 °C) the medium from the wells was removed by aspiration and wells were gently washed with 100 μL of phosphate buffer saline (PBS, pH 7.4). PBS was removed and biofilm was stained with 100 μL of MTT reagent dissolved in PBS (0.1 mg/mL). After 2 h incubation at 37 °C MTT was replaced with 150 μL of DMSO and incubated for 15 min at room temperature on rotary shaker. The absorbance was measured at wavelength of 540 nm (iEMS, Labsystems). To assess the MBEC,

bacterial cultures were grown in TSBGlc as it was previously described. The overnight cultures were diluted in TSBGlc 1:20 and after 24 h lasting biofilm formation the medium was removed, and biofilm was treated with samples (at (relevant) melatonin concentration of 0.08–2.7 mg/mL) that showed inhibitory effect on biofilm formation in the previous experiment. After overnight incubation, the viability of the biofilm was assessed in the same manner as previously described. To obtain the IC_{50} from the results of antibiofilm assays, non-linear dose-response fitting was applied using Eq. (13):

$$Y = A1 + (A2 - A1)/(1 + 10\hat{}((LogIC_{50} - X) * HillSlope) \quad (13)$$

where A1 is maximal viability (on y-axis), A2 is minimal viability (on y-axis), X is concentration of the inhibitor and HiLLSlope represents steepness of the curve.

2.12. In vitro cytotoxicity

2.12.1. Cell culture conditions

Human keratinocyte cell line HaCaT (Cell Line Services, Germany) and human fibroblast cell line BJ (American Type Culture Collection [ATCC], Rockville, MD, USA) were cultured in DMEM medium (GIBCO, Invitrogen, Paisley, UK) supplemented with 10% foetal bovine serum (GIBCO) and penicillin, streptomycin and amphotericin B (Sigma–Aldrich).

To assess the potential cytotoxicity of microspheres, HaCaT and BJ cells were seeded onto 24-well plates (Sarstedt, Newton, NC, USA) at a density of 10^5 and 5×10^4 cells/well, respectively, and allowed to reach confluence in 2 days. Microspheres were resuspended in the Hank's balanced salt solution (HBSS) buffered with 30 mM N-2-hydroxyethylpiperazine-N0-2-ethanesulfonic acid (HEPES) (pH 6.3 and pH 7.4), resulting in melatonin and chitosan concentration ranging from 0.015 to 0.30 and 0.03 to 0.06 mg/mL, respectively.

Prior to the treatment with microspheres, cell culture medium was withdrawn, and the cells were washed with HBSS. The cells were then exposed to the microsphere suspensions for 2 h. Cells incubated in HBSS were used as negative control, while cells treated with 1% Triton X-100 served as positive control. After the treatment, *in vitro* cytotoxicity was determined by MTT and lactate dehydrogenase (LDH) leakage assay.

2.12.2. MTT assay

Colorimetric MTT assays were performed to assess the metabolic activity of cells 24 h after the treatment with microspheres and melatonin solution. After 2 h treatment with melatonin-loaded and corresponding blank microspheres, HBSS suspension was removed, cells washed twice with PBS and replaced with fresh medium. After 24 h, a 0.5 mL of MTT solution in DMEM (0.5 mg/mL) was added to each well, and cells were then incubated for 30 min at 37 °C. Subsequently, medium was removed, cells were lysed and formazan was dissolved with DMSO. The amount of formazan was quantified spectrophotometrically at 595 nm (Spectra Max 190, Molecular Devices, Berkshire, UK). Mitochondrial activity was expressed relative to a control group treated with HBSS. No interference between microspheres and MTT assay was observed.

2.12.3. LDH leakage assay

LDH leakage assay was performed to assess the integrity of the plasma membrane following the treatment with microspheres. Due to the well-known melatonin antioxidant activity and possible interference with LDH test, blank microspheres were used for the determination of cell plasma membrane integrity. After 2 h treatment with blank microspheres, the activity of the enzyme present in HBSS was determined spectrophotometrically (Cary 50 Bio, Varian, Vistoria Australia) at λ_{max} 340 nm against distilled water as a blank using an LDH kit (Pointe Scientific Inc., Canton, MI, USA). Cells exposed to 1% Triton X-100 were used as a positive control (100% lysis) and non-treated cells as a negative control. No interference between microspheres and LDH assay was observed. Cell viability was calculated by the Eq. (14):

$$Cell\ viability\ (\%) = 100 - \frac{\text{experimental value} - \text{negative control}}{\text{positive control} - \text{negative control}} \times 100 \quad (14)$$

3. Results and discussion

3.1. Experimental design: analysis of results

In this study the fractional factorial experimental design was employed to investigate the effect of five process/formulation parameters and their possible interactions on the product characteristics with aim to direct the product development towards the one with the favourable performance.

The obtained characterization data (Table 2) were used to fit multiple linear regression models whose equations are given in Table 3. Equations with fitted coefficients for the investigated parameters are shown. The main factors and major interactions between main factors included in each equation were significant for the model at the 95% confidence level. The models were chosen using stepwise regression with minimum P-value threshold as a stopping rule. A positive parameter coefficient in equation means that an increase in the parameter value results in an increase in the response value and a negative coefficient that the response values increase with decreasing parameter value.

The yields varied between 34.2 and 64.6% (Table 2). Obtained yields were relatively high for the method employed [27]. Four main factors were found to significantly influence the yield: the inlet temperature, feed flow, presence of Pluronic® F127 and chitosan concentration (Table 3, Eq. (15)). It was noted that the increase in inlet temperature decreased the yield. Although not common, such relationship was reported previously in the literature and was ascribed to different events such as heating the particles beyond their glass transition temperature or creation of agglomerates leading to a lower yield [28–30]. The yield decreased with the increase of the feed flow, which could be explained by higher moisture content resulting in sticking of liquid or solid mass to the walls of the drying chamber or the cyclone separator [31]. As expected, better production yields were obtained for solutions with higher chitosan concentrations and if Pluronic® F127 was added [32,33]. Except the individual parameters, combinations of chosen factors were also responsible for controlling the process yield. The strongest interaction observed was between the inlet temperature and presence of Pluronic® F127 in the system, as indicated by the regression equation (Table 3, Eq. (15)).

All microspheres prepared were positively charged (Table 2) with values similar to those reported in the literature [34], indicating the presence of chitosan at the surface of all microspheres formed. Chitosan concentration distinctly had the greatest influence on zeta-potential values (Table 3, Eq. (16)). Increased inlet temperature was related to decreased zeta potential. This could be related to the conversion of chitosan acetate to acetyl amide form at high temperatures as reported in the literature [35]. In addition, interaction of chitosan concentration with inlet temperature was observed to be significant. As expected, addition of Pluronic® F127 to the spray drying solutions lowered particle surface charge [33]. Obtained microspheres are chitosan/Pluronic® F127 matrix systems with neutral Pluronic® F127 present on the

Table 2
The design matrix of fractional experimental design with variable values and resulting product characteristics (mean values ± SD, n = 3).

Sample ID	CC (g/L)	T (°C)	C/M	F (ml/min)	C/Pluronic® F127	Yield (%)	Mean diameter (μm)	Zeta-potential (mV)	Moisture content (%)
S1	4	145	2/1	2.59	5/1	64.6 ± 2.3	2.31 ± 0.30	23.9 ± 1.9	5.4 ± 0.1
S2	4	145	2/1	7.69	–	49.0 ± 1.9	1.94 ± 0.09	22.1 ± 1.6	6.7 ± 0.1
S3	4	145	2/1	7.69	5/1	56.3 ± 1.0	2.16 ± 0.01	21.1 ± 1.7	5.9 ± 0.6
S4	4	175	5/1	7.69	–	34.2 ± 5.2	2.21 ± 0.03	26.5 ± 1.4	6.1 ± 0.2
S5	4	145	2/1	2.59	–	63.3 ± 3.0	2.25 ± 0.19	24.0 ± 1.6	6.3 ± 0.5
S6	4	175	5/1	2.59	5/1	55.9 ± 0.6	2.31 ± 0.22	21.3 ± 1.9	5.3 ± 0.5
S7	4	175	5/1	2.59	–	37.9 ± 4.3	2.11 ± 0.07	20.8 ± 1.7	4.1 ± 0.2
S8	4	175	5/1	7.69	5/1	53.5 ± 3.7	2.44 ± 0.10	25.4 ± 1.0	4.3 ± 1.0
S9	8	175	5/1	7.69	5/1	50.4 ± 4.3	2.41 ± 0.13	26.8 ± 1.0	5.9 ± 0.9
S10	8	175	5/1	2.59	–	40.8 ± 3.1	2.03 ± 0.06	27.3 ± 1.5	5.6 ± 0.4
S11	8	175	5/1	2.59	5/1	53.0 ± 3.2	2.25 ± 0.01	19.6 ± 1.4	3.3 ± 0.1
S12	8	145	2/1	2.59	–	64.6 ± 3.0	2.18 ± 0.04	35.0 ± 0.6	3.7 ± 1.7
S13	8	175	5/1	7.69	–	52.2 ± 4.1	2.06 ± 0.17	29.3 ± 1.3	3.8 ± 0.4
S14	8	145	2/1	7.69	–	58.6 ± 4.2	2.19 ± 0.11	35.0 ± 1.3	5.9 ± 0.4
S15	8	145	2/1	2.59	5/1	62.9 ± 1.0	2.23 ± 0.04	27.0 ± 1.3	5.4 ± 0.5
S16	8	145	2/1	7.69	5/1	47.9 ± 4.2	2.54 ± 0.04	31.2 ± 1.8	5.8 ± 1.1

Table 3
Regression equations of the interaction models linking the formulation and process parameters (in terms of coded factors) with responses. R^2 values are given to indicate the goodness of fit of the theoretical models to the experimental values.

Regression equation of the interaction model	R^2
Yield (%) = 52.81 − 5.58T − 2.56F + 2.74C/P + 0.98CC + 2.99CC ∗ C/P − 2.89T ∗ F − 3.23T ∗ C/P (15)	0.9067
Zeta-potential (mV) = 26.20 + 2.59CC − 1.75T − 1.6C/P − 1.23CC ∗ T (16)	0.8502
Moisture content (%) = 4.94 − 0.44T − 0.59CC + 0.3C/M + 0.61F − 0.04 C/P + 0.37CC ∗ F − 0.25CC ∗ C/P − 0.33T ∗ C/M − 0.23T ∗ C/P (17)	0.9679
Mean diameter (μm) = 2.22 + 0.11C/P + 0.01F − 0.002 C/M + 0.0003 T + 0.01 CC + 0.05CC ∗ F − 0.05CC ∗ T + 0.05C/M ∗ C/P − 0.04 F ∗ C/P (18)	0.7870

particles surfaces which manifest in lower positive zeta-potential values.

Moisture content for all microsphere samples ranged from 3.2 to 6.7% (w/w) (Table 2). These values are in line with values reported in other studies indicating the moisture content of spray-dried powders to be up to 7.5% w/w [36,37]. The parameter having the greatest impact on this response is feed flow rate (Table 3, Eq. (17)). It is well known that high feed rates lead to poorer evaporation of solvent and higher moisture contents. Increase in inlet air temperature resulted in decrease in moisture content (Table 3, Eq. (17)). Supplying more heat energy, high inlet air temperature lowers relative humidity of air, thus lowering final product moisture. Increase in chitosan and melatonin concentration also decreased the microsphere moisture content. Generally, the more the feed is concentrated, better is the drying process. All significant interactions of main factors in the obtained fitted model are in accordance with the individual factor influence on the moisture content.

All microspheres prepared had uniform and narrow particle size distribution with the mean diameter range between 1.94 ± 0.09 (PDI = 0.004) and 2.54 ± 0.04 (PDI = 0.001) μm (Table 2). The observed differences in particle mean diameter do not have practical impact on microsphere performance and were found not to be significant as obtained regression equation contained high number of parameters with small coefficients and poor R^2 value (Table 3, Eq. (18)).

Entrapment efficiency was close to 100% for all microsphere samples (data not shown), indicating that no loss of active compound occurred during the spray-drying process. Therefore, entrapment efficiency was not suitable for statistical analysis.

Based on results obtained through fractional factorial experimental design, optimal process and formulation parameters for the establishment of efficient drying process resulting in melatonin-loaded microspheres with highly positive charge and low moisture content were identified (samples S15 and S12, with and without Pluronic® F127, respectively). Optimal parameters included usage of chitosan solution at the concentration of 8 g/L in the preparation of feed solution (giving higher values of zeta-potential and lower moisture content), chitosan to melatonin weight ratio of 2/1 (giving lower moisture content), inlet temperature of 145 °C (giving higher yields and zeta-potential values) and feed flow rate of 2.59 mL/min (giving higher yields and lower moisture content). Selected samples, S15 and S12, referring to melatonin-loaded chitosan/Pluronic® F127 and chitosan microspheres, are further denoted as MCP and MC, respectively. Both microsphere samples were characterized by high process yield (62.9 and 64.6%, respectively). MCP had a mean diameter of 2.23 ± 0.04 μm, with 72% of particles smaller than 1 μm. MC had a mean diameter of 2.18 ± 0.01 μm, with 67% of particles smaller than 1 μm. The positive zeta potential for MC (35.0 ± 0.6 mV) was higher than for MCP (27.0 ± 1.3 mV). For both samples entrapment efficiency was 99.7% so employed C/M weight ratio of 2/1 resulted in microspheres with relatively high drug loadings (29.4 and 33.3% for MCP and MC, respectively). Moisture content for samples MCP and MC was 5.4 ± 0.5 and 3.7 ± 1.7%, respectively. Optimized microsphere samples, were reproduced in triplicate (under selected process parameters) and characterized to confirm batch-to-batch repeatability.

3.2. Powder characterization

No significant difference in microsphere characteristics was observed between different batches of the same microsphere sample, confirming batch-to-batch repeatability (Table 4).

Flowability characteristics were expressed as Hausner ratio and ranged from 1.7 to 1.8, which is in accordance with literature values for chitosan-based spray-dried systems [38,39].

MCP and MC were further evaluated in terms of physical state of the drug, swelling ability, water vapour transmission rate, evaporative water loss, *in vitro* drug release, antimicrobial activity and cell biocompatibility.

3.3. Solid state characterization

X-ray diffractographs of crystalline melatonin and melatonin-loaded spray dried microspheres (MCP, MC) are shown in Fig. 1.

Melatonin diffraction peaks can be observed in both MCP and MC diffractographs indicating incomplete melatonin conversion to amorphous state during spray-drying process. Crystalline mela-

Table 4
Characteristics of selected melatonin loaded chitosan (MC) and chitosan/Pluronic® F127 (MCP) microspheres (mean values ± S.D., n = 3).

Sample ID	Yield (%)	Mean diameter (μm)	Zeta potential (mV)	Moisture content (%)	Entrapment efficacy (%)	Hausner ratio	WVTR (g m^{-2} day^{-1})	SWF uptake at pH 6.3 (μl/mg)	SWF uptake at pH 7.4 (μl/mg)
MCP	65.2 ± 5.3	2.3 ± 0.3	28.1 ± 2.2	3.6 ± 0.2	99.7 ± 0.0	1.8 ± 0.12	2357.1 ± 162.3	58.0 ± 6.3	47.6 ± 1.3
MC	69.3 ± 8.7	2.1 ± 0.6	34.3 ± 2.9	3.8 ± 0.3	99.7 ± 0.0	1.7 ± 0.1	2933.0 ± 201.7	78.3 ± 5.3	53.9 ± 3.3

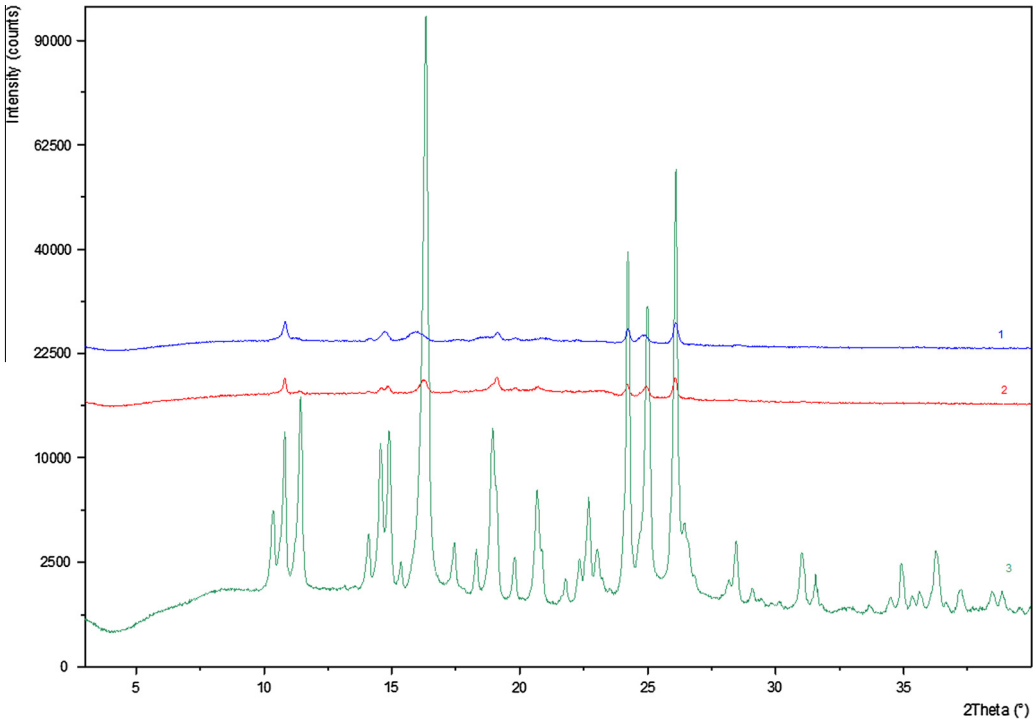

Fig. 1. X-ray diffractographs of spray dried melatonin-loaded chitosan microspheres (1), chitosan/Pluronic® F127 microspheres (2) and crystalline melatonin (3).

tonin in spray dried systems was identified by diffraction peaks at 10.8°, 14.9°, 16.3°, 18.9°, 24.2°, 25.0° and 26.1° 2θ.

Thermal analyses were employed in order to determine behaviour and possible interactions between drug and polymers. Fig. 2 presents the thermographs of the melatonin and melatonin-loaded microspheres. The thermograph of crystalline drug is characterized by an endothermic peak appearing at the midpoint temperature of 117.88 °C and was attributed to the melting point (T_m). Compared to the pure crystalline melatonin, shift of the melting point from 117.88 °C to 110.48 °C is detected, which indicates an interaction of the drug with polymers. The heat of fusion of melatonin in particles decreased compared to the pure drug indicating occurrence of partially amorphous melatonin due to the spray-drying process. Diminution of enthalpy is more prominent in chitosan/Pluronic® F127 than in chitosan microspheres. In case of MCP, the heat of fusion decreased from 140.2 J/g for the pure drug to 8.637 J/g which implies that about 80% of melatonin in MCP is amorphous. In case of MC microspheres the heat of fusion decreased to 30.43 J/g which corresponds to about 35% of amorphous melatonin. Shift in Pluronic® F127 melting peak can also be observed (from 56.23 °C to 47.09 °C), which suggests polymers interaction within the microspheres.

3.4. Swelling studies

Rapid hydrogel formation is a crucial characteristic for dry powders intended be applied to the open wound with excessive exudate production. Chitosan based microspheres are known for their ability to swell in the aqueous medium. However, the kinetics of the swelling process was shown to be dependent on the microsphere preparation method as well as on the type of chitosan and swelling medium used [40].

Swelling behaviour of MC and MCP microspheres was determined in SWF media with two pH values: physiologically relevant pH 7.4 and pH 6.3 that has been measured in the bacterial broth. Since the wound temperature is one of the critical factors of healing process, swelling behaviour was evaluated at 32 °C and 37 °C. Dermal surface temperature is lower than the body temperature and in wound bed it can be even lower than 32 °C. Wound temperature highly depends on vascular network and influences the healing process. Several studies have demonstrated that 33 °C is the minimal temperature required for normal cellular activity [41]. Also, elevated wound bed temperature (about 36 °C) is one of the signs of the infection [42], which is a condition relevant for our study. There was no significant difference in the swelling profiles evaluated at 32 °C and 37 °C.

SWF uptake of MC and MCP powder formulations at 37 °C is shown in Fig. 3. In both tested media (pH 6.3 and 7.4) swelling of powders followed a second order kinetics (Table 5, $R^2 \geqslant 0.99$ for all samples), as it has already been reported for various types of chitosan hydrogels [43]. The Korsmeyer-Peppas diffusion exponents ranging from 0.23 to 0.45 were obtained (Table 5). This indicates that diffusion of SWF to the microspheres follows a Fickian diffusion mechanism. At pH 7.4, MC absorbed higher volume of SWF (53.9 ± 3.3 μL/mg) than MCP (47.6 ± 1.3 μL/mg). However, when swelling ability was expressed as the volume of absorbed

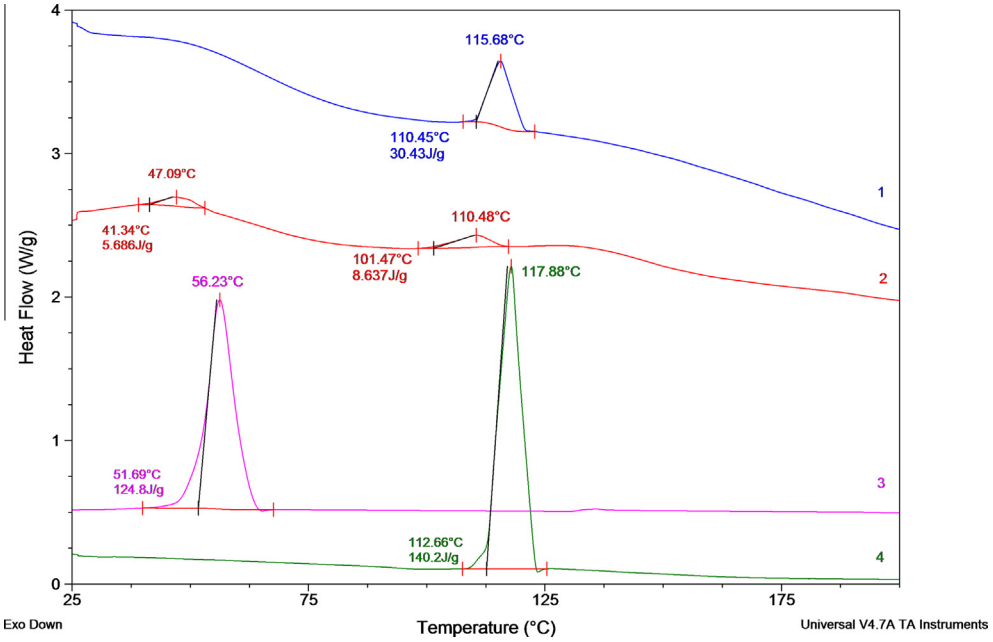

Fig. 2. DSC thermographs of melatonin-loaded chitosan microspheres (1), chitosan/Pluronic® F127 microspheres (2), Pluronic® F127 (3) and melatonin (4).

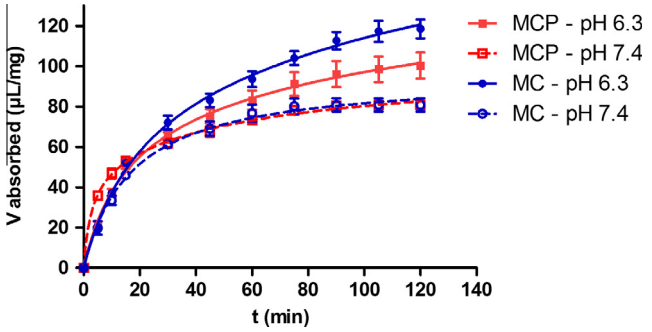

Fig. 3. Simulated wound fluid pH 7.4 and pH 6.3 uptake profiles of chitosan (MC) and chitosan/Pluronic® F127 (MCP) melatonin-loaded microspheres expressed as the volume of absorbed SWF per milligram of chitosan at 37 °C (mean values ± S.D, n = 3).

Table 5
Determination coefficients (R^2) for Zero, First, Second order and Higuchi models for MCP and MC swelling profiles in SWF pH 6.3 and 7.4 media and corresponding values of Korsmeyer-Peppas diffusion exponents (n_s). Bold values represent the highest R^2.

Kinetic model	pH 6.3		pH 7.4	
	MCP	MC	MCP	MC
	R^2			
Zero order	0.9166	0.8904	0.9140	0.8836
First order	0.9106	0.9722	0.9217	0.9419
Second order	**0.9952**	**0.9974**	**0.9976**	**0.9972**
Higuchi	0.9734	0.9621	0.9583	0.9679
Korsmeyer-Peppas	$n_s = 0.4548$	$n_s = 0.3843$	$n_s = 0.2280$	$n_s = 0.3432$

SWF per milligram of chitosan, no difference between MCP and MC was observed (80.9 *vs.* 80.7 µL/mg, respectively) indicating that the relative difference between absorbed water corresponds to the content of chitosan in different spray-dried systems.

Greater SWF uptake was observed at pH 6.3 due to the protonation of the chitosan free amine groups (58.0 ± 6.3 and 78.3 ± 5.3 µL/mg for MCP and MC, respectively). It was observed that at pH 6.3 MC absorb higher amount of SWF per milligram of chitosan (117.4 µL/mg) in comparison with MCP (98.5 µL/mg) indicating that Pluronic® F127 influenced swelling ability of chitosan in slightly acidic medium. DSC analysis had shown existence of polymer interactions, so it may be assumed that ion-dipole binding between positively charged chitosan amine groups and electro-negative oxygen of polyethers occurred, providing control over polymer matrix swelling extent [44].

3.5. Water vapour transmission rate and evaporative water loss

Wound dressing must be able to control the water loss from a wound at optimal rate. It has been recommended that rate of 2000–2500 g/m^2/day would provide adequate level of moisture without risking wound dehydration [18,45]. Hydrogel formed from MCP microspheres with SWF pH 6.3 and 7.4 has ideal WVTR of 2357.1 ± 162.3 g m^{-2} day^{-1} and 2421.5 ± 102.8 g m^{-2} day^{-1}, respectively (Table 4) that provides a proper fluid balance on the wound bed, which can facilitate cellular migration and enhance epithelization. MC hydrogel showed a value of 2933.0 ± 201.7 g m^{-2} day^{-1} for pH 6.3 and 2995.4 ± 183.6 g m^{-2} day^{-1} for pH 7.4 SWF hydrogel, which is close to optimal range as well.

The extent of water loss from the hydrogel on exposure to the air was evaluated to examine its behaviour when used as a dressing over a wound with less exudate. As shown in Fig. 4, the loss of water was approximately 10% after 60 min and within 5 h it reached 60%. After 10 h, water from the samples completely drained out. The highest rate of water loss was shown by MCP hydrogel prepared with SWF pH 7.4 ($t_{50\%} \sim 3$ h), while SWF pH 6.3 MCP gel had lower rate of water loss ($t_{50\%} \sim 4.2$ h). MC hydrogels showed slightly lower water loss rate which is in accordance with observed higher amount of fluid uptake during the swelling process. There was no difference in water loss between MC hydrogels prepared with SWF pH 6.3 ($t_{50\%} \sim 4.6$ h) and pH 7.4 ($t_{50\%} \sim 4.4$ h). It is clear that the material will lose its water content when exposed to the air under dry conditions during the short period. Thus, these dressings may be more advantageous to wounds with more exudates. Water loss may enable dressing to

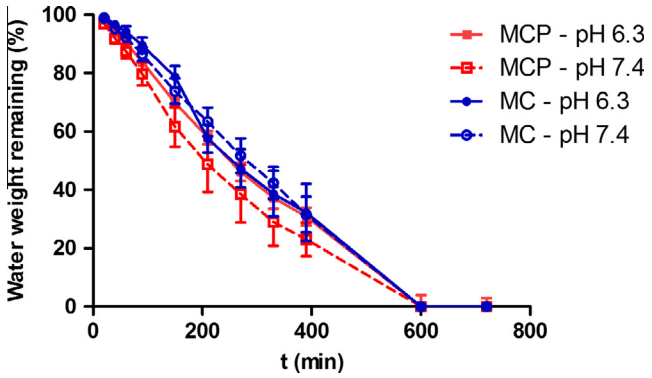

Fig. 4. Evaporative water loss from hydrogels prepared from melatonin-loaded chitosan (MC) and chitosan/Pluronic® F127 (MCP) microspheres (mean values ± S.D, n = 3).

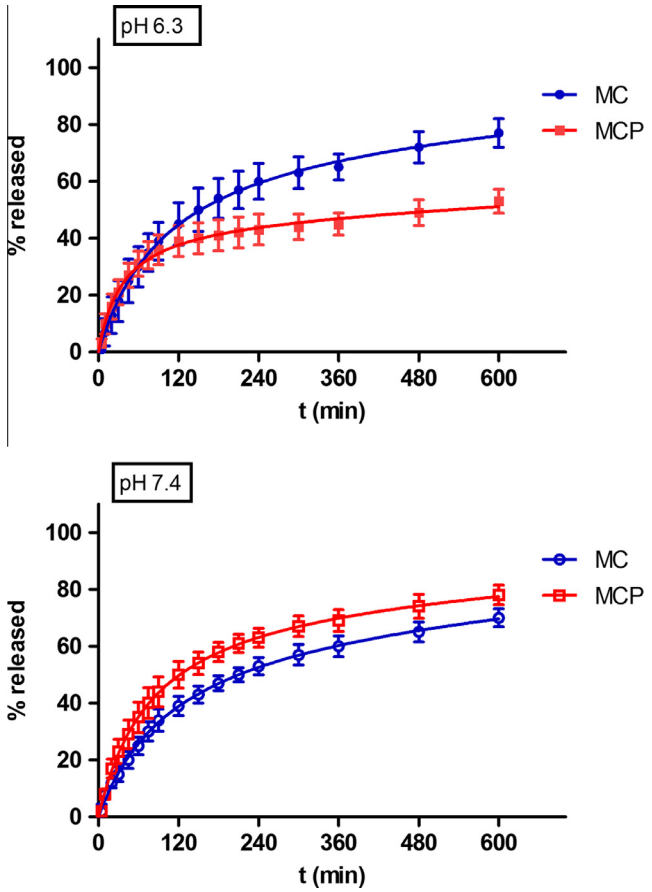

Fig. 5. The release profiles of melatonin from the chitosan (MC) and chitosan/Pluronic® F127 (MCP) microspheres in the phosphate buffer pH 7.4 and pH 6.3 at 37 °C (mean values ± S.D., n = 3).

take up exudate and oedema fluid from the wound by an active upward-directed process when used in exuding wounds.

3.6. In vitro drug release

In vitro drug release studies were performed at 32 °C and 37 °C, and similarly to swelling studies there was no significant difference in the release profiles evaluated at two depicted temperatures. The results of *in vitro* melatonin release from MCP and MC in phosphate buffer (pH 6.3 and 7.4) at 37 °C are shown in Fig. 5. In all cases, a biphasic release profile of the drug was observed: the initial rapid release (within first two hours) followed by a slower phase of release. This mode of release could be useful in prevention of infection occurrence and spreading at the beginning of a local therapy.

Melatonin release was shown to be dependent on both, the pH of the release medium and microsphere matrix composition. Thus, at pH 7.4, melatonin release profiles from MCP and MC were similar (in 10 h 70 and 78% of melatonin entrapped was released from MC and MCP, respectively) with higher release rate observed for MCP (for MC and MCP $t_{50\%}$ was about 3.5 and 2 h, respectively). This phenomenon could be explained by faster dissolving of amorphous melatonin which is (as confirmed by DSC analysis) in higher amount present in MCP than in MC. At pH 6.3, the initial release of melatonin from MCP was similar to MC. However, after the completion of the swelling process, melatonin release from MCP was significantly slower ($t_{50\%} \sim 8$ h) than from MC ($t_{50\%} \sim 2.5$ h). This observation can be explained by the fact that, due to its positive charge in slightly acidic media, chitosan could electrostatically interact with electronegative oxygen atoms of poly(ethylene oxide) segments of Pluronic® F127 and might produce gel with improved mechanical properties and slower drug release rate [46,47].

The diffusion of melatonin through the membrane from melatonin aqueous solution was significantly faster ($t_{50\%} \sim 1$ h) than for the investigated microspheres (data not shown). Therefore, melatonin release from microspheres was the rate-limiting factor that determined the release profile obtained for MCP and MC.

Table 6 shows that the best-fit release kinetic data with the highest values of determination coefficients were shown by Higuchi model ($R^2 \geqslant 0.99$ for all samples), as previously reported for chitosan spray-dried systems [48]. The release mechanism of the melatonin from MCP and MC samples indicates non-Fickian diffusion or anomalous transport, with release controlled by diffusion

Table 6
Determination coefficients (R^2) for Zero, First order and Higuchi models for MCP and MC drug release profiles in SWF pH 6.3 and 7.4 media and corresponding values of Korsmeyer-Peppas diffusion exponents (n_c). Bold values represent the highest R^2.

Kinetic model	pH 6.3		pH 7.4	
	MCP	MC	MCP	MC
	R^2			
Zero order	0.6850	0.9351	0.8452	0.8852
First order	0.7377	0.9283	0.9379	0.9381
Higuchi	**0.9918**	**0.9987**	**0.9952**	**0.9918**
Korsmeyer-Peppas	$n_c = 0.3931$	$n_c = 0.6022$	$n_c = 0.5644$	$n_c = 0.5905$

Table 7
Antimicrobial activity of melatonin-loaded and melatonin-free chitosan/Pluronic® F127 and chitosan microspheres against planktonic *S. aureus*.

Strains	MIC of mupirocin (μg/mL)[a]	MIC (mg/mL)[b]					
		MCP	MC	CP	C	Melatonin	P
ATCC 29213	0.125	0.125	0.250	0.250	0.250	>1	>1
MRSA strains	0.125 0.156 (MFBF 10677)	0.250	0.250	0.250	0.250	>1	>1

DMSO as vehicle control was applied at 2.5% v/v which was shown not to alter bacterial viability, while MHB without DMSO and antimicrobials was bacterial growth control.

[a] Mupirocin served as positive control.

[b] Minimal inhibitory concentration (MIC) was expressed as the (relevant) concentration of melatonin in the system.

Table 8
Antimicrobial activity of melatonin-loaded chitosan/Pluronic® F127 microspheres against *S. aureus* biofilm.

Strains	Inhibition of biofilm formation MCP (mg/mL)[a]				Biofilm eradication MCP (mg/mL)[a]			
	MBIC	Viability (%)			MBEC	Viability (%)		
		20	50[b]	100		20	50[b]	100
ATCC 29213	0.67	0.34	0.17	0.08	2.7	1.35	0.9	0.67
MRSA 101	1.35	–	–	0.34	2.7	1.35	0.9	0.67
MRSA 124-177	1.35	–	–	0.67	2.7	1.35	0.9	0.67

[a] Refers to (relevant) concentration of melatonin in the system.
[b] To calculate the viability of 50% (IC_{50}) non-linear dose-response fitting was applied using Eq. (13).

and swelling (n_c = 0.5644–0.6022). For an anomalous mechanism the coupling between molecular transport and stress relaxation during swelling causes deviations with respect to Fickian mechanism. However, melatonin release mechanism from MCP sample in pH 6.3 buffer indicates the predominance of diffusion (n_c = 0.3931). This observation is in accordance with observed MCP lower SWF uptake at pH 6.3 (Fig. 3).

3.7. Antimicrobial activity against planktonic bacteria and biofilm of *S. aureus*

Results of antimicrobial activity of melatonin-loaded chitosan and chitosan/Pluronic® F127 microspheres and all relevant controls are presented in Table 7. Minimal inhibitory concentration was expressed as the (relevant) concentration of melatonin in the system.

All microspheres showed the same antimicrobial activity against tested MRSA strains (MIC = 0.250 mg/mL), regardless the presence or absence of melatonin and/or Pluronic® F127 in the microsphere matrix. However, MCP microspheres showed the strongest antimicrobial activity against planktonic *S. aureus* ATCC 29213 resulting in MIC (0.125 mg/mL) twice as lower than all other microsphere formulations (0.250 mg/mL). As melatonin and Pluronic® F127 used alone exert no antibacterial activity on *S. aureus* strains, it seems that melatonin and Pluronic® F127 together potentiated antimicrobial activity of chitosan. Comparing to MICs of mupirocin (positive control) tested antimicrobials showed three orders of magnitude lower antimicrobial activity. Antimicrobial activity of mupirocin against planktonic *staphylococci* used in this study is in line with results reported by Kifer et al. [26].

In the literature, MICs of chitosan have been reported to range from 0.1 to 10.0 mg/mL against Gram-negative bacteria and from 0.1 to 1.25 mg/mL against Gram-positive bacteria [49]. It is very hard to compare antibacterial activity of chitosan demonstrated in different studies since it depends on numerous factors such as the bacterial strain, chitosan molecular weight, degree of deacetylation, pH, temperature, and composition of the medium [50–54]. However, in this study, the concentration of chitosan in the systems in which inhibition of bacterial growth was observed was relatively low (twice as high as melatonin concentration, namely 0.25 and 0.5 mg/mL for ATCC and resistant MRSA strains, respectively) which could be partially due to pH of broth with planktonic bacteria below pK_a of chitosan (pH about 6.3). Although chitosan has been confirmed as an attractive biomacromolecule with relevant

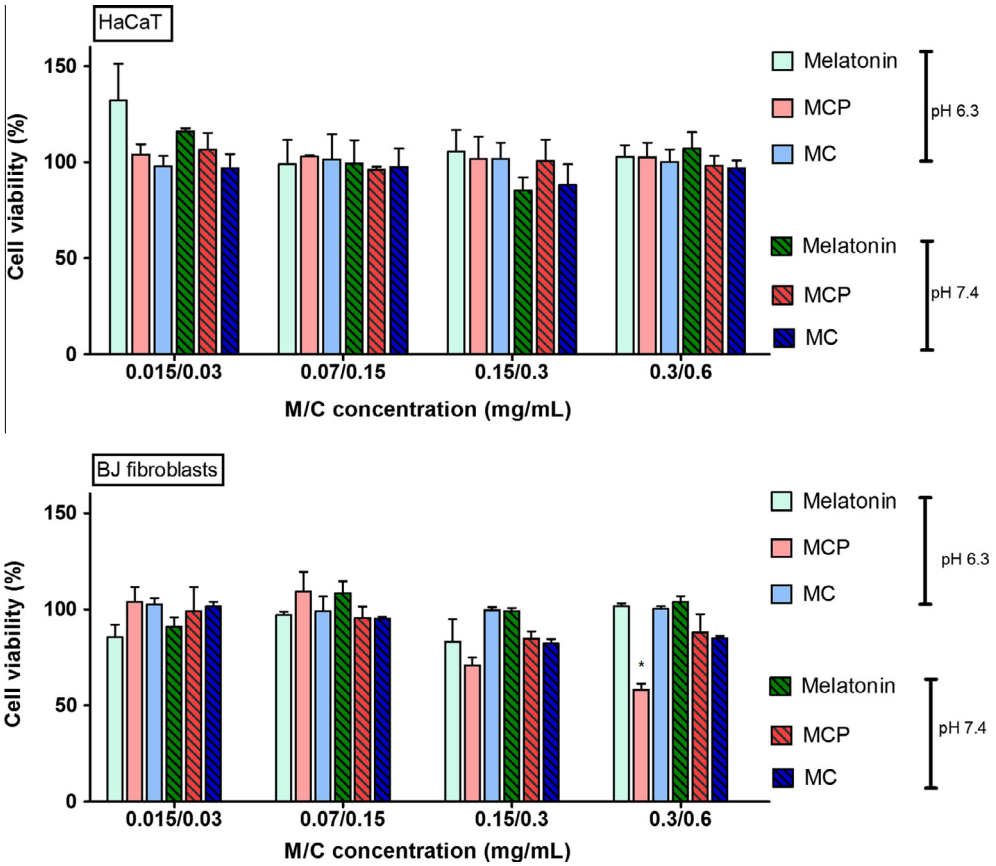

Fig. 6. Keratinocytes (HaCaT) and fibroblasts (BJ) viability (%) determined by MTT after 2 h of incubation at 37 °C with melatonin solution (Melatonin), melatonin-loaded chitosan/Pluronic® F127 (MCP) and chitosan (MC) microspheres resuspended in HBSS buffer pH 6.3 and pH 7.4 (mean values ± S.D, n = 3). *Cell viability below 70%.

antimicrobial properties, being a week base its application is sometimes limited due to low water-solubility. However, in case of saccharolytic bacteria, chitosan pH-dependent solubility/net charge is advantageous as decrease in microenvironmental pH owing to their metabolic activity can serve as a trigger for chitosan antimicrobial activity [55,56]. It is well known that all bacterial pathogens require iron to replicate and infect their human hosts [57]. Pathogens have developed efficient mechanisms to enable them to acquire iron in the highly iron-restricted environment of the host's tissues and body fluids. In case of *S. aureus*, it has been demonstrated that under conditions of iron starvation, a redirection of the central metabolic pathways occurs, causing the bacteria to produce large amounts of acidic end products. Lowering of the local microenvironment pH facilitates the release of iron from host iron-binding proteins and increases the availability of nutrient iron [58]. The idea of synergistic antimicrobial effect of melatonin and chitosan is based on these findings, as melatonin intracellular chelation of iron [12,59] could contribute to the lowering of pH in the bacteria microenvironment and promote subsequent increase in chitosan charge density and antimicrobial activity.

Tekbas et al. [10] reported on antibacterial activity of melatonin against *S. aureus* ATCC 29213 with MIC concentration of 0.25 mg/mL. In twofold serial dilution experiment authors used melatonin dissolved in DMSO (99.9%) in concentration of 2 mg/mL because melatonin is weakly soluble in water. In our experiment melatonin was successfully dissolved in MHB broth supplemented with 5% DMSO but melatonin didn't show antimicrobial activity, not even at highest concentration (1 mg/mL, 2.5% DMSO in solution). Next, we dissolved melatonin in the same manner as it was described by Tekbas et al. [10] and treated *S. aureus* in concentrations ranging from 0.008 mg/mL to 1 mg/mL. The MIC was recorded at 0.5 mg/mL of melatonin in MHB supplemented with DMSO (12.5%) as well as for DMSO (12.5%) in MHB used as control, but not for any lower applied concentrations of melatonin.

Potentiating effect of melatonin on antimicrobial activity of chitosan in the presence of Pluronic® F127 observed in this study could be attributed to the improved melatonin solubility. As shown by thermal analyses, Pluronic® F127 promoted melatonin amorphization during spray-drying process (Fig. 2). Even though entrapment of melatonin in chitosan/Pluronic® F127 microspheres promoted chitosan antibacterial activity only against ATCC strain, results obtained are significant. Developing new systems with improved and non-specific mechanism of antibacterial activity lowers the chance for resistance development.

All microspheres inhibited biofilm formation of tested MRSA strains and resulted in the same MBIC values (1.35 mg/mL). However, MCP microspheres showed the strongest inhibitory effect on biofilm formation of *S. aureus* ATCC 29213 resulting in MBIC (0.67 mg/mL) twice as lower than all other microsphere formulations (1.35 mg/mL), suggesting that melatonin and Pluronic® F127 potentiated the effect of chitosan biofilm inhibitory effect (Table 8). In addition, only MCP microspheres exerted stronger activity on *S. aureus* ATCC 29213 at melatonin concentration 0.34 mg/mL, which was recorded as 80% inhibition of biofilm formation. As it was expected, either melatonin or Pluronic® F127 applied alone did not show any antibiofilm activity (data not shown).

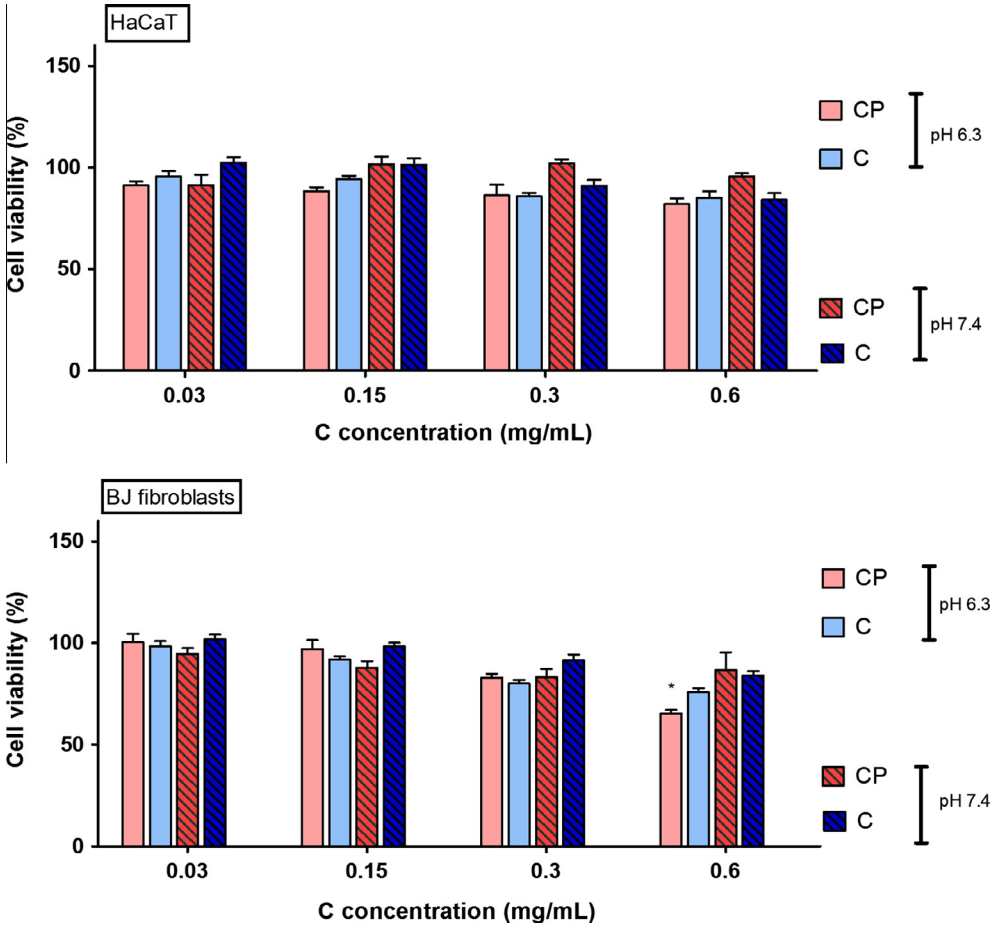

Fig. 7. Keratinocytes (HaCaT) and fibroblasts (BJ) viability (%) determined by LDH after 2 h of incubation on 37 °C with chitosan/Pluronic® F127 (CP) and chitosan (C) microspheres resuspended in HBSS buffer pH 6.3 and pH 7.4 (mean values ± S.D, n = 3). *Cell viability below 70%.

The MBEC value of MCP microspheres was 2.7 mg/mL in all tested strains of *S. aureus*. MC microspheres at melatonin concentrations of 2.7 and 1.35 mg/mL only reduced viability of ATCC and MRSA strains for about 20–30%, while blank chitosan/Pluronic® F127 (CP) and chitosan (C) microspheres, as well as melatonin and Pluronic® F127 applied alone, had no biofilm eliminating effect. These results suggested that chitosan made *S. aureus* biofilms susceptible to melatonin and confirmed that the best antimicrobial effects were achieved when both, melatonin and Pluronic® F127 were incorporated in the microsphere matrix. Similarly, Zhang et al. [60] have studied the effect of chitosan, streptomycin, chitosan-streptomycin conjugate and physical mixture against *S. aureus* preformed biofilms and have shown more pronounced effect of conjugate and physical mixture than streptomycin or chitosan alone on biofilm mass and cell viability [60]. They highlighted that the polycationic property enabled chitosan as an efficient Trojan horse to deliver streptomycin into preformed biofilms.

3.8. Cytotoxicity study

The biocompatibility of MCP and MC microspheres with human keratinocyte HaCaT and BJ fibroblasts was assessed by monitoring cell metabolic activity (MTT assay) and membrane integrity (LDH assay). The membrane integrity was tested for blank microspheres only, due to possible interaction of melatonin with LDH test because of its antioxidant activity. The effect on cell metabolic activity and membrane integrity was tested in concentration range relevant to determined antimicrobial activity against planktonic bacteria. Tested microsphere concentrations were in range (expressed as the melatonin concentration in the system) from 0.015 mg/mL to 0.29 mg/mL. Cells were treated for 2 h with MCP, MC, CP and C microspheres resuspended in pH 6.3 and pH 7.4 HBSS buffer. According to the guideline for determination of *in vitro* cytotoxicity of medical devices [61], materials are considered non-toxic if the viability of cells is $\geqslant$70% after exposure. The results of the cytotoxicity assays (MTT test, Fig. 6; and LDH assay, Fig. 7) indicate that tested chitosan based microspheres were well tolerated by keratinocytes and fibroblasts. Only in case of MCP at pH 6.3 and highest concentration tested, cell viability of fibroblasts, known to be more sensitive *in vitro*, marginally decreased below 70%. Chitosan is well-known biocompatible material for various types of cells related to wound healing process [62]. It was demonstrated that chitosans with relatively high degrees of deacetylation strongly stimulate fibroblast proliferation, while human keratinocyte mitogenesis is concentration depended [63]. Pluronic® F127 has also shown biocompatibility and potential to stimulate wound healing when applied topically as gel [64,65]. Melatonin protective effect on irradiated human keratinocytes and fibroblasts has been reported [66], although findings regarding melatonin effect on wound healing are controversy [67,68]. When applied topically, melatonin displays antioxidant, antiapoptotic, and p53-inhibitory effects [69] and exerts positive effects on wound healing [70].

4. Conclusion

In this study, QbD approach was successfully employed to produce fine-tuned melatonin-loaded chitosan based microspheres in terms of characteristics related to process applicability and microsphere performance in biological environment. Entrapment of melatonin in chitosan/Pluronic® F127 microspheres potentiated chitosan antimicrobial activity against *S. aureus* and five clinical isolates *S. aureus* MRSA strains. Developed wound dressing has shown the potential to improve wound management especially in cases of excessive exudate production as it rapidly forms hydrogel in contact with simulated wound fluid and provides optimal water vapour transmission rate. Described dual activity of developed wound dressing is beneficial since excessive wound exudation can be indicative of underlying bacterial infection.

References

[1] R.A.A. Muzzarelli, Chitins and chitosans for the repair of wounded skin, nerve, cartilage and bone, Carbohyd. Polym. 76 (2) (2009) 167–182.
[2] F. De Cicco et al., In situ forming antibacterial dextran blend hydrogel for wound dressing: SAA technology vs. spray drying, Carbohyd. Polym. 101 (2014) 1216–1224.
[3] R.P. Aquino et al., Design and production of gentamicin/dextrans microparticles by supercritical assisted atomisation for the treatment of wound bacterial infections, Int. J. Pharm. 440 (2) (2013) 188–194.
[4] J.W. Costerton, P.S. Stewart, E.P. Greenberg, Bacterial biofilms: a common cause of persistent infections, Science 284 (5418) (1999) 1318–1322.
[5] A.J. Huh, Y.J. Kwon, "Nanoantibiotics": a new paradigm for treating infectious diseases using nanomaterials in the antibiotics resistant era, J. Control. Release 156 (2) (2011) 128–145.
[6] K. Forier et al., Lipid and polymer nanoparticles for drug delivery to bacterial biofilms, J. Control. Release 190 (2014) 607–623.
[7] R.Y. Pelgrift, A.J. Friedman, Nanotechnology as a therapeutic tool to combat microbial resistance, Adv. Drug Deliv. Rev. 65 (13–14) (2013) 1803–1815.
[8] R.J. Reiter et al., Chapter 8 – Melatonin: A Multitasking Molecule, in: Progress in Brain Research, Elsevier, 2010, pp. 127–151.
[9] M. Gomez-Florit, J.M. Ramis, M. Monjo, Anti-fibrotic and anti-inflammatory properties of melatonin on human gingival fibroblasts in vitro, Biochem. Pharmacol. 86 (12) (2013) 1784–1790.
[10] O.F. Tekbas et al., Melatonin as an antibiotic: new insights into the actions of this ubiquitous molecule, J. Pineal Res. 44 (2) (2008) 222–226.
[11] V. Srinivasan, M. Mohamed, H. Kato, Melatonin in bacterial and viral infections with focus on sepsis: a review, Recent Pat. Endocr. Metab. Immune Drug Discov. 6 (1) (2012) 30–39.
[12] I. Gulcin, M.E. Buyukokuroglu, O.I. Kufrevioglu, Metal chelating and hydrogen peroxide scavenging effects of melatonin, J. Pineal Res. 34 (4) (2003) 278–281.
[13] D. Jacek, Wound healing and the effect of pineal gland and melatonin, J. Exp. Integr. Med. 2 (1) (2012) 3–14.
[14] A.S. Sahib, F.H. Al-Jawad, A.A. Al-Kaisy, Burns, endothelial dysfunction, and oxidative stress: the role of antioxidants, Ann. Burns Fire Disast. 22 (1) (2009) 6–11.
[15] A.S. Sahib, F.H. Al-Jawad, A.A. Alkaisy, Effect of antioxidants on the incidence of wound infection in burn patients, Ann. Burns Fire Disast. 23 (4) (2010) 199–205.
[16] R.C. Goy, D.d. Britto, O.B.G. Assis, A review of the antimicrobial activity of chitosan, Polymeros 19 (2009) 241–247.
[17] R.M. Nalbandian et al., Pluronic F-127 gel preparation as an artificial skin in the treatment of third-degree burns in pigs, J. Biomed. Mater. Res. 21 (9) (1987) 1135–1148.
[18] I.Y. Kim et al., Evaluation of semi-interpenetrating polymer networks composed of chitosan and poloxamer for wound dressing application, Int. J. Pharm. 341 (1–2) (2007) 35–43.
[19] L. Tajber et al., Spray drying of budesonide, formoterol fumarate and their composites—I. Physicochemical characterisation, Int. J. Pharm. 367 (1–2) (2009) 79–85.
[20] F. Sansone et al., Physical characteristics and aerosol performance of naringin dry powders for pulmonary delivery prepared by spray-drying, Eur. J. Pharm. Biopharm. 72 (1) (2009) 206–213.
[21] P.G. Bowler et al., Multidrug-resistant organisms, wounds and topical antimicrobial protection, Int. Wound J. 9 (4) (2012) 387–396.
[22] T. Higuchi, Mechanism of sustained-action medication. Theoretical analysis of rate of release of solid drugs dispersed in solid matrices, J. Pharm. Sci. 52 (1963) 1145–1149.
[23] R.W. Korsmeyer et al., Mechanisms of potassium chloride release from compressed, hydrophilic, polymeric matrices: effect of entrapped air, J. Pharm. Sci. 72 (10) (1983) 1189–1191.
[24] NCCLS, Methods for Dilution Antimicrobial Susceptibility Tests for Bacteria that Grow Aerobically: Approved Standard, Wayne, PA, fifth ed., vol. M07–A5, 2001.
[25] A. Klančnik et al., Evaluation of diffusion and dilution methods to determine the antibacterial activity of plant extracts, J. Microbiol. Methods 81 (2) (2010) 121–126.
[26] D. Kifer, V. Muzinic, M. Segvic Klaric, Antimicrobial potency of single and combined mupirocin and monoterpenes, thymol, menthol and 1,8-cineole against *Staphylococcus aureus* planktonic and biofilm growth, J. Antibiot. (2016) 1–8.
[27] P. Giunchedi et al., Formulation and in vivo evaluation of chlorhexidine buccal tablets prepared using drug-loaded chitosan microspheres, Eur. J. Pharm. Biopharm. 53 (2) (2002) 233–239.
[28] P. Lebrun et al., Design space approach in the optimization of the spray-drying process, Eur. J. Pharm. Biopharm. 80 (1) (2012) 226–234.
[29] A.M. Telang, B.N. Thorat, Optimization of process parameters for spray drying of fermented soy milk, Dry Technol. 28 (12) (2010) 1445–1456.

[30] S.P. Tan et al., Effects of the spray-drying temperatures on the physiochemical properties of an encapsulated bitter melon aqueous extract powder, Powder Technol. 281 (2015) 65–75.
[31] S. Kumar, R. Gokhale, D.J. Burgess, Quality by design approach to spray drying processing of crystalline nanosuspensions, Int. J. Pharm. 464 (1–2) (2014) 234–242.
[32] R. Lin, L. Shi Ng, C.H. Wang, In vitro study of anticancer drug doxorubicin in PLGA-based microparticles, Biomaterials 26 (21) (2005) 4476–4485.
[33] Y.C. Huang, C.H. Chiang, M.K. Yeh, Optimizing formulation factors in preparing chitosan microparticles by spray-drying method, J. Microencapsul. 20 (2) (2003) 247–260.
[34] A. Martinac et al., Development and bioadhesive properties of chitosan-ethylcellulose microspheres for nasal delivery, Int. J. Pharm. 291 (1–2) (2005) 69–77.
[35] M.F. Cervera et al., Effects of spray drying on physicochemical properties of chitosan acid salts, AAPS PharmSciTech 12 (2) (2011) 637–649.
[36] T.P. Learoyd et al., Chitosan-based spray-dried respirable powders for sustained delivery of terbutaline sulfate, Eur. J. Pharm. Biopharm. 68 (2) (2008) 224–234.
[37] K. Ståhl et al., The effect of process variables on the degradation and physical properties of spray dried insulin intended for inhalation, Int. J. Pharm. 233 (1–2) (2002) 227–237.
[38] J. Nunthanid et al., Characterization of chitosan acetate as a binder for sustained release tablets, J. Control. Release 99 (1) (2004) 15–26.
[39] J. Nunthanid et al., Development of time-, pH-, and enzyme-controlled colonic drug delivery using spray-dried chitosan acetate and hydroxypropyl methylcellulose, Eur. J. Pharm. Biopharm. 68 (2) (2008) 253–259.
[40] A. Martinac et al., Spray-dried chitosan/ethylcellulose microspheres for nasal drug delivery: swelling study and evaluation of in vitro drug release properties, J. Microencapsul. 22 (5) (2005) 549–561.
[41] V. Dini et al., Correlation between wound temperature obtained with an infrared camera and clinical wound bed score in venous leg ulcers, Wounds 27 (10) (2015) 274–278.
[42] M. Fierheller, R.G. Sibbald, A clinical investigation into the relationship between increased periwound skin temperature and local wound infection in patients with chronic leg ulcers, Adv. Skin Wound Care 23 (8) (2010) 369–379. quiz 380–1.
[43] A. Pourjavadi, G.R. Mahdavinia, Superabsorbency, pH-sensitivity and swelling kinetics of partially hydrolyzed chitosan-g-poly(acrylamide)hydrogels, Turk. J. Chem. 30 (2006) 595–608.
[44] P. Calvo et al., Chitosan and chitosan/ethylene oxide-propylene oxide block copolymer nanoparticles as novel carriers for proteins and vaccines, Pharm. Res. 14 (10) (1997) 1431–1436.
[45] D. Queen et al., The preclinical evaluation of the water vapour transmission rate through burn wound dressings, Biomaterials 8 (5) (1987) 367–371.
[46] T. Gratieri et al., Enhancing and sustaining the topical ocular delivery of fluconazole using chitosan solution and poloxamer/chitosan in situ forming gel, Eur. J. Pharm. Biopharm. 79 (2) (2011) 320–327.
[47] I. Pepic, J. Filipovic-Grcic, I. Jalsenjak, Bulk properties of nonionic surfactant and chitosan mixtures, Colloids Surfaces A: Physicochem. Eng. Aspects 336 (1–3) (2009) 135–141.
[48] C. Liu et al., Drug release kinetics of spray-dried chitosan microspheres, Dry. Technol. 24 (2006) 769–776.
[49] Y. Tao, L.-H. Qian, J. Xie, Effect of chitosan on membrane permeability and cell morphology of *Pseudomonas aeruginosa* and *Staphyloccocus aureus*, Carbohyd. Polym. 86 (2) (2011) 969–974.
[50] Y.-L. Chen, C.-C. Chou, Factors affecting the susceptibility of *Staphylococcus aureus* CCRC 12657 to water soluble lactose chitosan derivative, Food Microbiol. 22 (1) (2005) 29–35.
[51] Y.C. Chung et al., Effect of abiotic factors on the antibacterial activity of chitosan against waterborne pathogens, Bioresour. Technol. 88 (3) (2003) 179–184.
[52] C. Qin et al., Water-solubility of chitosan and its antimicrobial activity, Carbohyd. Polym. 63 (3) (2006) 367–374.
[53] R. Muzzarelli et al., Antimicrobial properties of N-carboxybutyl chitosan, Antimicrob. Agents Chemother. 34 (10) (1990) 2019–2023.
[54] H.K. No et al., Antibacterial activity of chitosans and chitosan oligomers with different molecular weights, Int. J. Food Microbiol. 74 (1–2) (2002) 65–72.
[55] H. Liu et al., Chitosan kills bacteria through cell membrane damage, Int. J. Food Microbiol. 95 (2) (2004) 147–155.
[56] T. Dai et al., Chitosan preparations for wounds and burns: antimicrobial and wound-healing effects, Expert Rev. Anti Infect. Ther. 9 (7) (2011) 857–879.
[57] E.P. Skaar, The battle for iron between bacterial pathogens and their vertebrate hosts, PLoS Pathog. 6 (8) (2010) e1000949.
[58] D.B. Friedman et al., Staphylococcus aureus redirects central metabolism to increase iron availability, PLoS Pathog. 2 (8) (2006) e87.
[59] T.M. Jasim, M.G. Alabbassi, S.F.H. Almuqdadi, J.K. Kamel, Anti-bacterial properties of melatonin against mycobacterium tuberculosis in vitro, Iraqi J. Pharm. Sci. 19 (2) (2010) 59–63.
[60] A. Zhang et al., Chitosan coupling makes microbial biofilms susceptible to antibiotics, Sci. Rep. 3 (2013) 3364.
[61] ISO10993-5, Biological Evaluation of Medical Devices-Part 5: Tests for Cytotoxicity: In Vitro Methods, 1992.
[62] K. Azuma et al., Chitin, chitosan, and its derivatives for wound healing: old and new materials, J. Funct. Biomater. 6 (1) (2015) 104–142.
[63] G.I. Howling et al., The effect of chitin and chitosan on the proliferation of human skin fibroblasts and keratinocytes in vitro, Biomaterials 22 (22) (2001) 2959–2966.
[64] V. Kant et al., Topical pluronic F-127 gel application enhances cutaneous wound healing in rats, Acta Histochem. 116 (1) (2013) 5–13.
[65] S. Demirci et al., Boron and poloxamer (F68 and F127) containing hydrogel formulation for burn wound healing, Biol. Trace Elem. Res. (2015).
[66] I. Izykowska et al., Effect of melatonin on human keratinocytes and fibroblasts subjected to UVA and UVB radiation in vitro, In Vivo 23 (5) (2009) 739–745.
[67] G. Soybir et al., The effects of melatonin on angiogenesis and wound healing, Surg. Today 33 (12) (2003) 896–901.
[68] N. Bulbuller et al., Effect of melatonin on wound healing in normal and pinealectomized rats, J. Surg. Res. 123 (1) (2005) 3–7.
[69] A. Şener et al., The effects of topical melatonin on oxidative stress, apoptosis signals, and p53 protein expression during cutaneous wound healing, Turk. J. Biol. 39 (2015).
[70] M. Ozler et al., Comparison of the effect of topical and systemic melatonin administration on delayed wound healing in rats that underwent pinealectomy, Scand. J. Clin. Lab. Invest. 70 (6) (2010) 447–452.

3. Melatonin loaded lipid enriched chitosan microspheres – Hybrid dressing for moderate exuding wounds

Journal of Drug Delivery Science and Technology 52 (2019) 431–439

Contents lists available at ScienceDirect

Journal of Drug Delivery Science and Technology

journal homepage: www.elsevier.com/locate/jddst

Melatonin loaded lipid enriched chitosan microspheres – Hybrid dressing for moderate exuding wounds

Marieta Duvnjak Romić[a], Drago Špoljarić[a], Maja Šegvić Klarić[b], Biserka Cetina-Čižmek[a], Jelena Filipović-Grčić[c], Anita Hafner[c,*]

[a] R&D, PLIVA Croatia Ltd, TEVA Group Member, Zagreb, Croatia
[b] University of Zagreb, Faculty of Pharmacy and Biochemistry, Department of Microbiology, Zagreb, Croatia
[c] University of Zagreb, Faculty of Pharmacy and Biochemistry, Department of Pharmaceutical Technology, Zagreb, Croatia

ARTICLE INFO

Keywords:
Melatonin
Nanoparticles
Microspheres
Chitosan
Spray-drying
Wound healing

ABSTRACT

The aim of this study was to develop nanostructured lipid carrier (NLC)-loaded chitosan-based microspheres as innovative dry powder wound dressing, with melatonin incorporated in both, NLC and chitosan matrix of the proposed hybrid system. Melatonin-loaded NLCs were prepared by a hot homogenization technique, while NLC-loaded microspheres were produced by a spray-drying method. To optimize the critical formulation and process parameters for both NLC and hybrid system, a definitive screening design was employed. NLC particle size, hybrid system production yield, particle size, moisture content, and zeta potential were investigated as responses. The optimized hybrid system was characterized by prolonged melatonin release, good flowability and appropriate extent of fluid uptake. In contact with simulated wound fluid, the hybrid system swelled, turning into a hydrogel layer. The presence of lipid nanoparticles attenuated the evaporative water loss showing the potential to provide optimal hydration for moderate exuding wounds. The hybrid system was proven to be biocompatible with skin keratinocytes and fibroblasts and moreover, showed antimicrobial activity against *Staphylococcus aureus* and *S. aureus* MRSA strain.

1. Introduction

Wound healing is a complex biological cascade which consists of multiple coordinated processes defined as hemostasis, inflammation, proliferation, and remodeling. Many internal and external factors, the infection being the most common one, can interfere with healing progress resulting in chronic and nonhealing wounds [1]. The problem of persistent wounds has significantly increased, presenting one of the biggest challenges in the healthcare system. Burn wounds are amongst the most challenging ones to manage. A burn injury causes tissue damage, leading to a significant fluid loss and providing a gateway for bacterial infection. With more than 50% of burn injury-associated deaths being caused by bacterial infections [2], appropriate burn wound management represents a crucial therapeutic objective. Growing bacterial resistance and potential biofilm formation represent a drawback in conventional antimicrobial treatments. Therefore, non-conventional approaches and advanced technologies are investigated in order to provide facilitated wound healing [3,4].

Melatonin, a pleiotropic molecule secreted by the pineal gland, is a well-known anti-inflammatory agent, free radical scavenger and stimulator of antioxidant enzymes [5]. The potential to fight bacterial [6], parasitic [7], and viral infections due to intracellular chelating activity has been reported [8]. Moreover, melatonin reduces inflammation and has been shown to promote cell proliferation and migration during the wound healing process *in vitro* [9]. When given orally as an antioxidant, melatonin has been proven to reduce the incidence of burn wound infections and shorten healing time [10]. Based on complementary antimicrobial and healing potential, melatonin is a good candidate for development of nonconventional wound dressings to improve healing and tissue regeneration.

One of the intensively investigated strategies for effective wound treatment is the development of lipid nanoparticles. In general, lipid carriers are biocompatible and biodegradable, improve skin hydration, provide controlled drug release and increase drug accumulation in the skin [11]. The latest generation of lipid nanoparticles are nanostructured lipid carriers (NLCs). NLCs are matrix nanoparticles composed of a blend of solid and liquid lipids [12], which have improved drug loading capacity and stability. NLCs are widely investigated for various topical applications [13]. In terms of wound dressings, NLCs act mainly as carriers of growth factors, providing controlled and increased

* Corresponding author. A. Kovačića 1, 10000, Zagreb, Croatia.
E-mail address: ahafner@pharma.hr (A. Hafner).

https://doi.org/10.1016/j.jddst.2019.05.004
Received 10 February 2019; Received in revised form 13 April 2019; Accepted 3 May 2019
Available online 04 May 2019
1773-2247/

drug penetration. In addition, promoted re-epithelialization was also reported [14]. In the management of burn wounds, NLCs also act as an occlusive factor helping to regulate the highly dehydrated wound bed [15]. Besides that, NLCs have been investigated as functional carriers for targeted and enhanced delivery of antimicrobial drugs [16].

Chitosan, a poly-N-acetyl-glucosaminoglycan obtained by alkaline deacetylation of chitin, is a well-known wound dressing material [17]. Depending on the molecular weight and degree of deacetylation, chitosan shows antibacterial activity by three proposed mechanisms: by interaction with bacterial DNA and cell membranes or by chelating intracellular metals [18]. Chitosan dressings are usually formulated as ready-to-use gel or film preparations [19]. When formulated as dry powder, chitosan can rapidly absorb exudate at the wound bed, forming a functional hydrogel *in situ*.

Our group has recently verified the idea of combining melatonin and chitosan in functional wound dressings by developing the fine-tuned, melatonin-loaded chitosan based microspheres with antimicrobial activity, applicable for wounds with excessive exudate production [20]. Following and expanding on our previous research, the aim of the present work was to develop NLC-loaded chitosan-based microspheres as an innovative melatonin dry powder formulation appropriate for moderate exuding wounds application. Lipid nanoparticulate system was introduced for two reasons – to prolong melatonin release and to alter hydrogel moisture transmission properties. NLC to chitosan ratio in the final powder was varied to empower characteristics of the NLC-free system, while maintaining chitosan as main structural component. Melatonin was incorporated in both the NLC and chitosan matrix of the proposed hybrid (nano-micro) system. NLCs were prepared by a hot homogenization technique to achieve prolonged release of the drug with an increased hydration effect due to lipids; while NLC-loaded chitosan microspheres were produced by a spray-drying method using Pluronic® F127 as a surfactant and healing enhancer [21]. To understand the critical formulation and process conditions for both systems, a novel screening design of experiment, called definitive screening design, was employed. The chosen design has many desirable properties, making it an appealing alternative to other screening designs [22]. The parameters investigated for NLCs were homogenization time, liquid lipid and total lipid content. Within the same design, other parameters, such as lipid to chitosan ratio, spray-drying feed flow rate, and inlet air temperature that have an impact on the characteristics of hybrid system, were also studied. The optimized hybrid system was additionally characterized in terms of flow properties, swelling, moisture transmission, and melatonin release profile. Finally, to assess the developed system wound dressing potential, *in vitro* biocompatibility with skin cell lines and antibacterial efficacy were evaluated and confirmed.

2. Materials and methods

2.1. Materials

Compritol® 888 ATO (glycerol dibehenate) was kindly gifted by Gattefosse (France). Melatonin (China) and low-viscosity chitosan (≥75% deacetylation degree, Japan) were purchased from Sigma-Aldrich. Pluronic® F127 was obtained from BASF (Germany). Miglyol® 812N was obtained from Sasol (Germany). Müller-Hinton broth (MHB) and Tryptic soy broth (TSB) were obtained from Merck (Germany). 2,3,5-triphenyltetrazolium chloride (TTC), 3-(4,5-dimethylthiazol-2-yl)-2,5-diphenyltetrazolium bromide (MTT), and DMSO were purchased from Sigma (St. Louis, MO, USA). All other chemicals and solvents used in this study were of analytical grade and purchased from Kemika (Croatia) and Sigma-Aldrich.

2.2. Experimental design

Quality by Design (QbD) principles were explored to understand the critical formulation and process conditions for both drug delivery systems. The influence of six factors at three levels was studied with a novel screening design of experiment, called definitive screening design (DSD) [22].

Table 1
Parameters considered in the experimental design and their levels.

	Parameter	Low (−1)	Central (0)	High (+1)
Investigated parameters for NLCs	H	10 min	15 min	20 min
	N-LC	5%	7.5%	10%
	LLC	10%	15%	20%
Investigated parameters for hybrid system	H-LC	15.5%	21.6%	26.9%
	F	1.8 mL/min	2.7 mL/min	3.6 mL/min
	T	110 °C	117.5 °C	125 °C

H - Homogenisation time; N-LC - Total lipid content in NLC suspension; LLC - Liquid lipid content in NLC; H-LC – Hybrid system lipid content; F - Feed rate; T - Inlet air temperature.

The parameters investigated for melatonin-loaded NLCs were homogenization time (H), total lipid content in the NLC suspension (N-LC), and liquid lipid content in NLCs (LLC). Within the same design, parameters influencing the characteristics of hybrid system, namely total lipid content (H-LC), feed flow rate (F), and inlet air temperature (T) were also studied (Table 1). Preliminary experiments were performed to determine appropriate values for low and high settings of these parameters.

NLC particle size, hybrid system production yield, particle size, moisture content, and zeta potential were investigated as responses. All experiments were performed in triplicate and ran in randomized order. Prediction models for the tested responses were built using the novel two-stage fitting procedure [23] or stepwise modelling. Design of experiments and data analyses were performed with the statistical software JMP® 13.1.0. (SAS Institute, USA).

2.3. Preparation of NLCs

Melatonin-loaded NLCs were prepared by a hot ultrasonication method. Briefly, a predetermined amount of melatonin was dissolved in a mixture of Compritol® 888 ATO and Miglyol® 812N at 90 °C to obtain a melatonin to lipid ratio of 2/5 (*w/w*). The aqueous phase containing Pluronic® F127 in the ratio 1/3 (*w/w*) with the dispersion lipid content heated to the same temperature, was added dropwise to the lipid phase under magnetic stirring at 1000 rpm for 3 min. The obtained pre-emulsion was subjected to probe sonication (UP200Ht Hielscher, Germany) at 100% amplitude for design-determined amount of time. The sample was cooled to room temperature to form melatonin-loaded NLCs.

2.4. Preparation of hybrid system

For preparation of the chitosan/melatonin/Pluronic® F127 solution, chitosan was solubilized in a 0.5% acetic acid solution at a concentration of 10 g/l and mixed with an ethanolic solution of melatonin and Pluronic® F127. For preparation of the final mixture, the melatonin loaded NLC dispersion was added dropwise to the chitosan/melatonin/Pluronic® F127 solution, under magnetic stirring (400 rpm).

The volume of ethanolic solution and the content of melatonin and Pluronic® F127 dissolved in ethanol were set up to provide the aqueous/ethanolic phase volume ratio of 8.5/1.5 in the final mixture, as well as a total melatonin to chitosan ratio of 1/2 (*w/w*) and a total Pluronic® F127 to chitosan ratio of 1/5 (*w/w*) (Table 2) [20]. The concentration of lipids in the final mixture was set up to provide the final product lipid content ranging from 15.5 to 26.9% (Table 1).

Microspheres as the hybrid system were produced by spray-drying the final mixture using a ProCept 4M8-TriX Spray Dryer with a standard 0.6 mm nozzle and compressed nitrogen flow rate of 0.3 m^3/min. The

Table 2
Composition of hybrid system.

Component	Amount (%)			Weight ratio to chitosan
Chitosan	43.0	46.1	49.7	–
Total lipid content in the hybrid system	26.9	21.6	15.5	5:8–2.5:8
Pluronic® F127	8.6	9.2	9.9	1:5
Total melatonin content in the hybrid system	21.5	23.1	24.9	1:2
Melatonin disposition ratio				
NLC matrix to chitosan matrix	1:1	1:2	1:3	/

other process parameters were set according to the requirements of the individual runs, as set in the DSD studies listed in Table 3. As a control, a melatonin free hybrid system was prepared following the same procedure. All experiments were performed in triplicate.

The process yield was calculated as the ratio between the weight of the obtained microspheres and the sum of the weights of all dry components introduced into the process.

2.5. Particle size, zeta potential and drug loading of NLCs

The particle size and polydispersity index (PDI) of melatonin loaded NLCs were determined by dynamic light scattering (Zetasizer 3000HS, Malvern Instruments, UK) at 25 °C. Before measurement, NLC suspensions were diluted 100-fold with ultra-purified water.

The zeta potential of the NLCs was determined by laser Doppler anemometry (Zetasizer 3000HS, Malvern Instruments, UK) at 25 °C. Before measurement, NLC suspensions were diluted 100-fold with 10 mM NaCl and placed in an electrophoretic cell, where a potential of 150 mV was established.

To assess the melatonin entrapped in the NLCs, the concentration of the free melatonin in the aqueous phase of NLC suspensions was determined by HPLC, as detailed in Supplementary Materials and Methods.

2.6. Particle size, zeta potential and drug loading of hybrid system

A microscopic imaging analysis technique for the determination of the hybrid system size distribution was applied. Hybrid system size and size distribution were determined with a Malvern Morphologi G3-ID (Malvern Instruments, UK). In all measurements at least 10000 particles were examined.

The zeta potential of the hybrid system was determined by laser Doppler anemometry (Zetasizer 3000HS, Malvern Instruments, UK) as described above.

The total amount of melatonin contained in the hybrid system was determined by the HPLC assay method detailed in Supplementary Materials and Methods.

2.7. Thermal analyses

Modulated differential scanning calorimetry (MDSC) analyses were carried out in a TA Instrument modulated DSC Q2000 (TA Instruments, USA), using aluminium standard pans with about 0.5–1.0 mg of the sample under dynamic nitrogen atmosphere (50 mL/min). The samples were heated at 5 °C/min from 20 °C to 220 °C using a modulation of ± 1 °C (amplitude) every 60 s (period).

The moisture content in the powder samples was analyzed by thermogravimetric analysis using TGA Q5000 (TA Instruments, USA). A powder sample weighing approximately 5 mg was heated from 25 °C to 500 °C at a rate of 10 °C/min under dynamic nitrogen atmosphere of 35 mL/min.

2.8. X-ray powder diffraction and FT-IR analyses

X-ray powder diffraction (XRPD) data were recorded on a Philips X'Pert PRO diffractometer (PAN Analytical, Germany) equipped with an X'Celerator detector (2.022° 2Θ) using Cu-Kα radiation at 45 kV and 40 mA. The scan angle range (2Θ) was 3–40°, the step size (2Θ) was 0.167°, and the time per step was 100 s.

Samples were applied directly into a Phillips' original zero background silicon plate holder with a spatula. Diffractograms were analyzed using X'Pert Data Collector software.

2.9. Analysis of flow properties of hybrid system powders

Bulk and tapped density of powders were measured by modifying the pharmacopoeia test, as reported in literature [24]. Approximately 30 mg of microsphere powders were loaded into a bottom-sealed 1 mL plastic syringe (Terumo Europe, Belgium), capped with a laboratory film and tapped until no change in the volume of the powder was observed. The bulk and tapped densities were calculated from the net

Table 3
The design matrix of definitive screening design with variable values and resulting mean product characteristics (mean values ± S.D., n = 3).

Sample ID	N-LC (%)	LLC (%)	H (min)	H-LC (%)	F (mL/min)	T (°C)	NLC particle size (nm)	NLC PdI	Hybrid system particle size (μm)	Hybrid system zeta potential (mV)	Hybrid system production Yield (%)	Hybrid system moisture content (%)
s1	10	20	10	15.5	2.7	125	227.8	0.21	2.71 ± 0.56	24.2 ± 1.5	60.21 ± 4.3	5.4 ± 0.2
s2	5	15	10	15.5	3.6	110	214.0	0.20	3.72 ± 0.86	27.7 ± 1.2	39.24 ± 3.8	5.3 ± 0.6
s3	10	20	20	15.5	3.6	110	213.5	0.22	3.07 ± 0.62	22.3 ± 1.0	59.5 ± 4.8	4.8 ± 0.4
s4	7.5	10	10	15.5	1.8	110	222.0	0.23	3.61 ± 1.24	22.1 ± 2.3	51.07 ± 2.9	5.7 ± 0.5
s5	5	20	20	21.6	1.8	110	199.1	0.23	3.11 ± 0.7	26.8 ± 0.3	62.18 ± 4.6	4.8 ± 0.2
s6	10	10	10	21.6	3.6	125	223.9	0.22	3.08 ± 0.9	19.8 ± 1.1	65.2 ± 3.4	4.1 ± 0.7
s7	10	10	15	26.9	3.6	110	215.4	0.19	3.00 ± 0.8	20.1 ± 1.2	44.49 ± 2.8	3.3 ± 0.5
s8	5	20	10	26.9	3.6	117.5	200.8	0.21	3.29 ± 0.92	17.9 ± 2.3	37.83 ± 3.7	5.4 ± 0.3
s9	10	10	20	15.5	1.8	117.5	219.6	0.23	3.44 ± 1.42	25.3 ± 1.5	49 ± 2.5	4.6 ± 0.4
s10	5	10	20	26.9	2.7	110	214.1	0.23	4.35 ± 1.17	20.4 ± 1.4	58.18 ± 3.3	4.8 ± 0.5
s11	5	10	10	26.9	1.8	125	220.6	0.20	3.61 ± 0.75	24.2 ± 0.5	55.67 ± 4.2	4.3 ± 0.6
s12	10	20	10	26.9	1.8	110	221.3	0.19	3.15 ± 1.44	25.9 ± 1.3	37.52 ± 1.8	3.5 ± 0.3
s13	10	15	20	26.9	1.8	125	213.8	0.22	4.92 ± 1.15	13.3 ± 0.5	34.39 ± 2.6	3.5 ± 0.7
s14	7.5	20	20	26.9	3.6	125	206.4	0.22	3.94 ± 0.92	24.5 ± 0.4	42.89 ± 3.8	6.1 ± 0.4
s15	5	10	20	15.5	3.6	125	206.4	0.22	4.54 ± 1.06	27.3 ± 0.1	59.79 ± 2.1	5.8 ± 0.7
s16	7.5	15	15	21.6	2.7	117.5	221.3	0.23	2.70 ± 0.17	24.8 ± 1.4	34.71 ± 3.2	3.9 ± 0.5
s17	5	20	15	15.5	1.8	125	204.2	0.20	2.72 ± 0.34	27.3 ± 1.4	47.89 ± 2.8	5.2 ± 0.3

N-LC - Total lipid content in NLC suspension; LLC - Liquid lipid content in NLC; H - Homogenisation time; H-LC – Hybrid system total lipid content; F - Feed rate; T - Inlet air temperature.

weight of the plastic syringe content divided by the volume in the syringe content before and after tapping, respectively. Experiments were performed in triplicate. The Hausner ratio was calculated as tapped density to bulk density ratio.

2.10. Wound dressing characterization

2.10.1. Swelling study

Franz diffusion cell apparatus was used to determine the simulated wound fluid (SWF pH 6.3 and 7.4, thermostated at 37 °C)-absorbing capacity and swelling kinetics of the hybrid system as detailed in Supplementary Materials and Methods. The liquid uptake of each sample was expressed as a volume of SWF added per milligram of the chitosan in 120 min swelling process.

2.10.2. Water vapour transmission rate (WVTR)

The hybrid system was swollen in SWF (pH 6.3 and 7.4) until the formation of a homogenous hydrogel. Hydrogels were mounted on the teflone mesh placed on the mouth of cylindrical plastic cups (15 mm diameter), containing 10 mL of water with negligible water vapor transmission, and placed in an oven at 35 °C for 24 h. The weight loss was measured at regular time intervals and a weight loss versus time plot was constructed. The WVTR was calculated using the formula (1):

$$WVTR = \frac{slope\ x\ 24}{A}\frac{g}{m^2}/day \quad (1)$$

where A represents the test area of the sample in m^2. Experiments were performed in triplicate with sealed cups as negative and open cup as positive controls.

2.10.3. Evaporative water loss

Hydrogels prepared as described above were kept at 37 °C and 35% relative humidity. After regular time intervals, the weight was noted. The percentage of the weight remaining was calculated by the equation (2):

$$Water\ weight\ remaining\ (\%) = \frac{Wt - Wt\ last}{Wo - Wt\ last}x100 \quad (2)$$

where W_0, W_t and $W_{t\ last}$ are initial weight, weight after time "t" and weight after 12 h, respectively. All experiments were performed in triplicate.

2.11. 11. In vitro drug release study

The melatonin release profiles from the hybrid system were evaluated using Franz diffusion cell apparatus and an HPLC assay method, as detailed in Supplementary Materials and Methods. Phosphate buffer pH 6.3 and 7.4, thermostated at 37 °C, were used as the receiving medium.

2.12. In vitro cytotoxicity

Human keratinocyte cell line HaCaT (Cell Line Services, Germany) and human diploid fibroblast strain MJ90hTERT (kindly provided by Dr. Ivica Rubelj, Institute Ruđer Bošković, Zagreb, Croatia) [25] were cultured in DMEM medium (GIBCO, UK) supplemented with 10% foetal bovine serum (GIBCO) and penicillin, streptomycin, and amphotericin B (Sigma–Aldrich).

Evaluation of *in vitro* cytotoxicity was described by the MTT and lactate dehydrogenase (LDH) leakage assay as detailed in Supplementary Materials and Methods. Hanks' Balanced Salt solution (HBSS) and 1% Triton X-100 were used as negative and positive controls, respectively.

2.13. Antimicrobial assay

2.13.1. Sample preparation

Prior to the experiment, the hybrid system was resuspended in a mixture of degassed sterile water and MH (1:1, v/v) and diluted in MH with respect to the concentration of melatonin. Antimicrobial activity of the prepared samples was tested on *Staphylococcus aureus* (ATCC 29213) and *S. aureus* MRSA strains (NCTC 12493) taken from the microbial collection of the Department of Microbiology, Faculty of Pharmacy and Biochemistry, University of Zagreb (Croatia). All experiments were performed in four replicates.

2.13.2. Antimicrobial activity against planktonic bacteria

For determination of minimal inhibitory concentrations (MICs) of samples, a two-fold microdilution assay on a 96-well plate using MH was carried out following NCCLS method [26]. Culture of *S. aureus* in the broth was treated with microspheres, melatonin or Pluronic® F127 solutions at (relevant) melatonin concentrations ranging from 0.08 mg/mL to 2.7 mg/mL. MH with or without 2.5% DMSO was used as a positive (growth) control, while melatonin-free microsphere samples, melatonin and Pluronic® F127 in appropriate dilutions at (relevant) melatonin concentrations without *S. aureus*, were used as negative controls. After 24 h of incubation at 35 ± 2 °C the MIC was assessed by absorbance measurement at 620 nm (iEMS, Labsystems), as described by Tekbas et al. [6]. MICs were confirmed using TTC reagent dissolved in water (20 mg/mL), in accordance with Klančnik et al. [27].

2.13.3. Antimicrobial activity against biofilm

Minimum biofilm inhibitory concentrations (MBICs) and minimum biofilm eliminating concentrations (MBECs) were determined in accordance with the methods described by Kifer et al. [28] using TSB supplemented with 0.25% D-(+)-glucose (TSBGlc). To assess MBIC, microsphere samples, melatonin or Pluronic® F127 solution in two-fold dilutions in TSBGlc at (relevant) melatonin concentrations ranging from 0.01 mg/mL to 1.35 mg/mL, were distributed on a 96-well plate. To assess the MBEC, the overnight cultures were diluted in TSBGlc 1:20 and after 24 h lasting biofilm formation, the medium was removed, and biofilm was treated with samples at (relevant) melatonin concentrations of 0.08–2.7 mg/mL. After overnight incubation, the viability of the biofilm was assessed by measurement at 540 nm.

To obtain the BIC_{50} and BEC_{50} from the results of antimicrobial assay, non-linear dose-response fitting was applied as described in Ref. [20].

3. Results and discussion

3.1. Lipid selection

Based on the technological procedure and topical application of the final delivery system, criteria for the selection of matrix lipids were (i) solid lipid melting point; (ii) solid lipid/liquid lipid compatibility, and (iii) solubility of melatonin in the lipids.

Melting point is the critical parameter of solid lipid, since the intention was to develop NLC-loaded microspheres using the spray-drying technique. Solid lipids were selected based on their melting points that had to be above 50 °C (70 °C, 56 °C and 72 °C for Compritol® 888 ATO, Precirol 5 ATO and Tristearin, respectively), which is the expected outlet temperature in the drying process.

Medium chain triglycerides Miglyol® 812N and 810N were tested as the most commonly used liquid lipid components for the preparation of NLCs. Polysorbate 80 and castor oil were taken into consideration due to their high melatonin solubility enhancing potential. Compatibility of solid lipids with liquid lipids was tested by heating lipid mixtures to 80 °C (details described in Supplementary Materials and Methods). All mixtures formed homogeneous liquid matrices. However, after 24-h storage at room temperature, mixtures containing Tristearin disjointed

with leaked liquid lipids (observed as liquid oil at the surface of the solid lipid). The same observation was recorded with the other two mixtures of solid lipids with castor oil. Thus, Tristearin and castor oil were excluded from further testing.

Solubility of melatonin in Compritol® 888 ATO, Precirol 5 ATO, Miglyol® 810N, Miglyol® 812N, Polysorbate 80, and all solid lipid/liquid lipid mixtures was determined. Melatonin solubility was higher in lipid mixtures compared to individual components, with the highest value for the Compritol® 888 ATO/Miglyol® 812N (9/1, *w/w*) mixture (data not shown).

Considering solid lipid melting point and the results of solubility testing, Compritol® 888 ATO and Miglyol® 812N were chosen as lipids to produce NLCs.

3.2. Experimental design: analysis of results

In this study, the DSD was employed to investigate the effect of six process/formulation parameters and their possible interaction on the product characteristics with the aim of directing the development towards the dressing with the targeted performance.

In comparison to traditional screening designs, the main advantages of DSDs are that, with a very small number of experiments/runs, information about parameters and their interactions can be obtained. Further, the main effects are orthogonal to two-factor interactions and any pair of second order effects is not confounded. Moreover, DSD with six or more factors allows projection of any three factors, fitting the full quadratic model without need to augment the design and run additional experiments. Furthermore, due to the beneficial properties mentioned above, DSD allows the analysis of experimental data using the novel method which exploits the specific structure of DSDs. It also allows building of models which could perform better than traditional models that use general procedures, like stepwise regression [22].

3.2.1. NLC particle size

NLCs with small and uniform size distribution are prerequisite for the stability and homogenous distribution of lipid phase within the hybrid system, therefore, sensitivity of this parameter was investigated within our statistical design. NLC mean nanoparticle size and size distribution were shown to be highly dependent on included components and process parameters [29]. NLCs prepared within this study had relatively smaller size (199.1–227.8 nm; Table 3) and narrower size distribution (PDI $\leq$0.24 for all samples; Table 3) compared to the NLCs prepared by the similar manufacturing process [30]. As expected, the statistical model revealed homogenization time (H), liquid lipid content in NLCs (LLC), and total lipid content in NLC suspension (N-LC) as critical parameters influencing NLC particle size (Table S1, Fig. 1 (a)).

The highest impact was observed for the N-LC. The model indicated that particle size increased with the increase of total lipid content, which was also reported by other researchers [31]. Also, longer homogenization time provided a higher total amount of energy available for lipid particle size reduction, which resulted in particles of smaller diameter. Smaller NLC particle sizes were observed in samples with a higher amount of liquid lipid, which could be assigned to lower particle surface tension [32] and decreased aggregation potential [31]. According to the prediction model, it can be concluded that the small NLC particles with narrow distribution can be manufactured by the hot homogenization technique, with 5% total lipid content in NLC suspension, 20% of Miglyol® 812 of total lipid content, and a homogenization time of 20 min (Table S1, Table 3).

3.2.2. Hybrid system particle size

The earlier mentioned two-stage fitting procedure specially designed for DSDs showed that two NLC related factors had a major influence on the hybrid system mean diameter: LLC and H (Table S1, Fig. 1 (b)). Interaction between these two factors and their squares are also part of the fitted multiple linear regression model.

According to the model, the largest microspheres were obtained when the longest homogenization time during NLC preparation was applied. A possible root cause of this observation could be the increased surface tension of the drying feed resulting from the homogenization time-related reduction of the NLCs size (Fig. 1a)) and consequently, increment of the surfactant-covered lipid surface. Even though the relationship between surface tension and droplet/particle size is commonly assumed, no clear correlation has been established by studying

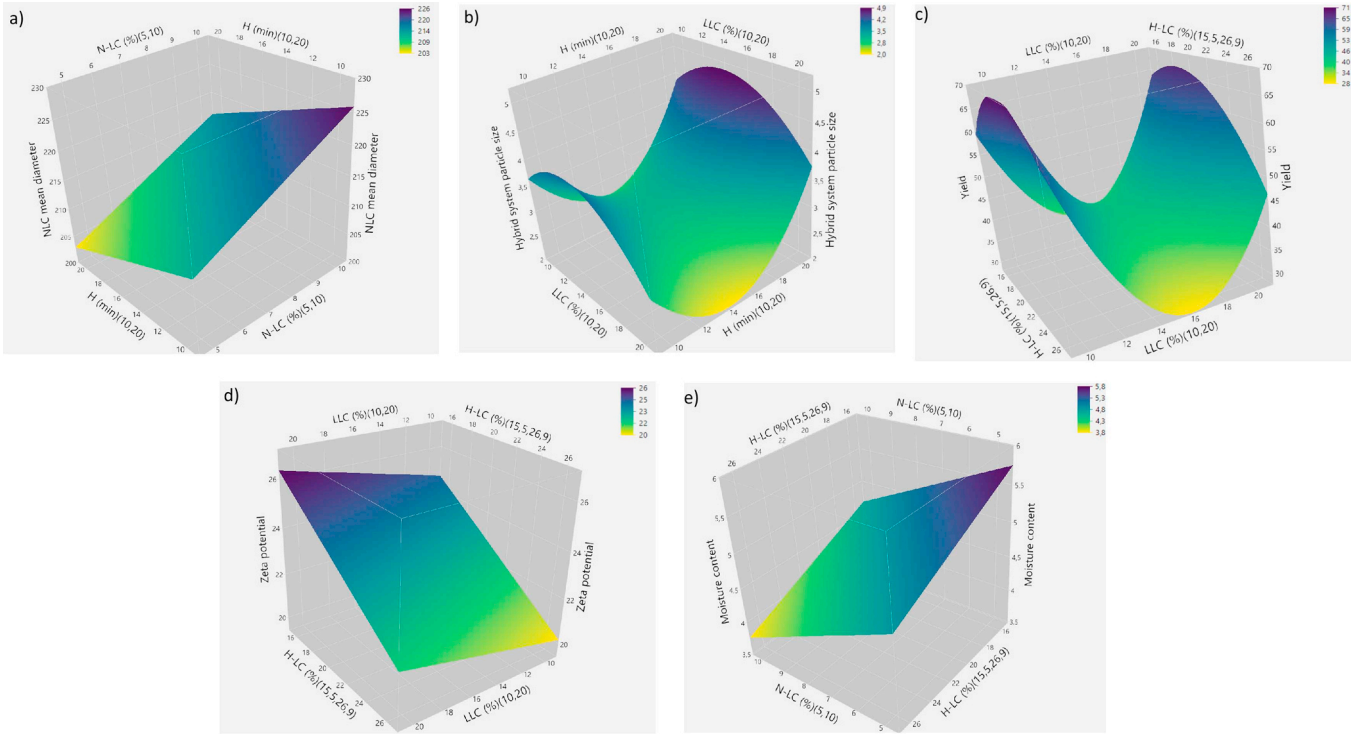

Fig. 1. Response surface analysis of the tested effects: (a) NLC particle size; (b) Hybrid system particle size; (c) Process yield; (d) Zeta potential; (e) Moisture content.

equilibrium surface tensions (data not shown). Kawakami and coworkers explained such phenomena by the fact that equilibrium surface tensions are not likely to be obtained in the spray-drying process, as particle formation is completed within a few seconds, and have shown that the droplet/particle size could be related to dynamic surface tension in the millisecond time scale [33].

The model also indicated that the increase in liquid lipid content resulted in production of microspheres with lower diameter. Wang et al. [34] obtained smaller and less aggregated microspheres for samples with higher liquid lipid content. They explained the effect by the lack of solid lipid crystallization during drying process due to inclusion of the liquid lipid. The same effect was observed in this study (Fig. 1b)), where s significant reduction in the hybrid system particle size was measured for samples containing NLCs with the highest amount of liquid lipid. Hybrid system mean particle size and distribution have direct impact on the swelling and consequent drug release rate [35]. Control of this parameter represents critical point in development of the in-situ gel forming drug delivery systems.

3.2.3. Process yield

The two most significant and nonlinear factors affecting spray drying process yield are liquid lipid content in NLCs (LLC) and total lipid content in the hybrid system (H-LC) (Table S1, Fig. 1 (c)). As mentioned above, high liquid lipid content in the hybrid system resulted in production of smaller microspheres. Also, smaller production yields were obtained when liquid lipid content was set to higher levels. The observed effect could be the consequence of the instrument configuration and the loss of the smallest microspheres, since completely efficient separation with the configuration used is expected for microspheres with a mean diameter above 1.5 μm [36]. The total amount of lipids has a negative impact on the process yield, as indicated by the negative sign for regression coefficients. The decrease in yield for the formulations with a high lipid to chitosan ratio could be caused by profound particle adhesion to the chamber walls, due to high lipid presence at the microsphere surface [37]. The interaction of the mentioned factors is also significant, implying major influence of the lipid component on production yield.

3.2.4. Zeta potential

All hybrid systems were positively charged (13.3–27.7 mV, Table 3), indicating the presence of the chitosan at the particle surface. The only significant parameter influencing zeta potential values was lipid to chitosan ratio, due to lipids' overall negative charge [38] (Table S1, Fig. 1 (d)). The zeta potential-lowering effect of lipids can be further indicated by the fact that NLC loaded microspheres were less positively charged than corresponding NLC-free chitosan based microspheres [20]. Although ionic interactions between components were not detected, weak ionic relationships could be present and manifest as lower positive zeta potential values for final product.

3.2.5. Moisture content

As shown in Table 3, the experimental results for moisture content varied between 3.31% and 6.05%. The factors in the model, their estimates, and statistical significance are given in Table S1 and Fig. 1 (e). The results obtained indicate an increase in the moisture content with a decrease in the lipid content in the NLC dispersions and the microspheres. Since chitosan is the only hygroscopic component in the system, it is expected that the moisture content of the hybrid system would be higher when the amount of lipid content in the system is lower. Additionally, when the NLC dispersions with lower lipid content were part of the mixture, higher amounts of the aqueous portion were introduced in the drying chamber, leading to the formation of a hybrid system with higher final moisture content.

Table 4
Optimised hybrid system – estimated and observed mean product characteristics (mean values ± S.D., n = 3).

Effect	Estimated	Observed
Process yield (%)	62.3 ± 4.7	60.9 ± 2.1
Hybrid system particle size (μm)	3.5 ± 0.4	3.3 ± 0.2
Moisture content (%)	4.8 ± 0.2	4.7 ± 0.1
Zeta potential (mV)	25.5 ± 5.2	26.6 ± 0.5
NLC particle size (nm)	201.3 ± 5.6	200.0 ± 2.3

3.3. Model optimization and validation

Combined inference from the obtained models resulted in the proposal for an optimized parameter set-up that was already included within design (conditions for sample number 5). The optimized hybrid system was reproduced under the selected process parameters in triplicate and characterized to validate the model and confirm batch-to-batch repeatability. The results obtained were within the predicted ranges, confirming the suitability of the developed model and repeatability of the product characteristics (Table 4).

3.4. Physico-chemical characterization of hybrid system

The crystalline nature of the hybrid system was assessed by X-ray analysis. Melatonin diffraction peaks can be observed in the hybrid system diffractograph (Fig. S1), indicating incomplete melatonin conversion to amorphous state during the spray-drying process. Crystalline melatonin in spray-dried systems was identified by diffraction peaks at 10.8°, 14.9°, 16.3°, 18.9°, 24.2°, 25.0° and 26.1° 2θ.

The thermographs of crystalline components (Fig. S2) revealed endothermic peaks, attributed to the melting points (Tm), appearing at the midpoint temperature of 70.29 °C and 117.99 °C for Compritol® 888 ATO and melatonin, respectively. Compared to the pure crystalline components, shifting of the melting point from 70.29 °C to 66.38 °C for Compritol® 888 ATO and from 117.99 °C to 106.06 °C for melatonin are detected. It is known that lipids can form various structures with different stability [39]. In NLCs, solid lipids are present in less ordered structures, allowing inclusion of drug molecules and improving their stability [40]. A shift in Tm for Compritol® 888 ATO demonstrates the presence of NLCs within the hybrid system, while a shift in the melatonin peak indicates the possible interaction of the drug with the polymers and/or lipids within the hybrid system. The heat of fusion of melatonin in the particles decreased compared to the pure drug, indicating the occurrence of partially amorphous melatonin due to the spray-drying process.

Melatonin content in the hybrid system was analyzed in order to confirm that no loss of drug substance during the preparation process occurred. The results in the Table 5 confirm complete entrapment of melatonin in the NLC loaded microspheres.

3.5. Wound dressing properties

3.5.1. Flow properties

As the developed dry powder hybrid system is intended for direct application to the wound bed, good flowability characteristics are

Table 5
Wound dressing characteristics of optimized hybrid system (mean values ± S.D, n = 3).

Entrapment efficiency (%)	Hausner ratio	WVTR - pH 6,3 (gm^{-2} day^{-1})	WVTR - pH 7.4 (gm^{-2} day^{-1})
99.3 ± 0.6	1.13 ± 0.11	2128 ± 105.3	2195 ± 112.7

WVTR - water vapour transmission rate.

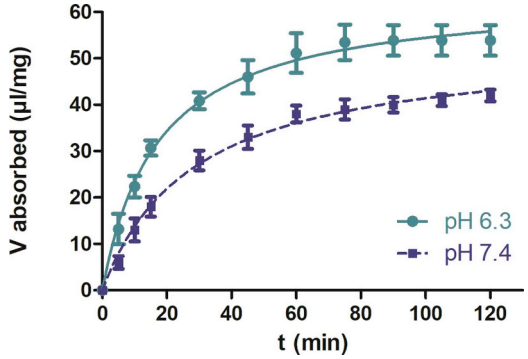

Fig. 2. Simulated wound fluid (SWF) pH 7.4 (dash line) and pH 6.3 (full line) uptake profiles of hybrid system expressed as the volume (V) of absorbed SWF per milligram of chitosan (mean values ± S.D., n = 3).

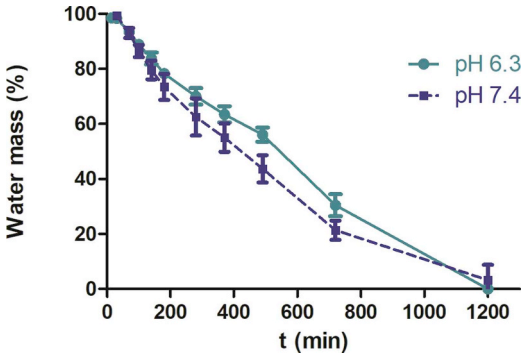

Fig. 3. Evaporative water loss from hydrogels prepared from hybrid system (mean values ± S.D., n = 3).

essential for dosing and application. The Hausner ratio for an optimized hybrid system is 1.13 ± 0.11, which characterizes good powder flow (Table 5). Observed flowability is superior compared to the literature reported values for chitosan based spray-dried systems [20]. When the microparticulate system contains lipid components, there is likelihood to obtain agglomerated and sticky powder with poor rheological properties [41]. Therefore, good flowability of the developed hybrid system confirms spray-drying as an appropriate technique to produce NLC loaded chitosan microspheres, as long as the formulation and process parameters crucial in tailoring the product characteristics are optimized.

3.5.2. Swelling properties

Swelling behavior plays an important role in microsphere *in situ* gelling/dressing formation and drug release. The hybrid system fluid uptake was determined in SWF media with two pH values: physiologically relevant pH 7.4 and pH 6.3, which has been measured in the bacterial broth at 37 °C (Fig. 2).

In accordance with previously reported results for various chitosan hydrogel types [20,42], swelling of powder followed second order kinetics (Table S2, $R^2 \geq 0.99$ for both pH values). Based on the Korsmeyer-Peppas diffusion exponent values, the fluid uptake mechanism can be described by anomalous transport coupled with the influence of polymer relaxation and fluid diffusion.

It was observed that microspheres at pH 6.3 absorbed significantly higher amounts of SWF in comparison to pH 7.4. In an acidic environment, chitosan amine groups are ionized, which results in increased solvent uptake [43]. However, when swelling ability at both pH values is compared with SWF uptake of NLC-free microspheres [20], a decrease in fluid uptake is observed. The presence of lipids in the system moderated the swelling capacity of the microspheres due to hydrophobicity [44]. This effect is in agreement with other researchers' observations [45].

3.5.3. Water vapor transmission rate and evaporative water loss

A moist environment represents one of the essential conditions for successful wound healing. The WVTR for normal skin is 204 g/m^2/day and for wounded skin from 278 to 5138 g/m^2/day, depending on the type and nature of the wound. The water vapor transmissivity of a dressing should be such that it maintains a satisfactory moisture balance within the repairing wound. It has been recommended that rate of 2000–2500 g/m^2/day would provide adequate levels of moisture without risking wound dehydration [21,46].

The hydrogel formed from the hybrid system with SWF pH 6.3 and 7.4 has an ideal WVTR of 2128.0 ± 105.3 g/m^2/day and 2195.0 ± 112.7 g/m^2/day, respectively (Table 5).

In order to investigate the behavior of the dressing when applied to less exuding wounds, water loss from the hydrogel was analyzed (Fig. 3). The hydrogel prepared with SWF at pH 6.3 showed a slightly lower water loss rate in relation to SWF at 7.4 ($t_{50\%}$–8.6 h for pH 6.3 and $t_{50\%}$–7.2 h for pH 7.4), which is in accordance with the observed higher amount of fluid uptake during the swelling process. Dissimilar to relatively high water loss of NLC-free chitosan dressing ($t_{50\%}$–4.2 h for pH 6.3 and $t_{50\%}$–3 h for pH 7.4 [20], adding the lipids in the system significantly reduced water loss due to the NLC occlusion effect.

Slower water loss and moderated fluid uptake capacity can be attributed to the solid state nature of the lipid components in the hydrogel [47]. Occlusivity offered by NLC-loaded chitosan system could be beneficial for application to moderately exuding wounds.

3.5.4. In vitro drug release

Release profiles of melatonin from the hybrid system in phosphate buffer (pH 6.3 and 7.4) at 37 °C are presented in Fig. 4. In both media, a characteristic drug release profile was observed: the initial burst release (within the first 2 h) followed by a slower phase of release [45]. This mode of release could be useful in prevention of infection occurrence and spreading at the beginning of a local therapy; while sustained release provides a therapeutic concentration for a prolonged period.

Chitosan's low solubility and corresponding lower swelling capacity in combination with lipids at physiological pH 7.4 caused relatively fast and less controlled melatonin release. At pH 6.3, chitosan chains rehydrated and formed a thick gel structure, which lead to an increased melatonin diffusional path length [45]. The initial phase of high release was governed by dissolution of drug incorporated within the chitosan matrix, while melatonin entrapment within NLCs contributed to the second phase, involving a slower release rate. Observed melatonin release retardation from the NLC-loaded microspheres verified the idea of partial melatonin-NLC entrapment.

Melatonin release from this nano-micro system can be described by the Higuchi model ($R^2 > 0.98$) and non-Fickian diffusion

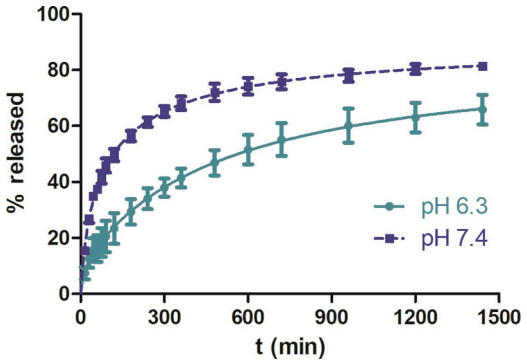

Fig. 4. The release profiles of melatonin from the hybrid system in the phosphate buffer pH 7.4 (dash line) and pH 6.3 (full line) as the release medium (mean values ± S.D., n = 3).

Table 6
Antimicrobial activity of hybrid system against planktonic bacteria and biofilm of *Staphylococcus aureus*.

S. aureus ATCC 29213					*S. aureus* MRSA NCTC 12493				
mg/mL of melatonin									
MIC	MBIC	BIC_{50}	MBEC	BEC_{50}	MIC	MBIC	BIC_{50}	MBEC	BEC_{50}
1.35	2.7	0.9	2.7	1.2	1.35	2.7	1.43	2.7	~1.3

MIC – minimal inhibitory concentration; MBIC – minimal biofilm inhibitory concentration; BIC50 – concentration that inhibits 50% bacteria in biofilm formation; MBEC – minimal biofilm eliminating concentration; BEC50 - concentration that eliminates 50% bacteria in formed biofilm.

(predominately)-swelling controlled release mechanism (ns = 0.4805–0.5259), as previously reported for similar delivery systems (Table S3) [48].

3.6. *In vitro* cytotoxicity

The biocompatibility of the hybrid system with human keratinocyte HaCaT and MJ90hTERT fibroblasts was assessed by monitoring cell metabolic activity (MTT assay) and membrane integrity (LDH assay) after exposure to developed microspheres in the same concentration range as in our previous study where systems were shown to be well tolerated [20]. Chitosan, the main component of the system, is characterized as a safe and undisputed biomaterial widely used for tissue engineering and drug delivery [49]. Newly introduced components were the lipids forming NLCs – Compritol® 888ATO and Miglyol 812. Both NLC constituents are considered biocompatible [40,50]. As expected, the hybrid system prepared in this study did not decrease cell viability under the experimental conditions employed. Thus, the evaluated system can be considered biocompatible with tested cell lines (Fig. S3).

3.7. *Antimicrobial activity against planktonic bacteria and biofilm of Staphylococcus aureus*

The results of antimicrobial activity of the hybrid system are presented in Table 6. Depicted (minimal) inhibitory and (minimal) biofilm inhibitory/eliminating concentrations were expressed as the (relevant) concentration of melatonin in the system. The hybrid system showed antimicrobial activity against planktonic bacteria and biofilm of both *Staphylococcus aureus* tested strains (MIC = 1.35 mg/mL, MBIC = 2.7 mg/mL), as well as biofilm eliminating effect (MBEC = 2.7 mg/mL for both strains). Considering the swelling extent of the hybrid system (Fig. 2) resulting in hydrogel dressing formation with theoretical melatonin concentration ranging between 9.0 and 12.5 mg/mL, it may be concluded that the developed hybrid system can provide overall antibacterial protection at the wound bed. Obtained MICs, MBICs and MBECs indicate a non-specific mechanism of antibacterial activity that lowers the chance of resistance and biofilm development. It is known that chitosan's positive charge has significant role in the antimicrobial efficacy due to the interaction with the negatively charged bacterial surface [51]. The idea of synergistic antimicrobial effects of melatonin and chitosan was postulated based on melatonin intracellular chelation of iron, which leads to lowering of pH in the bacteria microenvironment and promotes subsequent increase in chitosan charge density [52].

3.8. *Manufacturing outlook*

In order to allow possible *in vivo* evaluation of the developed hybrid system, sterility of the product must be ensured. According to EMA Decision tree for sterilization choices for dry powder products [53], dry heat is the first option. However, this cannot be the method of choice for the hybrid system since required sterilization temperature is above the melting point of both, solid lipid and melatonin. Ionizing radiation is a frequently used sterilization method for chitosan-based hydrogels. Irradiation causes size reduction of the chitosan chains, improving antibacterial and wound healing properties [54,55]. At the same time, ionizing radiation may cause oxidation of the lipids [56] and/or activation of melatonin as antioxidative agent [57], therefore is not suitable for developed system. Considering the latter, a sterile filtration and processing is the most appropriate sterilization option. However, aseptic spray drying is expensive process, which may represent a potential limitation for the production of the hybrid system.

4. Conclusion

This study confirms the sustainability of a spray-drying technique for the manufacturing of melatonin-NLC-loaded chitosan microspheres as hybrid wound dressings with antimicrobial and moderately occlusive properties. A novel DoE approach was successfully employed to understand and optimize the formulation and process parameters for the preparation of the hybrid system, ensuring quality built in during product development. Microspheres showed non-specific antimicrobial activity against *S. aureus* and *S. aureus* MRSA strains, lowering the chances of resistance and biofilm development. This *in vitro* proof-of-concept evaluation shows a promising potential of the developed swellable dry powder dressing to provide an adequate protection to moderately exuding wounds at risk of bacterial infection.

Acknowledgments

This research was supported by PLIVA Croatia Ltd, TEVA Group Member, as part of the project “Development of functional wound dressings with drug delivery nanosystems”.

Appendix A. Supplementary data

Supplementary data to this article can be found online at https://doi.org/10.1016/j.jddst.2019.05.004.

References

[1] T. Shipperley, C. Martin, B. Healthcare, The Physiology of Wound Healing : an Emergency Response, Surgeon 35 (2011) 8–10 http://www.sciencedirect.com/science/article/pii/S0263931917301369.
[2] W. Norbury, D.N. Herndon, J. Tanksley, M.G. Jeschke, C.C. Finnerty, Infection in burns, Surg. Infect. 17 (2016) 250–255, https://doi.org/10.1089/sur.2013.134.
[3] A.J. Huh, Y.J. Kwon, Nanoantibiotics A new paradigm for treating infectious diseases using, J. Control. Release 156 (2011) 128–145 http://www.ncbi.nlm.nih.gov/entrez/query.fcgi?cmd=Retrieve&db=PubMed&dopt=Citation&list_uids=21763369.
[4] M.A. Mofazzal Jahromi, P. Sahandi Zangabad, S.M. Moosavi Basri, K. Sahandi Zangabad, A. Ghamarypour, A.R. Aref, M. Karimi, M.R. Hamblin, Nanomedicine and advanced technologies for burns: preventing infection and facilitating wound healing, Adv. Drug Deliv. Rev. 123 (2018) 33–64, https://doi.org/10.1016/j.addr.2017.08.001.
[5] M. Gómez-Florit, J.M. Ramis, M. Monjo, Anti-fibrotic and anti-inflammatory properties of melatonin on human gingival fibroblasts in vitro, Biochem. Pharmacol. 86 (2013) 1784–1790, https://doi.org/10.1016/j.bcp.2013.10.009.
[6] O.F. Tekbas, R. Ogur, A. Korkmaz, A. Kilic, R.J. Reiter, Melatonin as an antibiotic: new insights into the actions of this ubiquitous molecule, J. Pineal Res. 44 (2008) 222–226, https://doi.org/10.1111/j.1600-079X.2007.00516.x.
[7] A. Daryani, M. Montazeri, A.S. Pagheh, M. Sharif, S. Sarvi, A. Hosseinzadeh, R.J. Reiter, R. Hadighi, M.T. Joghataei, H. Ghaznavi, S. Mehrzadi, The potential use of melatonin to treat protozoan parasitic infections: a review, Biomed. Pharmacother. 97 (2018) 948–957, https://doi.org/10.1016/j.biopha.2017.11.007.
[8] J.R. Vielma, E. Bonilla, L. Chacín-Bonilla, M. Mora, S. Medina-Leendertz, Y. Bravo, Effects of melatonin on oxidative stress, and resistance to bacterial, parasitic, and viral infections: a review, Acta Trop. 137 (2014) 31–38, https://doi.org/10.1016/j.actatropica.2014.04.021.
[9] R. Song, L. Ren, H. Ma, R. Hu, H. Gao, L. Wang, X. Chen, Z. Zhao, J. Liu, Melatonin promotes diabetic wound healing in vitro by regulating keratinocyte activity, Am. J. Transl. Res. 8 (2016) 4682–4693.
[10] A.S. Sahib, F.H. Al-Jawad, A.A. Al-Kaisy, Burns, endothelial dysfunction, and oxidative stress: the role of antioxidants, Ann. Burns Fire Disasters 22 (2009), pp. 6–11 http://www.pubmedcentral.nih.gov/articlerender.fcgi?artid=3188210&tool=

pmcentrez&rendertype=abstract.
[11] I. Garcia-Orue, J.L. Pedraz, R.M. Hernandez, M. Igartua, Nanotechnology-based delivery systems to release growth factors and other endogenous molecules for chronic wound healing, J. Drug Deliv. Sci. Technol. 42 (2017) 2–17, https://doi.org/10.1016/j.jddst.2017.03.002.
[12] J. Pardeike, A. Hommoss, R.H. Müller, Lipid nanoparticles (SLN, NLC) in cosmetic and pharmaceutical dermal products, Int. J. Pharm. 366 (2009) 170–184, https://doi.org/10.1016/j.ijpharm.2008.10.003.
[13] S. Jain, N. Patel, M.K. Shah, P. Khatri, N. Vora, Recent advances in lipid-based vesicles and particulate carriers for topical and transdermal application, J. Pharm. Sci. 106 (2017) 423–445, https://doi.org/10.1016/j.xphs.2016.10.001.
[14] I. Garcia-Orue, G. Gainza, C. Girbau, R. Alonso, J.J. Aguirre, J.L. Pedraz, M. Igartua, R.M. Hernandez, LL37 loaded nanostructured lipid carriers (NLC): a new strategy for the topical treatment of chronic wounds, Eur. J. Pharm. Biopharm. 108 (2016) 310–316, https://doi.org/10.1016/j.ejpb.2016.04.006.
[15] G. Gainza, M. Pastor, J.J. Aguirre, S. Villullas, J.L. Pedraz, R.M. Hernandez, M. Igartua, A novel strategy for the treatment of chronic wounds based on the topical administration of rhEGF-loaded lipid nanoparticles: in vitro bioactivity and in vivo effectiveness in healing-impaired db/db mice, J. Control. Release 185 (2014) 51–61, https://doi.org/10.1016/j.jconrel.2014.04.032.
[16] N. Karimi, B. Ghanbarzadeh, H. Hamishehkar, B. Mehramuz, H.S. Kafil, Antioxidant, antimicrobial and physicochemical properties of turmeric extract-loaded nanostructured lipid carrier (NLC), Colloids Interface Sci. Commun. 22 (2018) 18–24, https://doi.org/10.1016/j.colcom.2017.11.006.
[17] R.A.A. Muzzarelli, Chitins and chitosans for the repair of wounded skin, nerve, cartilage and bone, Carbohydr. Polym. 76 (2009) 167–182, https://doi.org/10.1016/j.carbpol.2008.11.002.
[18] Z. Ma, A. Garrido-Maestu, K.C. Jeong, Application, mode of action, and in vivo activity of chitosan and its micro- and nanoparticles as antimicrobial agents: a review, Carbohydr. Polym. 176 (2017) 257–265, https://doi.org/10.1016/j.carbpol.2017.08.082.
[19] G.D. Mogoşanu, A.M. Grumezescu, Natural and synthetic polymers for wounds and burns dressing, Int. J. Pharm. 463 (2014) 127–136, https://doi.org/10.1016/j.ijpharm.2013.12.015.
[20] M.D. Romić, M.Š. Klarić, J. Lovrić, I. Pepić, B. Cetina-Čižmek, J. Filipović-Grčić, A. Hafner, Melatonin-loaded chitosan/Pluronic® F127 microspheres as in situ forming hydrogel: an innovative antimicrobial wound dressing, Eur. J. Pharm. Biopharm. 107 (2016) 67–79, https://doi.org/10.1016/j.ejpb.2016.06.013.
[21] I.Y. Kim, M.K. Yoo, J.H. Seo, S.S. Park, H.S. Na, H.C. Lee, S.K. Kim, C.S. Cho, Evaluation of semi-interpenetrating polymer networks composed of chitosan and poloxamer for wound dressing application, Int. J. Pharm. 341 (2007) 35–43, https://doi.org/10.1016/j.ijpharm.2007.03.042.
[22] B. Jones, C.J. Nachtsheim, A class of three-level designs for definitive screening in the presence of second-order effects, J. Qual. Technol. 43 (2011) 1–15, https://doi.org/10.2514/6.2000-4890.
[23] B. Jones, C.J. Nachtsheim, Effective design-based model selection for definitive screening designs, Technometrics 59 (2017) 319–329, https://doi.org/10.1080/00401706.2016.1234979.
[24] F. Sansone, R.P. Aquino, P. Del Gaudio, P. Colombo, P. Russo, Physical characteristics and aerosol performance of naringin dry powders for pulmonary delivery prepared by spray-drying, Eur. J. Pharm. Biopharm. 72 (2009) 206–213, https://doi.org/10.1016/j.ejpb.2008.10.007.
[25] I. Rubelj, Telomere Q-PNA-FISH–reliable results from stochastic signals, PLoS One 9 (2014) e92559, , https://doi.org/10.1371/journal.pone.0092559.
[26] N.C.C.L.S. Standards, Approved Standard: M7-A6. Methods for Dilution Antimicrobial Susceptibility Tests for Bacteria that Grow Aerobically, Wayne, PA, (2003).
[27] A. Klančnik, S. Piskernik, B. Jeršek, S.S. Možina, Evaluation of diffusion and dilution methods to determine the antibacterial activity of plant extracts, J. Microbiol. Methods 81 (2010) 121–126, https://doi.org/10.1016/j.mimet.2010.02.004.
[28] D. Kifer, V. Mužinić, M.Š. Klaric, Antimicrobial potency of single and combined mupirocin and monoterpenes, thymol, menthol and 1,8-cineole against Staphylococcus aureus planktonic and biofilm growth, J. Antibiot. (Tokyo) 69 (2016) 689–696, https://doi.org/10.1038/ja.2016.10.
[29] M. Sznitowska, E. Wolska, H. Baranska, K. Cal, J. Pietkiewicz, The effect of a lipid composition and a surfactant on the characteristics of the solid lipid microspheres and nanospheres (SLM and SLN), Eur. J. Pharm. Biopharm. 110 (2017) 24–30, https://doi.org/10.1016/j.ejpb.2016.10.023.
[30] C. Puglia, M.G. Sarpietro, F. Bonina, F. Castelli, M. Zammataro, S. Chiechio, Development, characterization, and in vitro and in vivo evaluation of benzocaine- and lidocaine-loaded nanostructured lipid carriers, J. Pharm. Sci. 100 (2011) 1892–1899, https://doi.org/10.1002/jps.22416.
[31] E. Lasoń, E. Sikora, J. Ogonowski, Influence of process parameters on properties of Nanostructured Lipid Carriers (NLC) formulation, Acta Biochim. Pol. 60 (2013) 773–777 http://www.ncbi.nlm.nih.gov/pubmed/24432330.
[32] W. Zhang, X. Li, T. Ye, F. Chen, X. Sun, J. Kong, X. Yang, W. Pan, S. Li, Design, characterization, and in vitro cellular inhibition and uptake of optimized genistein-loaded NLC for the prevention of posterior capsular opacification using response surface methodology, Int. J. Pharm. 454 (2013) 354–366, https://doi.org/10.1016/j.ijpharm.2013.07.032.
[33] K. Kawakami, C. Sumitani, Y. Yoshihashi, E. Yonemochi, K. Terada, Investigation of the dynamic process during spray-drying to improve aerodynamic performance of inhalation particles, Int. J. Pharm. 390 (2010) 250–259, https://doi.org/10.1016/j.ijpharm.2010.02.018.
[34] T. Wang, Q. Hu, M. Zhou, J. Xue, Y. Luo, Preparation of ultra-fine powders from polysaccharide-coated solid lipid nanoparticles and nanostructured lipid carriers by innovative nano spray drying technology, Int. J. Pharm. 511 (2016) 219–222, https://doi.org/10.1016/j.ijpharm.2016.07.005.
[35] E.M. Ahmed, Hydrogel: preparation, characterization, and applications: a review, J. Adv. Res. 6 (2015) 105–121 https://doi.org/10.1016/j.jare.2013.07.006.
[36] ProCepT 4M8-TriX: Installation and Operation Manual: Fluid Bed, pan Coater, Spray Dryer, Nitrogen Unit, Zelzate, Belgium, n.D.
[37] K.P. Drapala, M.A.E. Auty, D.M. Mulvihill, J.A. O'Mahony, Influence of emulsifier type on the spray-drying properties of model infant formula emulsions, Food Hydrocolloids 69 (2017) 56–66, https://doi.org/10.1016/j.foodhyd.2016.12.024.
[38] D.P. Gaspar, C. Serra, P.R. Lino, L. Gonçalves, P. Taboada, C. Remuñán-López, A.J. Almeida, S.L.N. Microencapsulated, An innovative strategy for pulmonary protein delivery, Int. J. Pharm. 516 (2017) 231–246, https://doi.org/10.1016/j.ijpharm.2016.11.037.
[39] C. Freitas, R.H. Müller, Correlation between long-term stability of solid lipid nanoparticles (SLN(TM)) and crystallinity of the lipid phase, Eur. J. Pharm. Biopharm. 47 (1999) 125–132, https://doi.org/10.1016/S0939-6411(98)00074-5.
[40] A. Garcês, M.H. Amaral, J.M. Sousa Lobo, A.C. Silva, Formulations based on solid lipid nanoparticles (SLN) and nanostructured lipid carriers (NLC) for cutaneous use: a review, Eur. J. Pharm. Sci. 112 (2018) 159–167, https://doi.org/10.1016/j.ejps.2017.11.023.
[41] G. Pilcer, T. Sebti, K. Amighi, Formulation and characterization of lipid-coated tobramycin particles for dry powder inhalation, Pharm. Res. 23 (2006) 931–940, https://doi.org/10.1007/s11095-006-9789-4.
[42] A. Pourjavadi, G.R. Mahdavinia, pH-sensitivity and swelling kinetics of partially hydrolyzed chitosan-g-poly(acrylamide) hydrogels, Turk. J. Chem. 30 (2006) 595–608.
[43] A. Martínez-Ruvalcaba, J.C. Sánchez-Díaz, F. Becerra, L.E. Cruz-Barba, A. González-Álvarez, Swelling characterization and drug delivery kinetics of polyacrylamide-co-itaconic acid/chitosan hydrogels, Express Polym. Lett. 3 (2009) 25–32, https://doi.org/10.3144/expresspolymlett.2009.5.
[44] F. Ahmadi, Z. Oveisi, M. Samani, Z. Amoozgar, Chitosan based hydrogels: characteristics and pharmaceutical applications, Res. Pharm. Sci. 10 (2015) 1–16 http://www.ncbi.nlm.nih.gov/pmc/articles/PMC4578208/.
[45] R.A.B. Sanad, H.M. Abdel-Bar, Chitosan–hyaluronic acid composite sponge scaffold enriched with Andrographolide-loaded lipid nanoparticles for enhanced wound healing, Carbohydr. Polym. 173 (2017) 441–450, https://doi.org/10.1016/j.carbpol.2017.05.098.
[46] D. Queen, J.D.S. Gaylor, J.H. Evans, J.M. Courtney, W.H. Reid, The preclinical evaluation of the water vapour transmission rate through burn wound dressings, Biomaterials 5 (1987) 367–371 http://www.ncbi.nlm.nih.gov/entrez/query.fcgi?cmd=Retrieve&db=PubMed&dopt=Citation&list_uids=3676423.
[47] S.N. Shrotriya, B.V. Vidhate, M.S. Shukla, Formulation and development of Silybin loaded solid lipid nanoparticle enriched gel for irritant contact dermatitis, J. Drug Deliv. Sci. Technol. 41 (2017) 164–173, https://doi.org/10.1016/j.jddst.2017.07.006.
[48] Y.Y. Liu, X.D. Fan, B.R. Wei, Q.F. Si, W.X. Chen, L. Sun, pH-responsive amphiphilic hydrogel networks with IPN structure: a strategy for controlled drug release, Int. J. Pharm. 308 (2006) 205–209, https://doi.org/10.1016/j.ijpharm.2005.10.013.
[49] S.M. Ahsan, M. Thomas, K.K. Reddy, S.G. Sooraparaju, A. Asthana, I. Bhatnagar, Chitosan as biomaterial in drug delivery and tissue engineering, Int. J. Biol. Macromol. (2017), https://doi.org/10.1016/j.ijbiomac.2017.08.140.
[50] S. Doktorovová, A.B. Kovačević, M.L. Garcia, E.B. Souto, Preclinical safety of solid lipid nanoparticles and nanostructured lipid carriers: current evidence from in vitro and in vivo evaluation, Eur. J. Pharm. Biopharm. 108 (2016) 235–252, https://doi.org/10.1016/j.ejpb.2016.08.001.
[51] D. Raafat, K. Von Bargen, A. Haas, H.G. Sahl, Insights into the mode of action of chitosan as an antibacterial compound, Appl. Environ. Microbiol. 74 (2008) 3764–3773, https://doi.org/10.1128/AEM.00453-08.
[52] İ. Gulcin, M.E. Buyukokuroglu, O.I. Kufrevioglu, Metal chelating and hydrogen peroxide scavenging effects of melatonin, J. Pineal Res. 34 (2003) 278–281, https://doi.org/10.1034/j.1600-079X.2003.00042.x.
[53] European Medicines Agency, Decision trees for the selection of sterilisation methods, CPMP/QWP/054/98), 2000. https://www.ema.europa.eu/en/documents/scientific-guideline/decision-trees-selection-sterilisation-methods-cpmp/qwp/054/98-annex-note-guidance-development-pharmaceutics-cpmp/qwp/155/96_en.pdf.
[54] N.G. Madian, M. El-Hossainy, W.A. Khalil, Improvement of the physical properties of chitosan by γ-ray degradation for wound healing, Results Phys (2018), https://doi.org/10.1016/j.rinp.2018.10.051.
[55] G. Zhang, X. Li, X. Xu, K. Tang, V.H. Vu, P. Gao, H. Chen, Y.L. Xiong, Q. Sun, Antimicrobial activities of irradiation-degraded chitosan fragments, Food Biosci (2019), https://doi.org/10.1016/j.fbio.2019.03.011.
[56] R. Shah, D. Eldridge, E. Palombo, I. Harding, Lipid Nanoparticles: Production, Characterization and Stability, Springer, Cham, Switzerland, 2015, https://doi.org/10.1007/978-3-319-10711-0.
[57] D. Zetner, L.P.H. Andersen, J. Rosenberg, Melatonin as protection against radiation injury: a systematic review, Drug Res. (Stuttg) (2016), https://doi.org/10.1055/s-0035-1569358.

Supplementary material

Melatonin loaded lipid enriched chitosan microspheres – hybrid dressing for moderate exuding wounds

Marieta Duvnjak Romić[a], Drago Špoljarić[a], Maja Šegvić Klarić[b], Biserka Cetina-Čižmek[a], Jelena Filipović-Grčić[c] and Anita Hafner[c,] *

1. Supplementary Materials and Methods

S1.1 Lipid screening

A compatibility screening between lipids was performed. Binary mixtures of each solid (Compritol® 888 ATO (glycerol dibehenate), Precirol ATO 5 (glycerol distearate) and glycerol tristearate), and liquid lipid (Miglyol® 812N, 810N, Polysorbate 80 and castor oil) in the ratio 9:1 (*w/w*) were prepared and heated at 85 °C for 30 min. The mixtures were cooled down to room temperature and inspected for visual homogeneity after 24 hours.

The solubility of melatonin in solid lipids, liquid lipids, and their mixtures was tested by successive addition of pre-weighted amounts of the drug substance. Evaluation was assessed by visual observation of dissolution extent, i.e. the possibility to form a transparent homogeneous system [1,2]

S1.2 NLCs drug loading

NLC suspensions were 2-fold diluted with ultra-purified water, placed in the upper chamber of the Amicon tube (Ultra-30kDa MWCO, Millipore, Germany) and centrifuged at 5000 rpm for 30 min. The filtrate containing free drug was evaluated for the melatonin content by high performance liquid chromatography (HPLC) assay method. An HPLC system, which consisted of an Agilent 1100 Series instrument (Agilent Technologies, Germany) equipped with a diode array detector set at 224 nm, was used to perform the assay. The mobile phase, consisting HPLC grade water and acetonitrile in the ratio of 52/48, was used at a flow rate of 1 mL/min. The column (Kinetex C18 column 50×4.6 mm^2, particle size 5 mm, Phenomenex, USA) suited with an in-line filter (KrudKatcher Ultra HPLC, 0.5 µm Depth Filter × 0.004 in, Phenomenex, USA) was operated at 30 °C. The sample injection volume was 10 µL. The elution was isocratic, and the run time was 1 min.

S1.3 Drug loading of hybrid system

Microspheres were dispersed in 1 M HCl/acetonitrile (volume ratio of 1/1). The dispersion was shortly sonicated, filtered (0.2 µm), and diluted with the mixture of 96 % ethanol and purified water in 1:4 volume ratio. Drug content in the diluted sample was evaluated by high performance HPLC assay method described above.

S1.4 Wound dressing characterisation

Swelling properties of hybrid system were determined by volumetric method. The receiver compartment was filled with the simulated wound fluid (SWF) consisting of 50% foetal calf serum (Sigma Aldrich, Italy) and 50% maximum recovery diluent (Sigma Aldrich, Italy, composed of 0.1% (w/v) peptone, peptic digest of animal

tissue, and 0.9% (w/v) sodium chloride) [3] with pH adjusted to 6.3 and 7.4. SWF was thermostated at 37 °C. A regenerated cellulose membrane (0.45 μm pore size) with 10 mg of microsphere sample was placed between the donor and the receiver compartment. SWF level in graduated part of receiver compartment lowered due to liquid uptake of the microspheres. At set time intervals, receiver compartment was filled with SWF up to the starting level.

The swelling kinetics was evaluated using five mathematical models [4,5] – zero-order, which describes the swelling independent of concentration; first-order model, where swelling rate is dependent on concentration; second-order, where swelling depends on the system factors, and Higuchi model, which characterizes swelling based on Fick's law of diffusion. The determination coefficient (R^2) was used as an indicator of the model fit quality. To elucidate the fluid uptake transport mechanism, swelling curve was fitted to Korsmeyer-Peppas model and diffusion coefficient was determined [6].

S1.5 In vitro drug release study

A dialysis membrane with 12-14 kDa MWCO was inserted between the donor and the receiver compartment of the Franz diffusion cell. Receiver compartment was filled with the phosphate buffer pH 6.3 or pH 7.4. The microspheres containing 1.5 mg of melatonin were placed on the donor side, fully covering the membrane. The system was thermostated at 37 °C. The receiving medium was continuously stirred (600 rpm) with a magnetic stirrer. At the set time intervals, the samples (1 mL) were withdrawn from the receiver compartment and replaced with the equal volume of the fresh medium. The drug was detected according to the HPLC assay method described above. All release experiments were performed in triplicate.

The *in vitro* release kinetics and transport mechanism were evaluated as described for swelling kinetics, omitting second-order kinetics.

S1.6 In vitro cytotoxicity

HaCaT and MJ90hTERT cells were seeded onto 24-well plates and, after reaching confluence, treated with hybrid system suspension in buffered Hank's balanced salt solution (HBSS) containing melatonin and chitosan at concentration ranging from 0.015 – 0.30 and 0.03 – 0.06 mg/mL, respectively. After the treatment, *in vitro* cytotoxicity was determined by MTT and lactate dehydrogenase (LDH) leakage assay. Cells incubated in HBSS were used as negative control, while cells treated with 1 % Triton X-100 served as positive control. Cell viability was calculated by the equation (1):

$$Cell\ viability\ (\%) = 100 - \frac{\text{experimental value} - \text{negative control}}{\text{positive control} - \text{negative control}}\, x\ 100 \qquad (1)$$

2. Supplementary Results

Table S1. Regression coefficient estimates of the interaction models linking the formulation and process parameters (in terms of coded factors) with responses. P-values are given to indicate the significance of the influence of the given parameter

Term	Estimate	p-value
NLC particle size		
Intercept	214.3647	<.0001
N-LC (%) (5,10)	5.4357	0.0013
LLC (%) (10,20)	-3.4929	0.0208
H (min) (10,20)	-4.1071	0.0086
Hybrid system particle size		
Intercept	3.1744	<.0001
LLC (%) (10, 20)	-0.2600	0.0400
H (min) (10,20)	0.3000	0.0212
H (min)*H (min)	0.9084	0.0064
Process yield		
Intercept	42.1300	<.0001
H-LC (%) (15.5,26.9)	-3.9807	0.0326
LLC (%)*H-LC (%)	-3.9867	0.0446
LLC (%)*LLC (%)	17.8500	0.0009
H-LC (%)*H-LC (%)	-9.0250	0.0431
Zeta potential		
Intercept	23.1706	<.0001
H-LC (%) (15.5,26.9)	-2.1357	0.0384
Moisture content		
Intercept	4.7371	<.0001
N-LC (%) (5,10)	-0.4519	0.0044
H-LC (%) (15.5, 26.9)	-0.4344	0.0055
LLC (%)*F (mL/min)	0.4057	0.0129
F (mL/min)*T (°C)	0.3690	0.0203

N-LC - Total lipid content in NLC suspension; LLC - Liquid lipid content in NLC; H - Homogenisation time; H-LC – Hybrid system total lipid content; F - Feed rate; T - Inlet air temperature

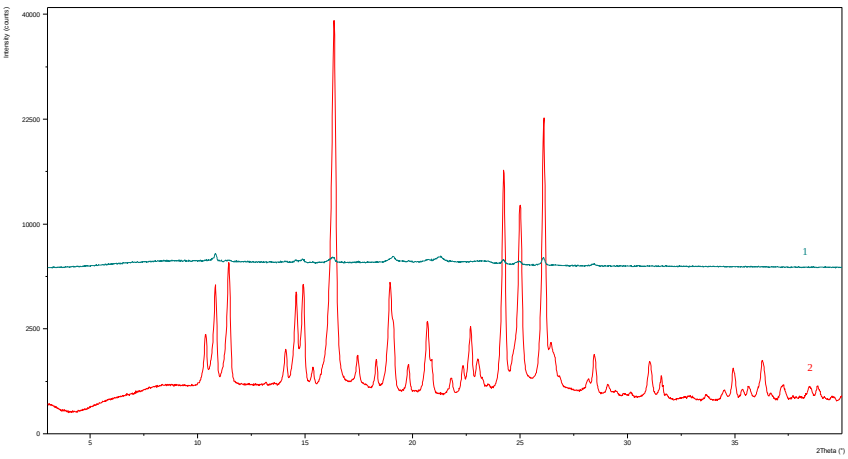

Figure S1. X-ray diffractographs of hybrid system (1) and crystalline melatonin (2)

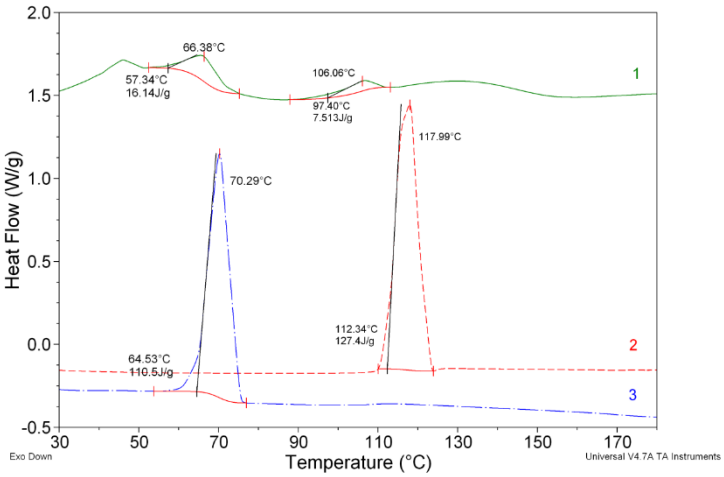

Figure S2. DSC thermographs of hybrid system (1), crystalline melatonin (2) and crystalline Compritol® 888 ATO (3)

Table S2. Determination coefficients for Zero, First, Second order and Higuchi models for swelling profiles in SWF pH 6.3 and 7.4 media and corresponding values of Korsmeyer-Peppas diffusion exponents (n_s)

Kinetic model	**pH 6.3**	**pH 7.4**
	R^2	
Zero order	0.9305	0.9708
First order	0.9327	0.9893
Second order	0.9972	0.9964
Higuchi	0.9679	0.9891
Korsmeyer-Peppas	n_s=0.5673	n_s=0.7668

Table S3. Determination coefficients for Zero, First order and Higuchi models for melatonin release profiles in pH 6.3 and 7.4 media and corresponding values of Korsmeyer-Peppas diffusion exponents (n_s).

Kinetic model	**pH 6.3**	**pH 7.4**
	R2	
Zero order	0.9346	0.7721
First order	0.9743	0.8939
Higuchi	0.9877	0.9816
Korsmeyer-Peppas	ns=0.5259	ns=0.4805

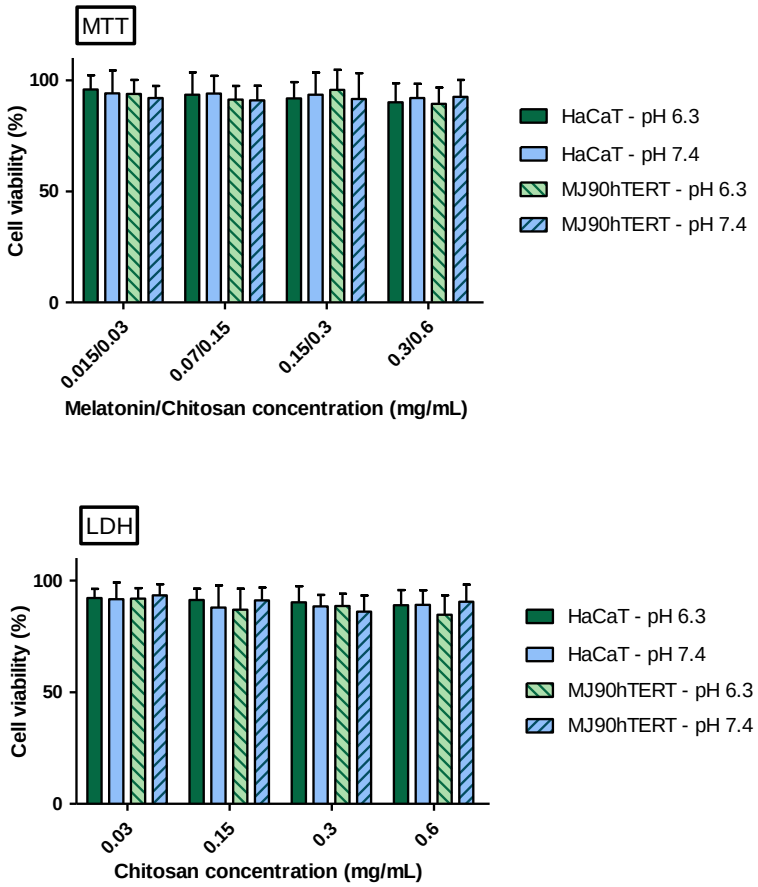

Figure S4 Keratinocytes (HaCaT, solid filling) and fibroblasts (MJ90hTERT, strapped filling) viability (%) determined by MTT (LDH) after 2h of incubation on 37°C with hybrid system resuspended in HBSS buffer pH 6.3 and pH 7.4 (mean values ± S.D. n=3)

Supplementary References

[1] S.N. Shrotriya, B. V. Vidhate, M.S. Shukla, Formulation and development of Silybin loaded solid lipid nanoparticle enriched gel for irritant contact dermatitis, J. Drug Deliv. Sci. Technol. 41 (2017) 164–173. doi:10.1016/j.jddst.2017.07.006.

[2] P.O. Nnamani, S. Hansen, M. Windbergs, C.M. Lehr, Development of artemether-loaded nanostructured lipid carrier (NLC) formulation for topical application, Int. J. Pharm. 477 (2014) 208–217. doi:10.1016/j.ijpharm.2014.10.004.

[3] P.G. Bowler, S. Welsby, V. Towers, R. Booth, A. Hogarth, V. Rowlands, A. Joseph, S.A. Jones, Multidrug-resistant organisms, wounds and topical antimicrobial protection, Int. Wound J. 9 (2012) 387–396. doi:10.1111/j.1742-481X.2012.00991.x.

[4] A. Martínez-Ruvalcaba, J.C. Sánchez-Díaz, F. Becerra, L.E. Cruz-Barba, A. González-Álvarez, Swelling characterization and drug delivery kinetics of polyacrylamide-co-itaconic acid / chitosan hydrogels, EXPRESS Polym. Lett. 3 (2009) 25–32. doi:10.3144/expresspolymlett.2009.5.

[5] T. Higuchi, Mechanism of sustained-action modification. Theoretical analysis of rate of release of solid drugs dispersed insolid matrices, J Pharm Sci. 52 (1963) 1145–1149. http://www.ncbi.nlm.nih.gov/entrez/query.fcgi?cmd=Retrieve&db=PubMed&dopt=Citation&list_uids=14088963.

[6] R.W. Korsmeyer, R. Gurny, E. Doelker, P. Buri, N.A. Peppas, Mechanisms of potassium chloride release from compressed, hydrophilic, polymeric matrices: Effect of entrapped air, J. Pharm. Sci. 72 (1983) 1189–1191. doi:10.1002/jps.2600721021.

4. Evaluation of stability and *in vitro* wound healing potential of melatonin loaded (lipid enriched) chitosan based microspheres

Acta Pharm. **69** (2019) 635–648
https://doi.org/10.2478/acph-2019-0049

Original research paper

Evaluation of stability and *in vitro* wound healing potential of melatonin loaded (lipid enriched) chitosan based microspheres

MARIETA DUVNJAK ROMIĆ[1]
ANJA SUŠAC[2]
JASMINA LOVRIĆ[2]
BISERKA CETINA-ČIŽMEK[1]
JELENA FILIPOVIĆ-GRČIĆ[2]
ANITA HAFNER[2,*]

[1] *R&D, PLIVA Croatia Ltd, TEVA Group Member, Zagreb, Croatia*

[2] *University of Zagreb Faculty of Pharmacy and Biochemistry, Department of Pharmaceutical Technology, Zagreb Croatia*

Accepted June 23, 2019
Published online July 31, 2019

The aim of this study was to evaluate long-term stability and assess the wound healing potential of the innovative melatonin-loaded lipid-enriched hybrid system compared to conventional melatonin-loaded chitosan microspheres. The hybrid system contained nanostructured lipid carrier incorporated in the chitosan matrix, in order to modify melatonin release and alter physicochemical characteristics of the delivery system. Stability testing was performed during a six-month period under two conditions: refrigerated (5 ± 3 °C) and at room temperature (25 ± 2 °C/60 ± 5 % RH). Samples stored at both conditions were analyzed in terms of particle size, zeta potential, moisture content and thermal properties. At the end of testing, drug content was determined in all samples. Dressings wound healing potential was assessed by *in vitro* scratch test using human skin fibroblast cell line. Although both systems showed good stability characteristics, the addition of lipids in the system has improved its wound healing potential.

Keywords: melatonin, nanoparticles, microspheres, chitosan, stability, wound healing

Persisting non-healing wounds represent a massive burden for the worldwide healthcare system, with more than 25 billion USD spent per year in the US only (1). Population aging, high incidence of obesity and diabetes and a large number of burn injuries are recognized as a major cause of increased chronic wound prevalence. Wound healing is a well-coordinated physiological process, governed by different cell types and signals. Generally, healing can be divided into four ordered but overlapping processes of haemostasis, inflammation, proliferation and remodelling (2). In most of the cases, the healing process is interrupted during the inflammation phase. Although the aetiology is highly variable, persistent infection, biofilm formation and reduction of granulation and reepithelialisation are common characteristics associated with non-healing wounds (3, 4). High incidence of chronic wounds accompanied by increasing bacterial resistance justifies enlarged interest in the development of nonconventional, more efficient therapies.

* Correspondence; e-mail: ahafner@pharma.hr

Melatonin, mainly perceived as the pineal gland hormone, has pleiotropic activities as a neurotransmitter, cytokine, biological-response modifier, anti-inflammatory agent and free-radical scavenger (5). While full melatonin potential as a cutaneous agent still needs to be discovered (6), recent *in vitro* studies showed a positive impact on corneal and diabetic wound healing models (7, 8). Owing to its anti-oxidant and anti-inflammatory properties, melatonin shows potential for application in nonconventional dressings for burn and chronic wound treatment (9).

Among many nano-sized drug delivery systems, nanostructured lipid carriers (NLCs) are highly investigated as wound-healing agents (10). NLCs are nanoparticles composed of a blend of solid and liquid lipids (11), with adequate drug loading capacity and stability (compared to solid lipid nanoparticles), providing controlled drug release and skin hydration effect (12). Even though mainly acting as carriers for growth factors or antimicrobial agents (12, 13), it was reported that NLCs themselves can promote wound healing in a rat burn model (14).

Chitosan, a linear amino polysaccharide, is widely used as a wound healing promoter, due to its antibacterial, haemostatic and mucoadhesive properties (15). Chitosan-based dressings in form of gels and films are already present as marketed products, whereas in terms of novel systems, chitosan can be formulated as part of artificial skin, powder formulation or coupled to peptides (16).

Our group has recently verified the idea of combining the above-mentioned components for the development of two drug delivery systems for wound management, prepared by spray drying technology. The first one refers to fine-tuned melatonin-loaded chitosan/Pluronic® F127 microspheres characterized by small diameter, positive surface charge, efficient melatonin encapsulation and high rate and extent of fluid uptake. Formulated dry powder acted as *in situ* gel-forming dressing with antimicrobial activity, applicable for highly exuding wounds (17). In order to alter microparticulate dressing properties, the novel lipid-enriched hybrid system was developed, comprising NLCs within the chitosan/Pluronic® F127 matrix, with melatonin incorporated in both, the NLC and chitosan matrix. Influence of formulation and process parameters, on characteristics of prepared lipid and hybrid systems, was evaluated using Design of Experiments approach. The optimized hybrid system showed prolonged melatonin release and good flowability properties while maintaining antimicrobial activity. Reduced swelling and water retaining characteristics made it suitable for application to moderate exuding wounds (18). Both systems were shown to be biocompatible with skin keratinocytes and fibroblasts (17, 18).

The aim of this study was to evaluate and compare aforementioned (NLC free and NLC enriched, in the further text indicated as MCP and MLCP) melatonin delivery systems in terms of long-term stability and *in vitro* wound healing potential.

There are some literature reports on the stability of spray-dried chitosan-based powders (19, 20). However, although the conversion of lipid particles to dry powder *via* spray drying has been evaluated by other researchers (21, 22), stability assessment of the lipid component and the dry powder over time is scarce (23). Stability testing was performed during a six-month period under two conditions: refrigerated (5 ± 3 °C) and at room temperature (25 ± 2 °C/60 ± 5 % RH). Samples stored at both conditions were analysed in terms of particle size, zeta potential, moisture content and thermal properties. At the end of the testing, drug content was determined in all samples.

Dressings wound healing potential was assessed by completion of *in vitro* scratch test using human skin fibroblast cell line. *In vitro* scratch assay is a widely used conventional

assay that provides insight about formulation influence on cell migration and proliferation (24). As fibroblasts play a major role in the healing process during inflammation and remodelling phase (25), they were used for the evaluation of developed microsphere-based dressings.

EXPERMENTAL

Materials

Compritol® 888 ATO (glycerol dibehenate) was a kind gift from Gattefosse (France). Melatonin (China) and chitosan (≥ 75 % deacetylated powder, Japan) were purchased from Sigma-Aldrich. Pluronic® F127 was obtained from BASF (Germany). Miglyol® 812N was obtained from Sasol (Germany). All other chemicals and solvents used in the study were of analytical grade and procured from Kemika (Croatia) or Sigma-Aldrich.

Preparation of melatonin loaded chitosan/Pluronic® F127 microspheres

Melatonin loaded chitosan/Pluronic® F127 microspheres (MCP; *i.e.* NLC free microspheres) were prepared by spray drying method as previously described (17). Briefly, spray drying feed was prepared by mixing (*i*) solution of chitosan (10 g L^{-1}) in 0.5 % acetic acid solution with (*ii*) melatonin and Pluronic® F127 solution prepared in 96 % ethanol. Solutions were mixed at a volume ratio of 4/1, respectively, resulting in the spray drying feed with chitosan to melatonin ratio of 2/1 (Table I) and chitosan to Pluronic® F127 ratio of 5/1 (Table I). Spray drying was performed using a Mini Spray Dryer Büchi 190 (Flawil, Switzerland) with an inlet temperature of 145 °C, feed flow rate of 2.59 mL min^{-1}, a standard 0.7 mm nozzle and compressed air flow rate of 700 NL h^{-1}.

Preparation of melatonin loaded NLC enriched chitosan/Pluronic® F127 microspheres

Preparation of NLCs: Melatonin loaded NLCs were prepared by hot ultrasonication method optimized by our group (18). Briefly, melatonin was dissolved in a Compritol® 888 ATO/Miglyol® 812N mixture heated to 90 °C, at melatonin to lipid weight ratio of 2/5 (Table I). The aqueous phase containing Pluronic® F127 was heated to the same temperature and added dropwise to the lipid phase under magnetic stirring. The mass ratio of Pluronic® F127 to dispersed lipids in the obtained pre-emulsion was 1/3. Pre-emulsion was then

Table I. Composition of melatonin-loaded NLC free (MCP) and NLC enriched (MLCP) microspheres

Component	MCP		MLCP	
	Amount (%)	Mass ratio to chitosan	Amount (%)	Mass ratio to chitosan
Chitosan	58.8	–	46.1	–
Lipids content in the microspheres	–	–	21.6	2.3/5
Pluronic® F127	11.8	1/5	9.2	1/5
Melatonin content in the microspheres	29.4	1/2	23.1	1/2

subjected to probe sonication (UP200Ht Hielscher, Germany) and melatonin loaded NLCs were formed after cooling down to room temperature.

Preparation of microspheres. – As described in our previous work (18), spray-drying feed for the preparation of melatonin loaded NLC enriched microspheres (MLCP) was prepared by dropwise addition of dispersion of melatonin loaded NLCs to chitosan/melatonin/Pluronic® F127 solution prepared as for above-mentioned NLC free microspheres. The volume ratio of NLC dispersion to chitosan/melatonin/Pluronic® F127 solution was set to ensure lipid to chitosan mass ratio of 2.3/5 (Table I). Spray drying was performed using a ProCept 4M8-TriX Spray Dryer, with an inlet temperature of 110 °C, feed flow rate of 1.8 mL min^{-1} with a 0.6 mm nozzle and compressed nitrogen flow rate of 0.3 m^3 min^{-1}.

Physico-chemical characteristics of melatonin loaded (NLC enriched) microsphere

Particle size. – NLC free microspheres (MCP) size and distribution were determined by microscopic imaging analysis technique, using Olympus BH-2 microscope, equipped with a camera (CCD Camera ICD-42E; Ikegami Tsushinki Co., Tokyo, Japan) and computer-controlled image analysis system (Optomax V, Cambridge, UK), with at least 3000 particles examined. NLC enriched microsphere (MLCP) size and distribution were evaluated using a Malvern Morphology G3-ID (Malvern Instruments, UK) with a minimum of 10000 particles examined.

Zeta potential. – The zeta potential of the microspheres was determined by laser Doppler anemometry (Zetasizer 3000HS, Malvern Instruments, UK) at 25 °C, as described in our previous work (17). Briefly, microspheres were dispersed in 10 mM NaCl. Measurement was performed in an electrophoretic cell under the potential of 150 mV. Conversion of the measured electrophoretic mobility to zeta potential using the Helmholtz-Smoluchowski equation was performed within the system software.

Drug loading. – The content of melatonin within the microspheres was determined by the HPLC assay method as described previously (18). In short, dispersion of microspheres in 1 mol L^{-1} HCl/acetonitrile mixture (1/1, *V*/*V*) was first sonicated, then filtered and diluted with the mixture of 96 % ethanol and purified water (1/4, *V*/*V*).

An HPLC analysis was performed on Agilent 1100 Series instrument (Agilent Technologies, Germany) equipped with a diode array detector set at 224 nm. The mobile phase contained HPLC grade water and acetonitrile in the ratio of 52/48, The column (Kinetex C18 column 50 × 4.6 mm^2, particle size 5 mm, Phenomenex, USA) suited with an in-line filter (KrudKatcher Ultra HPLC, 0.5 μm Depth Filter × 0.004 in, Phenomenex, USA) was used. The analysis was performed under chromatographic conditions as follows: sample injection volume of 10 μL, isocratic elution, the run time of 1 min, the flow rate of 1 mL min^{-1} and the column temperature of 30 °C.

Thermal analyses. – Modulated differential scanning calorimetry (MDSC) analyses were performed using a TA Instrument modulated DSC Q2000 (TA Instruments, USA). Quantity of about 0.5–1.0 mg of the powder sample was weighed in aluminium standard pans. The analysis was performed under dynamic nitrogen atmosphere at the flow rate of 50 mL min^{-1}. Samples were scanned at the heating rate of 5 °C min^{-1} from 20 to 220 °C, with modulation of ± 1 °C (amplitude) each 60 s (period).

TGA Q5000 (TA Instruments, USA) was used to determine the moisture content in the microsphere samples. Thermogravimetric analysis was performed on the microsphere sample (about 5 mg) under dynamic nitrogen atmosphere at a flow rate of 35 mL min^{-1}. The samples were analysed at the heating rate of 10 °C min^{-1} in the temperature range of 25 to 500 °C.

Stability testing scheme. – Stability testing was performed during a six-month period. Sample containers were sealed, protected from light and kept refrigerated (5 ± 3 °C) and at room conditions (25 ± 2 °C/60 ± 5 % RH). Samples stored at both conditions were analysed in terms of particle size, zeta potential, moisture content and thermal properties. At the end of testing, drug content was determined in all samples.

In vitro *scratch assay*

In vitro scratch assay was performed using Human diploid fibroblast strain MJ90hTERT (kindly provided by Dr. Ivica Rubelj, Institute Ruđer Bošković, Zagreb, Croatia) (26), cultured in DMEM medium (GIBCO, UK) under supplementation with 10 % foetal bovine serum (FBS, GIBCO) and antimicrobial solution (Sigma-Aldrich).

MJ90hTERT cells were seeded onto 24-well plates and allowed to reach confluence over 1 day in DMEM medium supplemented with 10 % FBS. Subsequently, medium was removed and replaced with serum-free medium. Next day (24 h later) a straight scratch was made with a 100 μL pipette tip, to simulate a wound (27). The cell monolayer was washed with HBSS (pH 7.4) to remove detached cells and cell debris. The wound was exposed to MCP and MLCP suspensions, in HBSS pH 7.4 and 6.3, at melatonin concentration of 0.3 mg mL^{-1} and corresponding chitosan concentration of 0.6 mg mL^{-1}, that were set based on our previous studies. Namely, MCP and NLCP systems were shown to exhibit antimicrobial effect and fibroblast cell line compatibility at selected melatonin and chitosan concentrations (17, 18). Non-treated cells incubated in HBSS (pH 7.4 or 6.3) served as control. After the 2-hour treatment, cells were washed with HBSS pH 7.4 and incubated with serum-free medium. The closure of the scratch (*in vitro* wound healing) was monitored over 24 h using an inverted microscope (5× magnification; Olympus CKX41) equipped with a camera (Samsung, 16 MP, f/1.9). To measure the rate of scratch closure, the difference between wound area at time 0 and after 24 h was determined. Each well was marked below the plate surface by drawing a vertical line, to enable exploration and evaluation of the same scratched zone. Scratch area was estimated using ImageJ software (National Institutes of Health, USA). Wound healing rate (WHR) was expressed as a percentage of the scratch closure on an initial area basis, according to the following equation:

$$WHR = \frac{A_0 - A_{24}}{A_0} \times 100$$

where A_0 is the scratch area at time 0, and A_{24} is the corresponding scratch area at 24 h. The values shown are the means of three wells from three independent experiments.

Statistical analysis

Statistical data analyses were performed on all *in vitro* data by one-way analysis of variance (ANOVA) followed by multiparametric Tukey's post hoc test with $p < 0.05$ as the minimal level of significance. Calculations were performed using GraphPad Prism software (GraphPad Software, Inc., USA).

RESULTS AND DISCUSSION

Physico-chemical characteristics of melatonin loaded (NLC enriched) microspheres

NLC free an NLC enriched microspheres were successfully prepared by spray drying method. Main characteristics of the microspheres (mean diameter, zeta potential and moisture content) are reported in Table II.

Mean diameter of MLCP was higher than the mean diameter of MCP (3.3 *vs.* 2.7 μm, Table II). During the six-month storage at both conditions (5 °C and 25 °C/60 % RH), no significant changes in particle size for both samples were observed. This is in agreement with the literature report on accelerated stability studies of chitosan-based spray dried microspheres conducted at 40 ± 2 °C and 75 ± 5 % RH for a period of 3 months (28).

Both types of microspheres were initially characterised with positive surface charge due to the presence of chitosan at the microsphere surface, with lower values for MLCP due to the presence of negatively charged lipids in the system. Although slight changes in zeta potential during storage were observed for both samples, the decrease was shown not to be significant (Table II).

MCP had lower initial moisture content compared to MLCP (Table II), which could be explained by higher inlet temperature employed (145 °C *vs.* 110 °C, respectively) during spray drying. Higher inlet temperature resulted in higher outlet temperature and consequent lower moisture content of the MCP microspheres at the end of the drying process (21). However, upon storage, moisture content of MCP increased by ~20 % for samples kept at 5 °C and by ~40 % for samples kept at 25 °C/60 % RH. No change in the moisture content

Table II. Characteristics of melatonin-loaded NLC free microspheres (MCP) and melatonin-loaded NLC enriched microspheres (MLCP) during stability testing[a]

Time (month)	Mean diameter (μm)		Zeta potential (mV)		Moisture content (%)	
	MCP	MLCP	MCP	MLCP	MCP	MLCP
start	2.7 ± 0.3	3.3 ± 0.2[b]	29.0 ± 2.0	26.6 ± 0.5[b]	2.5 ± 0.1	4.7 ± 0.1[b]
Stored at 5 °C						
1	2.7 ± 0.9	3.2 ± 0.4	25.3 ± 1.0	26.1 ± 0.5	3.0 ± 0.1	4.4 ± 0.1
2	2.6 ± 0.4	3.0 ± 0.2	29.9± 0.8	26.4 ± 0.9	3.0 ± 0.1	4.4 ± 0.2
3	2.6 ± 0.1	3.1 ± 0.3	26.8 ± 2.8	25.7 ± 1.1	2.9 ± 0.2	4.5 ± 0.1
6	2.6 ± 0.5	3.2 ± 0.5	25.9 ± 3.8	25.3 ± 1.0	3.1 ± 0.3	4.5 ± 0.1
Stored at 25 °C/60 % RH						
1	2.8 ± 0.0	3.3 ± 0.3	23.0 ± 0.5	25.9 ± 0.7	3.4 ± 0.1	4.5 ± 0.2
2	2.4 ± 0.8	3.4 ± 0.4	24.6 ± 1.1	26.0 ± 0.4	3.6 ± 0.6	4.6 ± 0.2
3	2.5 ± 0.8	3.2 ± 0.3	24.6 ± 1.8	25.4 ± 0.5	3.5 ± 0.1	4.5 ± 0.0
6	2.4 ± 0.3	3.4 ± 0.5	23.7 ± 0.7	25.1 ± 1.1	± 0.1	4.5 ± 0.2

[a] mean values ± SD, $n = 3$

[b] Characterization results at the start of testing for MLCP have already been reported by Duvnjak Romić *et al*. (18).

for MLCP microspheres was observed, regardless of the storage conditions employed. It is well known that chitosan's positively charged amino groups are prone to capture water (29). Lower water sorption of MLCP microspheres in comparison to MCP microspheres might be explained by the interaction between positively charged chitosan and negatively charged lipids acting as matrix stabilizing agents. Although ionic interactions between components were not previously detected, weak ionic associations that manifest as lower positive zeta potential in case of MLCP microspheres could be present (18).

It is known that melatonin is susceptible to degradation on exposure to air and light (30), while when formulated in dosage form, its stability is improved (31). Thus, melatonin content in microspheres was determined after six-month storage. In the case of MCP sample, no changes in melatonin content were observed. Samples stored refrigerated and at room temperature contained more than 97 % of the melatonin at the end of the testing period. The MLCP microspheres showed a slight decrease in content, with 93 % melatonin remaining in the MLCP microspheres after 6 months at 5 °C and 91 % under room conditions.

Thermal characteristics of melatonin loaded NLC free and NLC enriched microspheres

Thermal analyses of microspheres were employed in order to determine and monitor components' behaviour and interactions during storage. Crystalline melatonin is characterized by an endothermic peak (melting point, T_m) appearing at midpoint temperature of

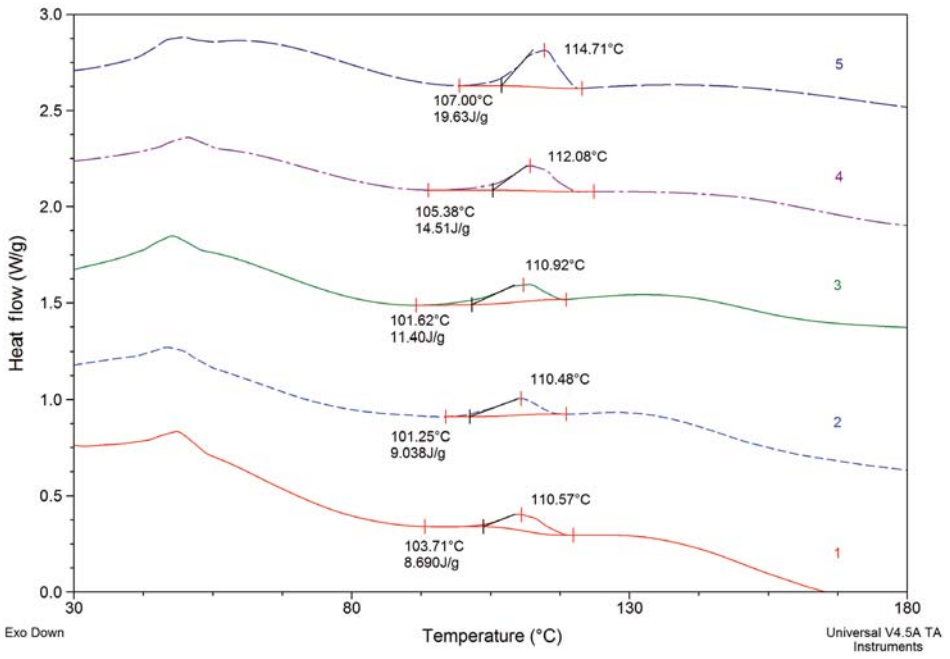

Fig. 1. DSC thermographs of melatonin loaded microspheres (MCP) immediately after the preparation (1), and after one (2), two (3), three (4) and six months (5) at 5 ± 3 °C.

117.88 °C with the heat of fusion of 140.2 J g^{-1} (17). Melatonin melting point in MCP immediately upon the preparation is detected at 110.57 °C (Fig. 1 and 2), which indicates an interaction of the drug with polymers (chitosan and lipids). The decrease in heat of fusion of melatonin in microspheres indicates the occurrence of partially amorphous melatonin due to the spray drying process (17). Therefore, midpoint temperature and heat of fusion were used as indicators of the melatonin state in the MCP during storage. In the Fig. 1 it can be seen that throughout the storage time at 5 °C, T_m and heat of fusion values increase, as a sign of the progressive transformation of amorphous melatonin to the crystalline state.

Fig. 2 presents the thermographs of the MCP throughout storage at 25 °C/60 % RH. Although the shift of melting point towards higher temperature is observed, the heat of fusion does not change significantly over time indicating improved stability of the MCP at a higher temperature. As microspheres contain a moderate amount of moisture, Pluronic® F127 could easily be dissolved at low temperatures (32). This effect could lead to the dissolution of amorphous melatonin and consequent precipitation as crystalline material when the temperature increases. The above hypothesis could explain improved MCP stability when stored at room temperature.

Thermographs of MLCP samples were characterized by an additional endothermic peak attributed to the melting point (T_m) of solid lipid Compritol® 888 ATO (Figs. 3 and 4). Compared to pure Compritol® 888 ATO that has T_m at 70.3 °C (18), the shift of the melting point towards lower temperature was observed in MLCPs. When formulated in NLCs, solid lipids are organised in less ordered structures, thus promoting the inclusion of drug

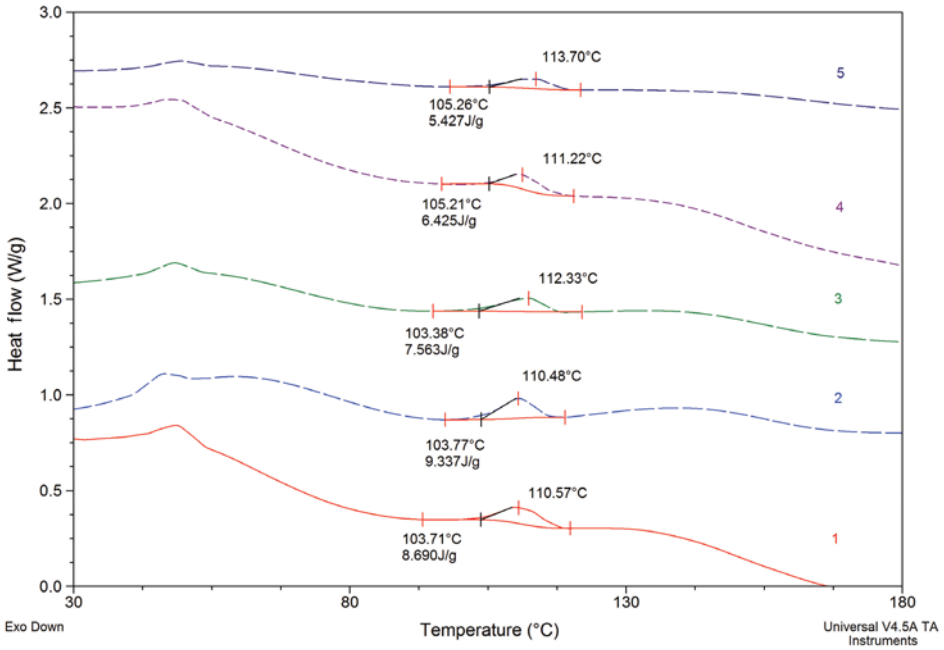

Fig. 2. DSC thermographs of melatonin loaded microspheres (MCP) immediately after the preparation (1) and after one (2), two (3), three (4) and six months (5) at 25 °C/60 % RH.

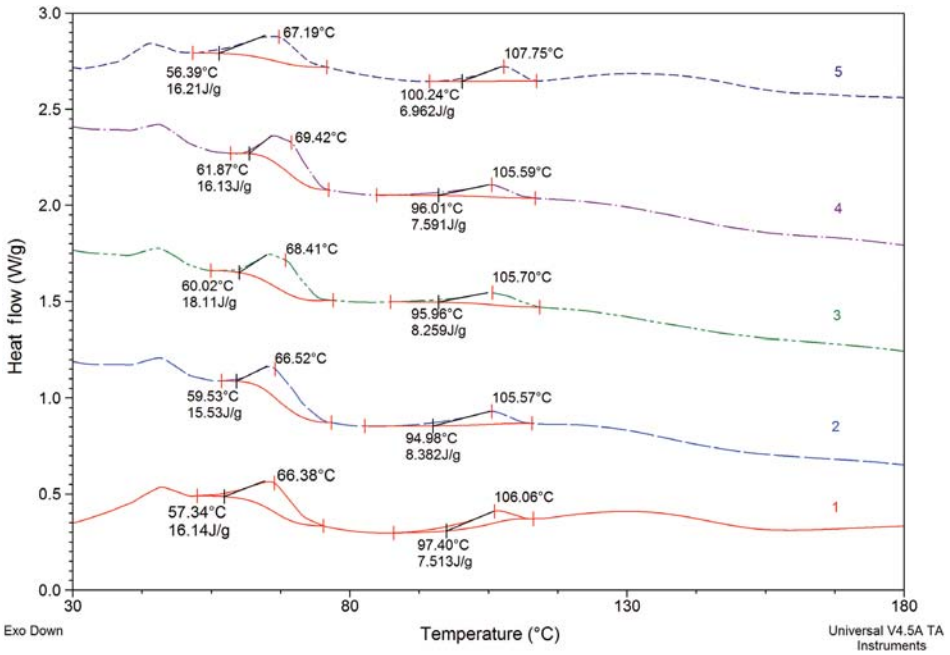

Fig. 3. DSC thermographs of melatonin loaded NLC enriched microspheres (MLCP) immediately after the preparation (1) and after one (2), two (3), three (4) and six months (5) at 5 ± 3 °C.

molecules and enhancing drug stability (33). Therefore, the shift in T_m for Compritol® 888 ATO demonstrates the presence of NLCs within the microspheres. Considering the latter, T_m and heat of fusion for both, melatonin and Compritol® 888 ATO were evaluated during MLCP stability study.

Fig. 3 represents thermographs of MLCP samples stored for 6 months at 5 °C. It was observed that no significant changes in T_m or heat of fusion for both melatonin and Compritol® 888 ATO occurred. Results indicate that after six months there was no change in the crystalline state of melatonin and that lipids still existed in the form of NLCs within the microspheres.

When stored at room temperature (Fig. 4), change in the state of Compritol® 888 ATO to the most stable form occurred, which is indicated with an increase in T_m and the heat of fusion. At the same time, there was no significant change in T_m and heat of fusion related to melatonin. Observed data showed that decomposition of NLC within microspheres progressed with time at 25 °C/60 % RH, while there was no significant change in melatonin state or content.

In vitro *scratch wound healing assay*

In vitro scratch wound healing assay was carried out to evaluate the effect of developed MCP and MLCP microspheres on fibroblast migration/proliferation and consequent wound repair potential. Microspheres were dispersed in HBSS buffer set to physiologically

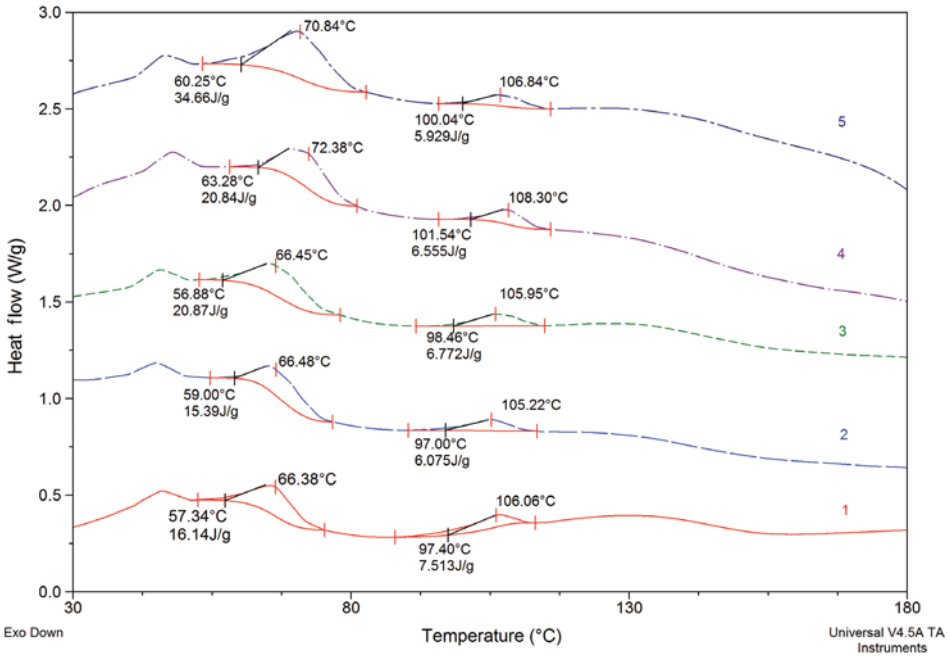

Fig. 4. DSC thermographs of melatonin loaded NLC enriched microspheres (MLCP) immediately after the preparation (1) and after one (2), two (3), three (4) and six months (5) at 25 °C/60 % RH.

relevant pH 7.4 and pH 6.3, that has been measured in the bacterial broth (17). Although it was postulated that an increase in wound bed pH indicates contamination and interruption in healing (35), lower micro-environmental pH milieu is expected for saccharolytic

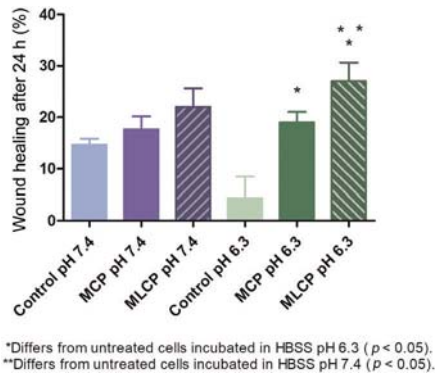

Fig. 5. Influence of melatonin loaded microspheres (MCP) and melatonin loaded NLC enriched microspheres (MLCP) dispersed in HBSS (pH 7.4 or 6.3) on scratch wound healing (mean values ± SD, $n = 3$). The wound closure rate is expressed as the percentage of scratch closure after 24 h compared to the initial area (0 h). Controls refer to untreated cells incubated in HBSS medium (pH 7.4 or 6.3).

bacterial infections (36). Our group has previously reported biocompatibility of MCP and MLCP systems with human skin cell lines at both pH levels, namely pH 7.4 and pH 6.3 (17, 18). Results presented in Fig. 5 reveal that MPC and MLPC accelerated wound healing when compared to the control in the 24-h period after cell treatment. These results indicate that developed systems retained the healing potential of the main components reported previously by other researchers (27, 37–39).

Although improvement in wound healing rate after treatment at pH 7.4 was observed, it was not found significant. However, major improvement of scratch closure was obtained at pH 6.3, indicating the beneficial effect of partially solubilized chitosan in slightly acidic conditions. Proliferation/migration of untreated fibroblasts incubated in HBSS at pH 6.3 (Control pH 6.3; Fig. 5) was the lowest among all the tested variants. Due to the simplicity of the scratch assay, replicating only a limited segment of the tissue structure and function of the wound bed, higher susceptibility of cell monolayer to non-physiological pH is anticipated. Therefore, healing of model wounds treated with microsphere suspensions in HBSS at pH 6.3 (MCP pH 6.3 and MLCP pH 6.3, Fig. 5) was also evaluated in comparison to the untreated model wound incubated in HBSS at pH 7.4 (Control pH 7.4; Fig. 5). Even in that case, the improved closure of wound treated with MLCP was found significant. More prominent wound closure for cells treated with MLCP in relation to MCP signifies the beneficial effect of lipids in the system. A similar concept where NLCs acted as an accompanying healing factor in the wound dressing was recently proposed and confirmed by other researchers (40, 41).

CONCLUSIONS

In this study, long term stability of NLC enriched and NLC free microspheres was assessed at refrigerated (5 ± 3 °C) and room temperature (25 ± 2 °C/60 ± 5 % RH) over a six-month period. Both systems showed good stability in general, with NLC free microspheres favouring storage at room temperature due to better preservation of amorphous melatonin. Oppositely, the lower temperature is the condition of choice for long term storage in case of NLC enriched microspheres, as a result of improved conservation of lipid nanosystem. *In vitro* scratch wound healing assay showed the respectable potential of developed systems for application as a functional wound dressing.

Acknowledgments. – This research was supported by PLIVA Croatia Ltd, TEVA Group Member, as part of the project "Melatonin-loaded chitosan (nano)systems".

REFERENCES

1. R. G. Frykberg and J. Banks, Challenges in the treatment of chronic wounds, *Adv. Wound Care* **4** (2015) 560–582; https://doi.org/10.1089/wound.2015.0635
2. T. Shipperley, C. Martin and B. Healthcare, The physiology of wound healing : an emergency response, *Surg.* **35** (2011) 8–10; http://www.sciencedirect.com/science/article/pii/S0263931917301369
3. K. Kaplani, S. Koutsi, V. Armenis, F. G. Skondra, N. Karantzelis, S. Champeris Tsaniras and S. Taraviras, Wound healing related agents: Ongoing research and perspectives, *Adv. Drug Deliv. Rev.* (2018); https://doi.org/10.1016/j.addr.2018.02.007

4. Y.-K. Wu, N.-C. Cheng and C.-M. Cheng, Biofilms in chronic wounds: pathogenesis and diagnosis, *Trends Biotechnol.* **37** (2019) 505–517; https://doi.org/10.1016/j.tibtech.2018.10.011
5. R. J. Reiter, D.-X. Tan, L. Fuentes-Broto and M. Luciano, *Chapter 8 – Melatonin: A multitasking molecule*, *Progress in Brain Res.* **181** (2010) 127–151; https://doi.org/10.1016/S0079-6123(08)81008-4
6. R. Hardeland, A. T. Slominski, R. M. Slominski, R. J. Reiter, M. A. Zmijewski and R. Paus, Melatonin: A cutaneous perspective on its production, metabolism, and functions, *J. Invest. Dermatol.* **138** (2018) 490–499; https://doi.org/10.1016/j.jid.2017.10.025
7. A. Crooke, A. Guzman-Aranguez, A. Mediero, P. Alarma-Estrany, G. Carracedo, T. Pelaez, A. Peral and J. Pintor, Effect of melatonin and analogues on corneal wound healing: involvement of Mt_2 melatonin receptor, *Curr. Eye Res.* **40** (2015) 56–65; https://doi.org/10.3109/02713683.2014.914540
8. R. Song, L. Ren, H. Ma, R. Hu, H. Gao, L. Wang, X. Chen, Z. Zhao and J. Liu, Melatonin promotes diabetic wound healing in vitro by regulating keratinocyte activity, *Am. J. Transl. Res.* **8** (2016) 4682–4693.
9. R. Murali, P. Thanikaivelan and K. Cheirmadurai, Melatonin in functionalized biomimetic constructs promotes rapid tissue regeneration in Wistar albino rats, *J. Mater. Chem. B* **4** (2016) 5850; https://doi.org/10.1039/c6tb01221c.
10. I. Garcia-Orue, J. L. Pedraz, R. M. Hernandez and M. Igartua, Nanotechnology-based delivery systems to release growth factors and other endogenous molecules for chronic wound healing, *J. Drug Deliv. Sci. Technol.* **42** (2017) 2–17; https://doi.org/10.1016/j.jddst.2017.03.002
11. J. Pardeike, A. Hommoss and R. H. Müller, Lipid nanoparticles (SLN, NLC) in cosmetic and pharmaceutical dermal products, *Int. J. Pharm.* **366** (2009) 170–184; https://doi.org/10.1016/j.ijpharm.2008.10.003
12. G. Gainza, M. Pastor, J. J. Aguirre, S. Villullas, J. L. Pedraz, R. M. Hernandez and M. Igartua, A novel strategy for the treatment of chronic wounds based on the topical administration of rhEGF-loaded lipid nanoparticles: In vitro bioactivity and in vivo effectiveness in healing-impaired db/db mice, *J. Control. Release* **185** (2014) 51–61; https://doi.org/10.1016/j.jconrel.2014.04.032
13. N. Karimi, B. Ghanbarzadeh, H. Hamishehkar, B. Mehramuz and H. S. Kafil, Antioxidant, antimicrobial and physicochemical properties of turmeric extract-loaded nanostructured lipid carrier (NLC), *Colloid. Interface Sci. Commun.* **22** (2018) 18–24; https://doi.org/10.1016/j.colcom.2017.11.006
14. F. Saporito, G. Sandri, M. C. Bonferoni, S. Rossi, C. Boselli, A. I. Cornaglia, B. Mannucci, P. Grisoli, B. Vigani and F. Ferrari, Essential oil-loaded lipid nanoparticles for wound healing, *Int. J. Nanomed.* **13** (2018) 175–186; https://doi.org/10.2147/IJN.S152529
15. Z. Ma, A. Garrido-Maestu and K. C. Jeong, Application, mode of action, and in vivo activity of chitosan and its micro- and nanoparticles as antimicrobial agents: A review, *Carbohydr. Polym.* **176** (2017) 257–265; https://doi.org/10.1016/j.carbpol.2017.08.082
16. V. Patrulea, V. Ostafe, G. Borchard and O. Jordan, Chitosan as a starting material for wound healing applications, *Eur. J. Pharm. Biopharm.* (2015); https://doi.org/10.1016/j.ejpb.2015.08.004
17. M. Duvnjak Romić, M. Š. Klarić, J. Lovrić, I. Pepić, B. Cetina-Čižmek, J. Filipović-Grčić and A. Hafner, Melatonin-loaded chitosan/Pluronic® F127 microspheres as in situ forming hydrogel: An innovative antimicrobial wound dressing, *Eur. J. Pharm. Biopharm.* **107** (2016) 67–79; https://doi.org/10.1016/j.ejpb.2016.06.013
18. M. Duvnjak Romić, D. Špoljarić, M. Š. Klarić, B. Cetina-Čižmek, J. Filipović-Grčić and A. Hafner, Melatonin loaded lipid enriched chitosan microspheres – Hybrid dressing for moderate exuding wounds, *J. Drug Deliv. Sci. Technol.* (2019); https://doi.org/10.1016/j.jddst.2019.05.004
19. B. N. Estevinho, F. Rocha, L. Santos and A. Alves, Microencapsulation with chitosan by spray drying for industry applications – A review, *Trends Food Sci. Technol.* **31** (2013) 138–155; https://doi.org/10.1016/j.tifs.2013.04.001

20. B. R. P. Cabral, P. M. de Oliveira, G. M. Gelfuso, T. de S. C. Quintão, J. A. Chaker, M. G. de O. Karnikowski and E. F. Gris, Improving stability of antioxidant compounds from *Plinia cauliflora* (jabuticaba) fruit peel extract by encapsulation in chitosan microparticles, *J. Food Eng.* **238** (2018) 195–201; https://doi.org/10.1016/j.jfoodeng.2018.06.004
21. D. P. Gaspar, M. M. Gaspar, C. V. Eleutério, A. Grenha, M. Blanco, L. M. D. Gonçalves, P. Taboada, A. J. Almeida and C. Remunán-López, Microencapsulated solid lipid nanoparticles as a hybrid platform for pulmonary antibiotic delivery, *Mol. Pharmaceutics* **14** (2017) 2977–2990; https://doi.org/10.1021/acs.molpharmaceut.7b00169
22. T. Wang, Q. Hu, M. Zhou, J. Xue and Y. Luo, Preparation of ultra-fine powders from polysaccharide-coated solid lipid nanoparticles and nanostructured lipid carriers by innovative nano spray drying technology, *Int. J. Pharm.* **511** (2016) 219–222; https://doi.org/10.1016/j.ijpharm.2016.07.005
23. H. Salminen, J. Ankenbrand, B. Zeeb, G. Badolato Bönisch, C. Schäfer, R. Kohlus and J. Weiss, Influence of spray drying on the stability of food-grade solid lipid nanoparticles, *Food Res. Int.* **119** (2018) 741–750; https://doi.org/10.1016/j.foodres.2018.10.056
24. D. G. Sami, H. H. Heiba and A. Abdellatif, Wound healing models: A systematic review of animal and non-animal models, *Wound Med.* **24** (2019) 8–17; https://doi.org/10.1016/j.wndm.2018.12.001
25. A. Stunova and L. Vistejnova, Dermal fibroblasts – A heterogeneous population with regulatory function in wound healing, *Cytokine Growth Factor Rev.* **39** (2018) 137–150; https://doi.org/10.1016/j.cytogfr.2018.01.003
26. I. Rubelj, Telomere Q-PNA-FISH – reliable results from stochastic signals, *PLoS One* **9** (2014) e92559; https://doi.org/10.1371/journal.pone.0092559
27. F. Felice, Y. Zambito, E. Belardinelli, A. Fabiano, T. Santoni and R. Di Stefano, Effect of different chitosan derivatives on in vitro scratch wound assay: A comparative study, *Int. J. Biol. Macromol.* **76** (2015) 236–241; https://doi.org/10.1016/j.ijbiomac.2015.02.041
28. A. D. Kulkarni, D. B. Bari, S. J. Surana and C. V Pardeshi, In vitro, ex vivo and in vivo performance of chitosan-based spray-dried nasal mucoadhesive microspheres of diltiazem hydrochloride, *J. Drug Deliv. Sci. Technol.* **31** (2016) 108–117; https://doi.org/10.1016/j.jddst.2015.12.004
29. S. Demarger-Andre and A. Domard, Chitosan carboxylic acid salts in solution and in the solid state, *Carbohydr. Polym.* **23** (1994) 211–219; https://doi.org/10.1016/0144-8617(94)90104-X
30. N. El Moussaoui and A. Bendriss, The influence of storage conditions on melatonin stability, *Int. J. Eng. Res. Technol.* **3** (2014) 2243–2246.
31. M. Friciu, T. Savji, S. Zaraa and G. Leclair, Evaluation of stability of melatonin in extemporaneously compounded oral suspensions, *J. Pharm. Pract. Res.* **46** (2016) 28–33; https://doi.org/10.1002/jppr.1171
32. P. Linse and M. Malmsten, Temperature-dependent micellization in aqueous block copolymer solutions, *Macromolecules* **25** (1992) 5434–5439; https://doi.org/10.1021/ma00046a048
33. A. Garcês, M. H. Amaral, J. M. Sousa Lobo and A. C. Silva, Formulations based on solid lipid nanoparticles (SLN) and nanostructured lipid carriers (NLC) for cutaneous use: A review, *Eur. J. Pharm. Sci.* **112** (2018) 159–167; https://doi.org/10.1016/j.ejps.2017.11.023
34. B. M. Dulmovits and I. M. Herman, Microvascular remodeling and wound healing: A role for pericytes, *Int. J. Biochem. Cell Biol.* **44** (2012) 1800–1812; https://doi.org/10.1016/j.biocel.2012.06.031
35. S. L. Percival, S. McCarty, J. A. Hunt, E. J. Woods, The effects of pH on wound healing, biofilms, and antimicrobial efficacy, *Wound Rep. Reg.* **22** (2014) 174–186; https://doi.org/10.1111/wrr.12125
36. D. B. Friedman, D. L. Stauff, G. Pishchany, C. W. Whitwell, V. J. Torres and E. P. Skaar, Staphylococcus aureus redirects central metabolism to increase iron availability, *PLoS Pathog.* **2** (2006) 0777–0789; https://doi.org/10.1371/journal.ppat.0020087
37. X. Chen, L. H. Peng, Y. H. Shan, N. Li, W. Wei, L. Yu, Q. M. Li, W. Q. Liang and J. Q. Gao, Astragaloside IV-loaded nanoparticle-enriched hydrogel induces wound healing and anti-scar activity through topical delivery, *Int. J. Pharm.* **447** (2013) 171–181; https://doi.org/10.1016/j.ijpharm.2013.02.054

38. V. Kant, A. Gopal, D. Kumar, A. Gopalkrishnan, N. N. Pathak, N. P. Kurade, S. K. Tandan and D. Kumar, Topical pluronic F-127 gel application enhances cutaneous wound healing in rats, *Acta Histochem.* **116** (2014) 5–13; https://doi.org/10.1016/j.acthis.2013.04.010

39. G. Soybir, C. Topuzlu, Ö. Odabaş, K. Dolay, A. Bilir and F. Köksoy, The effects of melatonin on angiogenesis and wound healing, *Surg. Today.* **33** (2003) 896–901; https://doi.org/10.1007/s00595-003-2621-3

40. I. Garcia-Orue, G. Gainza, P. Garcia-Garcia, F. B. Gutierrez, J. J. Aguirre, R. M. Hernandez, A. Delgado and M. Igartua, Composite nanofibrous membranes of PLGA/Aloe vera containing lipid nanoparticles for wound dressing applications, *Int. J. Pharm.* (2019); https://doi.org/10.1016/j.ijpharm.2018.12.010.

41. M. Ghodrati, M. R. Farahpour and H. Hamishehkar, Encapsulation of Peppermint essential oil in nanostructured lipid carriers: In-vitro antibacterial activity and accelerative effect on infected wound healing, *Colloids Surfaces A Physicochem. Eng. Asp.* (2019); https://doi.org/10.1016/j.colsurfa.2018.12.043

5. GENERAL DISCUSSION

Given the complexity of wound healing process and milieu in chronic wound bed, development of innovative "multitasking" dressings is essential for successful therapy. Key features of effective dressing include assurance of moist environment and gas exchange, protection of the wound bed from external contamination and delivery of incorporated drug in effective and controlled manner (Kim et al., 2018; Leaper et al., 2012). Additionally, due to increasing antimicrobial resistance and the prevalence of infected chronic wounds, development of dressings with antibacterial properties becomes an imperative (Simões et al., 2018). Patient comfort and adherence present additional important aspects, especially for the ones with chronic, long-lasting wounds. Considering above, design of the dressing's final form is complex challenge. Films and hydrocolloid dressings usually have pre-defined dimensions, while foams and hydrogels are directly applied in the wound bed and their dose and quantity depend on the wound size. *In situ* gelling systems are the sub-type of hydrogel dressings with the most convenient properties, as they directly gel or swell in the wound bed and mould in the affected tissue. *In situ* gelling systems are usually developed as liquid or dry powder formulation, that form a hydrogel in contact with wound exudate (De Cicco et al., 2014a, 2014b), with change of temperature (Basha et al., 2018; Du et al., 2016), by enzymatic reaction (Ying et al., 2019) or UV energy (Lu et al., 2010).

The aim of this thesis was to develop novel chitosan-based wound dressing in the form of dry powder by spray drying technology, and to prepare, characterize and evaluate complementary dry powder dressings in terms of their potential application to different types of wounds. Chitosan was selected as a main carrier due to its well-known antimicrobial and wound healing effects, while melatonin was evaluated as a drug because of antioxidant and anti-inflammatory properties that could influence chronic wounds environment in nonconventional way. Pluronic® F127 was added to the system in order to fine-tune physic-chemical microsphere characteristics and potentially support healing effect, while lipid component in form of nano delivery system (NLCs) was introduced to alter the dressing in terms of drug release and moist related properties, making it applicable to wounds with diverse pathologies. Spray dried microspheres with/without Pluronic® F127 and/or NLCs were characterized, and statistically compared when appropriate, in terms of physico-chemical properties, *in vitro* swelling, drug release, moist-related properties, antibacterial efficacy, *in vitro* biocompatibility with skin cell lines and *in vitro* healing potential, using Analysis of Variance and Tukey's Multiple Comparison Test. Finally, long-term stability of the dry

powders that were shown promising for application as *in situ* forming wound dressings was evaluated.

Melatonin-loaded chitosan/Pluronic® F127 microspheres (in further text denoted as MCP) and melatonin-loaded chitosan microspheres (in further text denoted as MC) were prepared by previously optimized spray drying process (Duvnjak, 2010). Melatonin loaded lipid enriched chitosan/Pluronic® F127 microspheres (in further text denoted as MLCP) were developed as a novel, complementary system. MLCP is described as hybrid system, as it comprises two different delivery systems – NLCs incorporated within the microspheres, with melatonin incorporated in both phases. Thus, evaluation and understanding of critical formulation and process parameters for both systems were critical. To achieve these goals, MLCP was developed and optimized by means of Quality by Design approach, employing definitive screening design. That allowed optimization of investigated parameters and their responses for nano and micro delivery systems within one statistical design. Liquid and solid lipids were chosen during preformulation assessment based on their compatibility, melatonin solubility and applicability to subsequent drying process, while NLCs themselves were prepared by hot homogenization technique. In order to obtain NLCs with high drug loading and small and uniform size, formulation parameters including hot homogenization time, liquid lipid content in the NLCs and total lipid content in the final NLC suspension were investigated. For MLCP, portion of NLC component, drying feed flow rate and inlet temperature, were investigated within the same statistical design, as critical parameters for the preparation of microspheres. MLCP were characterised in terms of drying process yield, moisture content, size and zeta potential. Optimised MLCP properties were achieved at following formulation and process parameters: NLC containing 20% of Miglyol 812N as liquid lipid, 5% total lipid content in NLC suspension, 20 min hot homogenization time, 21.6% of NLC in MLCP, feed flow rate of 1.8 mL/min and inlet drying temperature of 110 °C.

All three type of microspheres were characterized by complete encapsulation efficacy (> 99.3% for all samples), meaning that no loss of melatonin during the preparation process occurred. For all samples amorphization of melatonin by spray drying was observed, however, traces of crystalline melatonin were present on X-ray diffractographs, which was also confirmed by DSC analysis. Interaction of melatonin with polymer components was indicated by shift of melatonin melting point present in all analysed samples. At the same time, significant increase of amorphous melatonin portion with addition of Pluronic® F127 in the system was observed (~35% amorphous melatonin in MC, ~80% in MCP and ~75% in MLCP). Latter could

be explained by increased melatonin solubility and/or improved stabilization potential of complex polymer system. For MLCP system, additional melting point of Compritol® 888ATO was detected. As solid lipid melting point indicates the order of crystalline state in which it is present within the NLCs (Garcês et al., 2018), melting point (T_m) was used as a control of the NLC system within the MLCP microspheres during long-term storage.

Flowability properties (expressed as Hausner ratio) of dried powders were evaluated to estimate their manufacturing, handling, packaging and administration perspective. Although addition of lipids in the system can increase agglomeration and adhesiveness (Pilcer et al., 2006), MLCP showed superior flowing properties, being the only sample characterized by free flowing (Hausner ratio 1.13 ± 0.11). While MC and MCP did not show advantageous flowability (Hausner ratio 1.7 ± 0.1 and 1.8 ± 0.12, respectively), they were in typical range for chitosan dried powders (Nunthanid et al., 2008). Superior flowing behaviour for MLCP confirmed successful optimization of the hybrid system.

Swelling behaviour was assessed by determination of simulated wound fluid (SWF) uptake set at physiologically relevant pH 7.4 and at pH 6.3. As the chitosan is the major swelling component in the systems and its portion differs between the systems, all SWF absorption curves were expressed as volume of absorbed SWF per mg of chitosan in relation to time (Figure 3). At pH 6.3, MC showed the highest SWF uptake as chitosan free amine groups were partially charged (pKa 6.5), with lower total uptake for MCP due to presence of weak ionic interactions between chitosan and Pluronic® F127 chains (Calvo et al., 1997). However, no significant difference in SWF absorption profile between MC and MCP was observed at pH 7.4 ($p>0.05$). When lipid component was introduced in the microspheres, pH dependency of SWF uptake ability was still present, but overall absorbing capacity significantly decreased, due to NLC hydrophobicity and weak interactions between positive charged chitosan and negatively charged lipids (Sanad and Abdel-Bar, 2017).

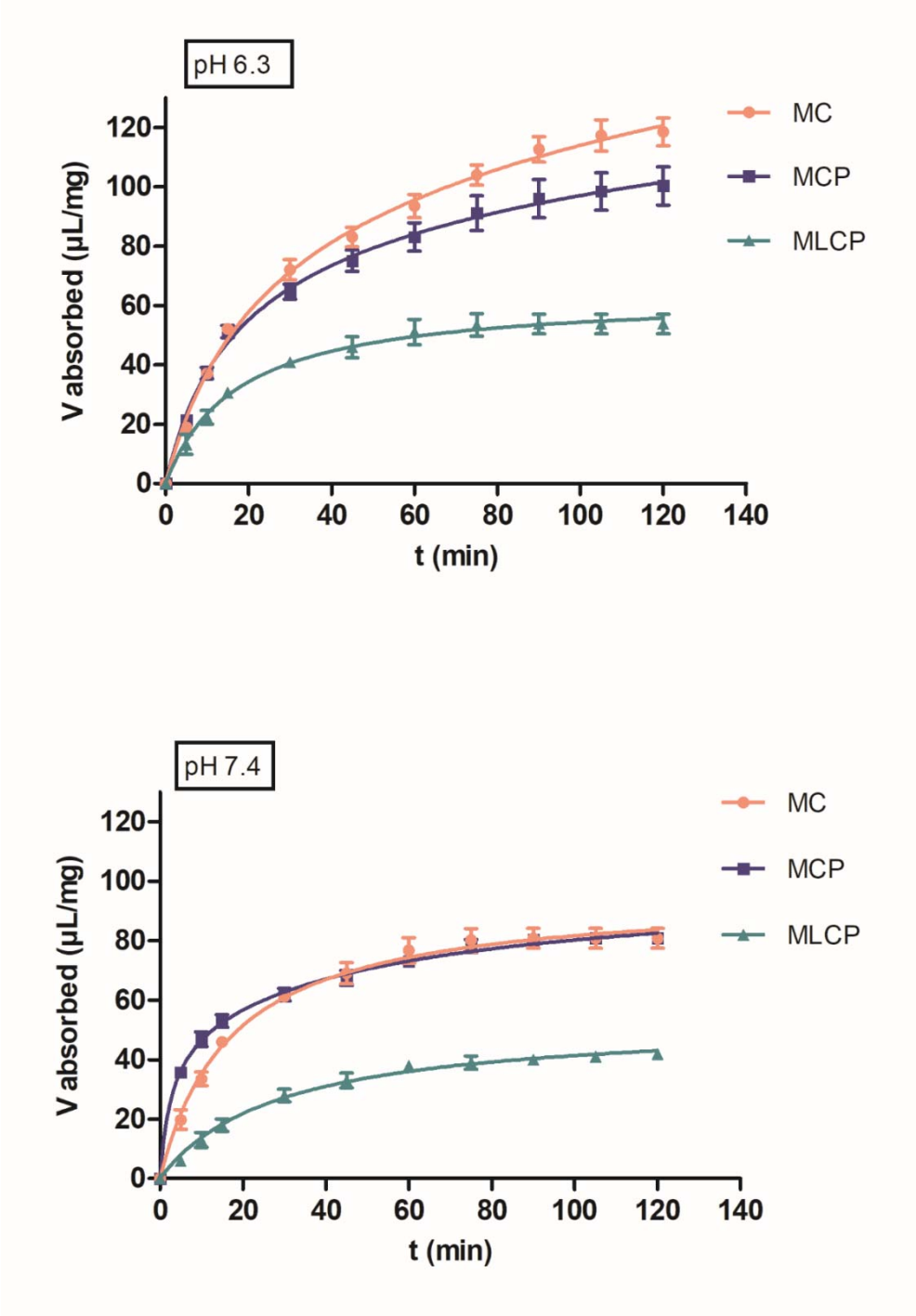

Figure 3. Simulated wound fluid (SWF) pH 6.3 and pH 7.4 uptake profiles of MC, MCP and MLCP expressed as the volume of absorbed SWF per milligram of chitosan in relation to time (mean values±S.D., n=3).

Establishment and preservation of moist environment in the wound bed is one of the essential features effective dressing must possess. Measured WVTRs for MCP and MLCP hydrogels were within recommended range of 2000–2500 g/m^2/day (2357.1 ± 162.3 g/m^2/day and 2128.0 ± 105.3 g/m^2/day, respectively). In parallel, MC hydrogel showed WVTR outside the recommended range (2933.0 ± 201.7 g/m^2/day). At the same time, no significant difference between measured WVTRs related to pH of SWF used for powder swelling (pH 6.3 vs 7.4) was observed ($p>0.05$). Measured values indicate that, regardless of pH conditions, after the swelling is complete and hydrogel dressings is formed, water permeation will remain constant and in optimal range, as long the exudate is produced in the wound bed. Lack of pH dependence is advantageous for developed dressings, as it is known that pH in the wound bed changes with the state and phase of healing process (Bennison et al., 2017).

Water loss from the prepared hydrogels was measured in order to characterize behaviour when dressing is applied to less exuding wounds. As shown in Figure 4, the loss from MLCP was significantly lower compared to MC and MCP ($p<0.05$ for $t_{50\%}$ evaluation). All three hydrogels swollen in pH 6.3 showed slightly slower water loss ($t_{50\%}$ ~4.6 h, ~4.2 h and ~8.6 h for MC, MCP and MLCP, respectively) compared to pH 7.4 hydrogels ($t_{50\%}$ ~4.4 h, ~3 h and ~7.2 h for MC, MCP and MLCP, correspondingly). Observed lipid effect was expected since it is known that lipids form a (semi)occlusion layer that hinders water loss from the system (Shrotriya et al., 2017). Considering more extensive SWF uptake, higher WVTR and faster water loss, it was concluded that MC and MCP powders could be beneficial for administration to highly exuding wounds, while moisture characteristics of MLCP dressing better suit needs of moderate exuding wounds.

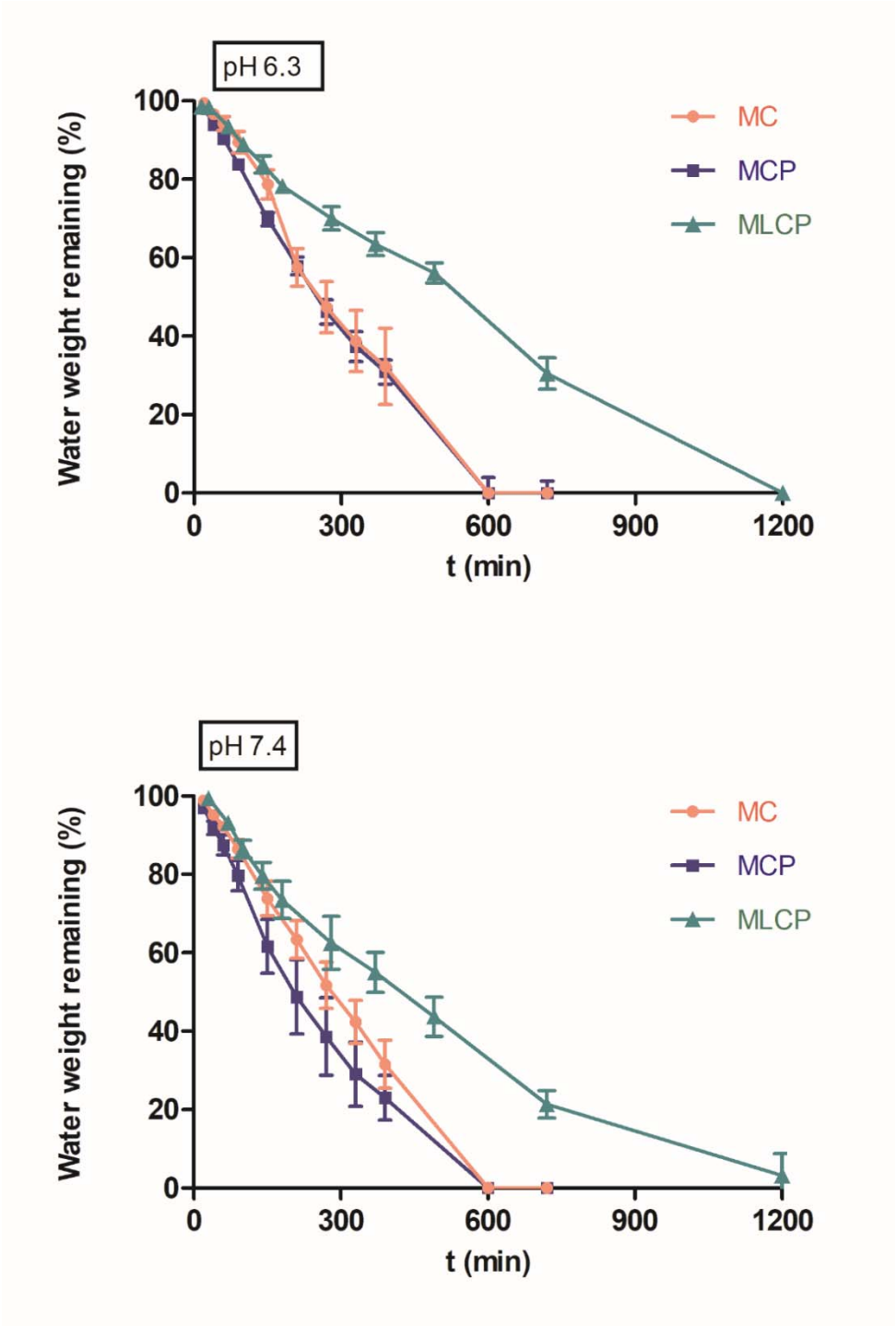

Figure 4. Evaporative water loss from hydrogels prepared from MC, MCP and MLCP powder with SWF pH 6.3 and pH 7.4 (mean values±S.D., n=3).

In vitro melatonin release profiles from MC, MCP and MLCP were evaluated in phosphate buffer with pH set to 6.3 and 7.4. All the profiles followed biphasic kinetics with initial burst release, followed by more controlled gel-diffusion driven phase (Figure 5). Release

profiles in pH 6.3 were in accordance with swelling properties of microspheres. Namely, melatonin release rate decreased in order MC>MCP>MLCP reflecting the swelling properties of the microspheres. At the beginning of experiment, release from MC and MCP is similar, indicating the release of melatonin close to the surface of microparticles due to hydration of chitosan chains. After the swelling is complete, slower melatonin release for MCP is observed, as a consequence of ionic interactions in hydrogel structure, caused by Pluronic® F127 (f_2 similarity factor =45 for MC *vs.* MCP). As for MLCP, retardation of melatonin release profile was also driven by its partial incorporation within the NLC phase that reduced its release rate in comparison to simple diffusion through the swollen gel (f_2 similarity factor =43 for MLCP *vs.* MCP). On the other hand, in the pH 7.4 there was no clear difference between release profiles of melatonin from different formulations (f_2 similarity factor >50 for all combinations). Due to the lack of chitosan protonation, formed hydrogels do not comprise thick and consistent diffusion layer, thus release of melatonin is much less controlled (Notario-Pérez et al., 2017). At the beginning of experiment, melatonin release from MCP and MLCP was slightly faster than MC, which can be explained by higher amount of amorphous drug in the presence of Pluronic® F127, while later MLCP profile showed more gradual slope due to NLC effect.

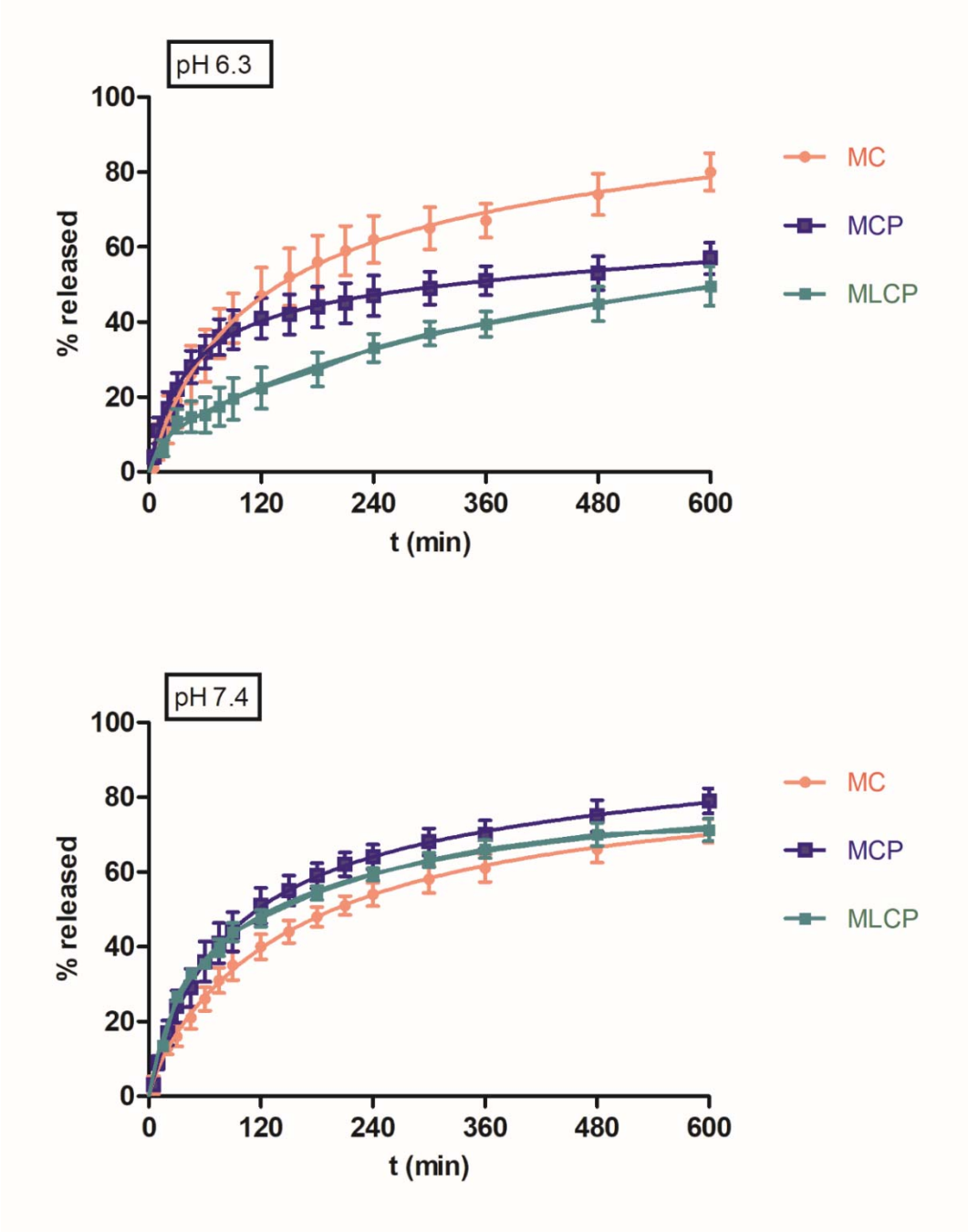

Figure 5. The release profiles of melatonin from the MC, MCP and MLCP in the phosphate buffer pH 6.3 and pH 7.4 as the release medium (mean values±S.D., n=3).

As the purpose of developed *in situ* forming hydrogels was administration to chronic, usually infected wounds, it was important to assess their antimicrobial potential. Antimicrobial activity against planktonic bacteria (*S. aureus* ATCC and MRSA strains), as well as biofilm inhibition and elimination effect, were evaluated using broth dilution method (Klančnik et al.,

2010). Minimum inhibitory concentrations (MIC) expressed as the melatonin concentration, of individual components and developed microparticulate dressings were evaluated. Compared to the other microspheres, MCP showed the most potent activity against ATCC strain of planktonic bacteria (Table 1), indicating synergistic antimicrobial action of chitosan with melatonin and Pluronic® F127. The observed values for MLCP microspheres showed that addition of lipids reduced antimicrobial potency. Microbial pathogens need iron to replicate (Skaar, 2010) and in case of low iron levels, *S. aureus* is prone to produce acid compounds to lower microenvironmental pH and provoke iron release from the host supplies (Friedman et al., 2006). The theory about novel, non-specific synergistic effect of chitosan and melatonin is based on above effects, since melatonin intracellular iron chelation (Jasim et al., 2010) could contribute to the lowering of bacterial microenvironmental pH and consequently increase in chitosan charge and antimicrobial activity. In this study potentiating effect of Pluronic® F127 on antimicrobial activity was also observed and it can be attributed to the state of melatonin in MCP microspheres. As already discussed, MCP consists of mainly amorphous melatonin which is more soluble and therefore sooner available for triggering iron-pH reaction.

Table 1. Antimicrobial activity of MC, MCP and MLCP against planktonic bacteria and biofilm of *Staphylococcus aureus*.

	***S. aureus ATCC*[1]**			***S. aureus MRSA*[2]**		
	MIC (mg/mL)	MBIC (mg/mL)	MBEC (mg/mL)	MIC (mg/mL)	MBIC (mg/mL)	MBEC (mg/mL)
MC	0.25	1.35	-	0.25	1.35	-
MCP	0.13	0.67	2.70	0.25	1.35	2.70
MLCP	1.35	2.70	2.70	1.35	2.70	2.70

[1] strain 29213

[2] strains MFBF 10674, 10676, 10677, 10679, 10680 for MC and MCP, strain NCTC 12493 for MLCP

Biofilm inhibition (MBIC) and elimination (MBEC) potential of microspheres were further tested following the same approach (Table 1). MBIC values showed the same trend in potency, especially for ATCC strain, namely MCP>MC>MLCP, while more interesting results were observed for biofilm eradication potential. At the highest tested concentration (2.70 mg/mL) only partial reduction in viability was observed for MC microspheres, while MLCP

had MBEC same as MBIC. Although MCP microspheres were shown more potent in terms of MIC and MBIC, interestingly, their biofilm eradication potency was the same as for MLCP.

As hydrogel dressing would be formed in the wound bed after powder swelling, relevant melatonin concentrations were calculated based on the swelling extent of tested systems. MCP hydrogel dressing would have theoretical melatonin concentration ranging between 5.0 and 6.25 mg/mL. As MLCP swelling extent is significantly lower, theoretical melatonin hydrogel concentrations are in range of 9.0-12.5 mg/mL. Based on above calculations, it can be concluded that melatonin concentration in the swollen hydrogels is well above minimal inhibitory concentrations, therefore, both tested dressings are expected to provide overall protection against microbial and biofilm activity.

In vitro cytotoxicity effect of developed MC, MCP and MLCP powders on human skin cell lines – keratinocyte HaCaT and BJ/MJ90hTERT fibroblasts was tested at concentration range of 0.015–0.29 mg/mL (expressed as the melatonin concentration in the microsphere suspension). Samples were dispersed in HBSS medium with pH values set to 6.3 and 7.4 and biocompatibility was evaluated by monitoring cell metabolic activity (MTT test, Figure 6) and membrane integrity (LDH assay, Figure 7). As melatonin could interact with LDH assay due to its antioxidant activity, the effect on membrane integrity was assessed with the blank (melatonin free) microspheres only – namely, chitosan (C), chitosan/ Pluronic® F127 (CP) and NLC loaded chitosan/ Pluronic® F127 (LCP). Chitosan is widely used, well tolerated wound dressing material (Azuma et al., 2015; Hamedi et al., 2018), while Pluronic® F127-based dressings are in the focus of many research (Demirci et al., 2015; Kant et al., 2014). NLC components (Compritol® 888ATO and Miglyol 812) are also proved safe for dermal application (Doktorovová et al., 2016; Garcês et al., 2018). Melatonin as endogen compound is generally well tolerated, with recent studies showing it's positive effect on wound healing (Slominski et al., 2018; Song et al., 2016). As mentioned, all individual components of the microspheres were known as biocompatible, therefore, all three types of dressings were also well tolerated (Supplemental figures 4 and 5). At pH 6.3, the highest tested concentration of MCP samples showed borderline decreased viability, however observed effect could be attributed to the simplicity and accompanying increased sensitivity of the employed cell-monolayers tests.

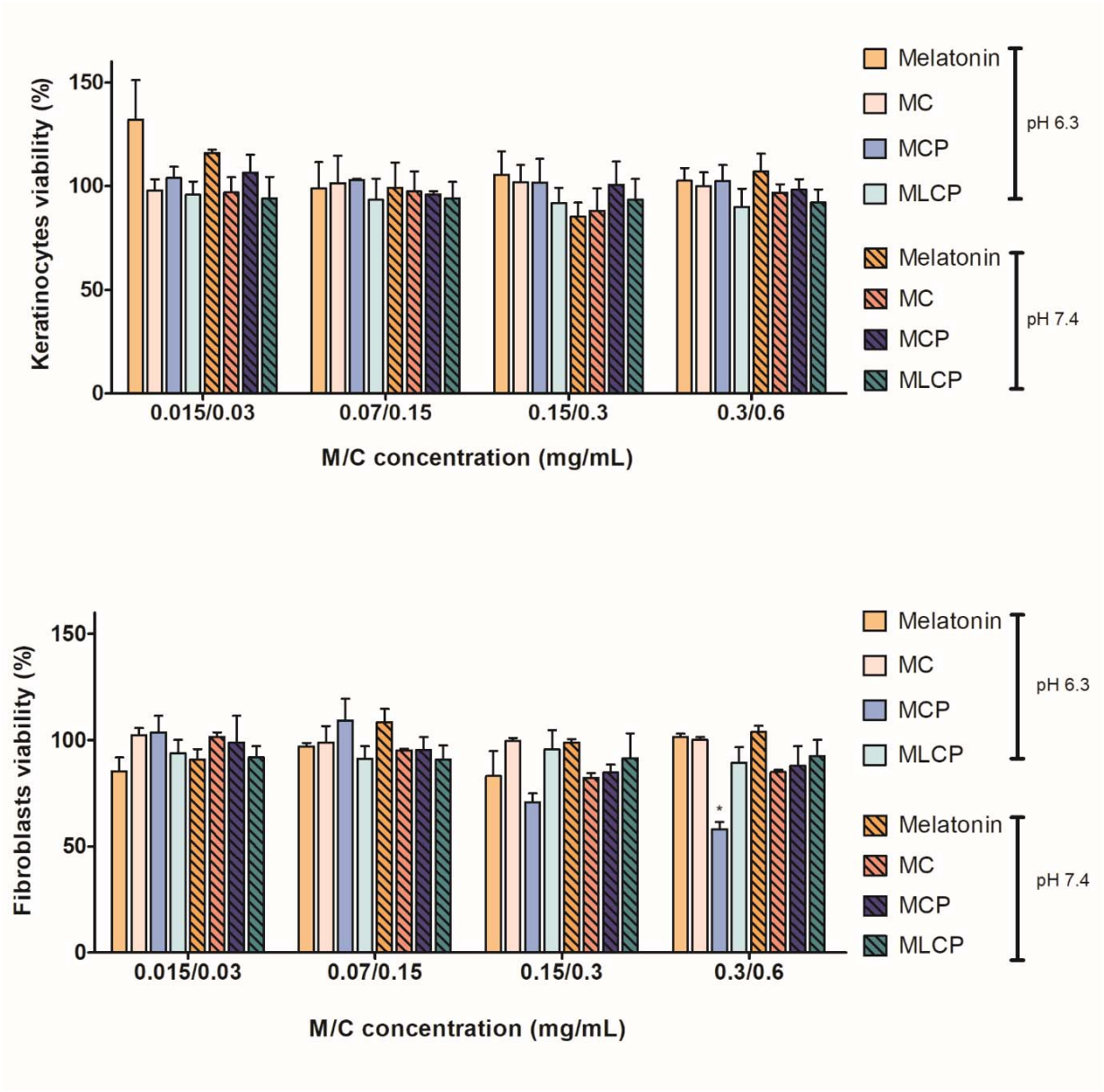

Figure 6. Keratinocytes (HaCaT) and fibroblasts (BJ/MJ90hTERT) viability (%) determined by MTT after 2 h of incubation at 37 °C with melatonin solution, MC, MCP and MLCP microspheres resuspended in HBSS buffer pH 6.3 and pH 7.4 (mean values ± S.D, n = 3). *Cell viability below 70%.

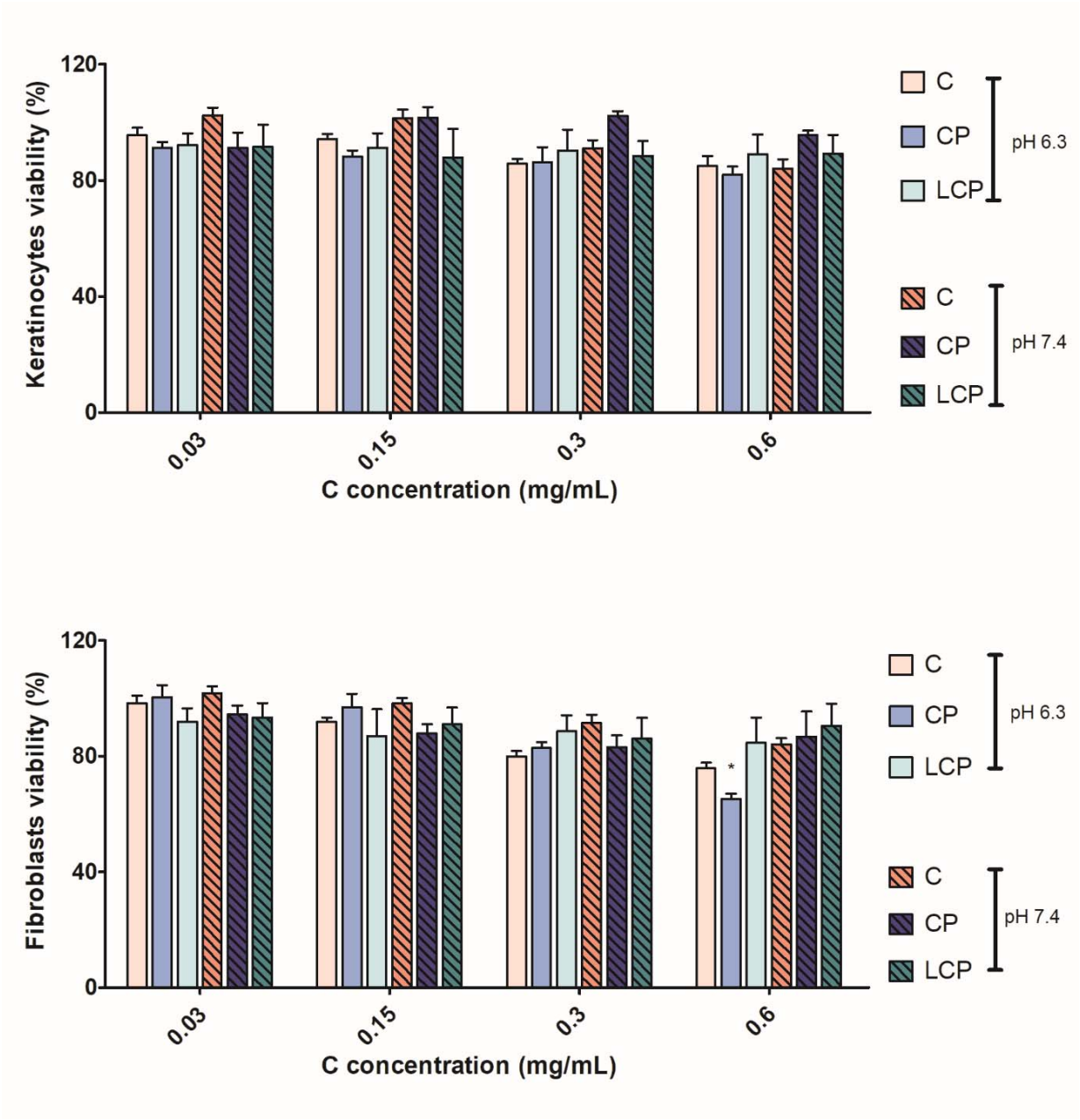

Figure 7. Keratinocytes (HaCaT) and fibroblasts (BJ/MJ90hTERT) viability (%) determined by LDH after 2 h of incubation at 37 °C with C, CP and LCP microspheres resuspended in HBSS buffer pH 6.3 and pH 7.4 (mean values ± S.D, n = 3). *Cell viability below 70%.

Following improved amorphous solid state, complementary moisture handling properties and drug release, proven biocompatibility of developed systems and antimicrobial efficacy, *in vitro* wound healing potential of MCP and MLCP dressings was assessed by scratch assay. Skin MJ90hTERT fibroblast cell line was incubated in serum-free medium and migration/proliferation was studied after 2-hour treatment with MCP and MLCP powders

dispersed in HBSS medium with pH set to 6.3 and 7.4. As previously shown nontoxic, melatonin concentration was set to 0.3 mg/mL. Wound closure was evaluated 24h after the treatment, and all treated cells showed improved healing compared to untreated cells. However, only increase in healing rate for samples dispersed in HBSS pH 6.3 were found significant. For both tested conditions, MLCP dispersion showed slightly faster wound closure, compared with MCP sample (27% vs. 19% closure at pH 6.3 and 22% vs. 17% closure at pH 7.4), implying lipids as complementary factor for improved healing, as recently observed by other researchers (Ghodrati et al., 2019).

Finally, as MCP and MLCP microspheres showed promising characteristics as *in situ* forming wound dressing materials, long-term stability of dry powders was tested. In order to reach the patient, drug product in the early development phase, should not suffer changes in any of important parameters in a period of at least six months (Food and Drug Administration Center for Drug Evaluation and Research, 2015). Therefore, physico-chemical stability of powder samples was evaluated at refrigerated (5 ± 3 °C) and at room conditions (25 ± 2 °C/60 ± 5% RH) for six months period. At designated time-points, samples were analysed in terms of particle size, zeta potential, moisture content and thermal properties. For all samples at all tested conditions no significant change in particles size and zeta potential were observed, while increase in moisture content was measured for MCP powder. Thermal properties were evaluated to monitor solid state and interactions between components. Transformation of amorphous melatonin to crystalline state was observed for MCP stored at 5 ± 3 °C, while samples stored at room temperature, maintained drug in mostly amorphous state. This effect could be explained by potential influence of Pluronic® F127 on melatonin solubility within the microspheres. At low temperatures, Pluronic® F127 could be dissolved (Linse and Malmsten, 1992) in the water present in the microspheres, causing dissolution of amorphous melatonin. However, temperature increase (to room conditions) would then lead to solidification of Pluronic® F127 and precipitation of melatonin in a crystalline form. In addition to melatonin melting peak, MLCP thermographs contain the melting peak of Compritol® 888ATO which characterizes its polymorphic state in NLC phase. In the stable NLC system, solid lipid is organized in less ordered structure, which can be confirmed by shift of melting point to the lower temperatures, as observed for MLCP particles at the beginning of testing. After 6 months of storage at 5 ± 3 °C, no change in solid lipid or melatonin melting peak was observed, indicating good stability. Thermographs of samples stored at 25 ± 2 °C/60 ± 5% RH showed conversion of the Compritol® 888ATO to the most stable form, indicating disruption in the

NLC phase. For all samples drug content was determined at the end of the testing; while no change in MCP drug content was observed (> 97%), slightly lower melatonin content in MLCP samples was measured (> 91%). Stability study revealed the room conditions as favorable for long-term storage of MCP microspheres, while the refrigerated conditions are the choice for MLCP microspheres.

As MCP and MLCP powders were shown as promising *in situ* gelling system, manufacturing potential was also considered. As products applied to open wounds must satisfy sterile requiremements, possible sterilization/manufacturing options were considered based on EMA Decision tree (European Medicines Agency, 2000). Considering the fact that liquid feed containts ethanol, the mixture itself should be self-preserved (Bouwman-Boer et al., 2015), however sterility of the final product must also be ensured. Dry heat sterilization, as first option, could not be employed since high temperature would cause melting of melatonin in MCP microspeheres as well as solid lipid in MLCP microspheres. Next method of option would be widely used ionizing radiation. Altough it is known that irradiation affects (and possibly improves) chitosan properties (Madian et al., 2018; Zhang et al., 2019), it could also activate melatonin antioxidative activity (Zetner et al., 2016) in both samples and cause oxidation of lipid component of MLCP (Shah et al., 2015). Aseptic processing is the final and most complex option in the decision tree. Although investigated and established for long time, FDA has only recently approved first drug product manufactured using aseptic spray drying, making it viable approach (Nema and Ludwig, 2019). Considering above, aseptic spray drying would be a method of option for the manufacturing of both, MCP and MLCP microspheres for wound healing application.

6. CONCLUSIONS

In this thesis, novel (nano)-microparticulate wound dressing was developed in form of dry powder by spray drying technology and evaluated and compared with complementary microparticulate dressings. Three variants of melatonin loaded wound dressings were evaluated - chitosan, chitosan/Pluronic® F127 and NLC enriched chitosan/Pluronic® F127 microspheres. Powder systems acting as *in situ* forming hydrogels were characterized in terms of physico-chemical properties, *in vitro* drug release, moisture related properties, antibacterial efficacy, *in vitro* biocompatibility with skin cell lines, *in vitro* healing potential and long-term stability in dry state.

A definitive screening design was successfully employed to understand and optimise the critical formulation and process parameters for the preparation of melatonin loaded NLC enriched chitosan/Pluronic® F127 microspheres, ensuring quality built in during the product development. Lipid enriched microspheres were characterized by high production yield, small and uniform particle size, positive zeta potential, relatively low moisture content and complete drug entrapment efficiency.

In comparison with melatonin loaded chitosan/Pluronic® F127 microspheres, corresponding NLC enriched microspheres showed improved flowability features and prolonged drug release when exposed to slightly acidic conditions. Introduction of lipid component in the system had a significant influence on moisture handling properties. NLC free dressing showed significantly higher fluid uptake capacity, water vapour transition and evaporation rate. Based on obtained results, it was concluded that melatonin loaded chitosan/Pluronic® F127 microspheres are suitable for application as dressing for wounds that produce high amounts of exudate. In the other hand, NLC enriched microspheres were shown as suitable for moderately exuding wounds.

Microspheres showed antimicrobial activity against *S. aureus* ATCC and *S. aureus* MRSA strains, with NLC free sample being more potent in terms of bacterial and biofilm formation inhibition, while no difference in concentrations required for biofilm eradication were observed. At the same time, effective antimicrobial concentration for both powders were well above theoretical concentration in the hydrogel dressing after swelling, making them suitable to provide antimicrobial shelter in the wound bed.

Both, melatonin loaded NLC enriched and NLC free chitosan/Pluronic® F127 microspheres were shown as biocompatible with dermal keratinocytes and fibroblasts *in vitro*.

In vitro scratch wound healing assay revealed respectable potential of developed systems to promote healing process, especially in case of lipid enriched system.

Long-term stability study of powders in dry state showed good stability in general, with NLC free microspheres favouring storage at room temperature due to better preservation of amorphous melatonin. Oppositely, lower temperature was the condition of choice for long term storage in case of NLC enriched microspheres, as a result of improved conservation of lipid phase.

Proposed *in situ* forming dressings had shown the complementary potential to improve wound management for different types of chronic wounds by maintaining favourable moist environment, providing antibacterial protection and promoting healing process.

7. REFERENCE LIST

Ahmed, S., Ikram, S., 2016. Chitosan Based Scaffolds and Their Applications in Wound Healing. Achiev. Life Sci. 10, 27–37. https://doi.org/10.1016/j.als.2016.04.001

Akakuru, O., Isiuku, B., 2017. Chitosan Hydrogels and their Glutaraldehyde-Crosslinked Counterparts as Potential Drug Release and Tissue Engineering Systems - Synthesis, Characterization, Swelling Kinetics and Mechanism. J. Phys. Chem. Biophys. 07. https://doi.org/10.4172/2161-0398.1000256

Anisimov, V.N., Popovich, I.G., Zabezhinski, M.A., Anisimov, S. V., Vesnushkin, G.M., Vinogradova, I.A., 2006. Melatonin as antioxidant, geroprotector and anticarcinogen. Biochim. Biophys. Acta - Bioenerg. 1757, 573–589. https://doi.org/10.1016/j.bbabio.2006.03.012

Archana, D., Dutta, J., Dutta, P.K., 2013. Evaluation of chitosan nano dressing for wound healing: Characterization, in vitro and in vivo studies. Int. J. Biol. Macromol. 57, 193–203. https://doi.org/10.1016/j.ijbiomac.2013.03.002

Ashtikar, M., Wacker, M.G., 2018. Nanopharmaceuticals for wound healing – Lost in translation? Adv. Drug Deliv. Rev. 129, 194–218. https://doi.org/10.1016/j.addr.2018.03.005

Azuma, K., Izumi, R., Osaki, T., Ifuku, S., Morimoto, M., Saimoto, H., Minami, S., Okamoto, Y., 2015. Chitin, Chitosan, and Its Derivatives for Wound Healing: Old and New Materials. J. Funct. Biomater. 6, 104–142. https://doi.org/10.3390/jfb6010104

Bagheri-Khoulenjani, S., Taghizadeh, S.M., Mirzadeh, H., 2009. An investigation on the short-term biodegradability of chitosan with various molecular weights and degrees of deacetylation. Carbohydr. Polym. 78, 773–778. https://doi.org/10.1016/j.carbpol.2009.06.020

Basha, M., AbouSamra, M.M., Awad, G.A., Mansy, S.S., 2018. A potential antibacterial wound dressing of cefadroxil chitosan nanoparticles in situ gel: Fabrication, in vitro optimization and in vivo evaluation. Int. J. Pharm. 544, 129–140. https://doi.org/10.1016/j.ijpharm.2018.04.021

Baxter, R.M., Dai, T., Kimball, J., Wang, E., Hamblin, M.R., Wiesmann, W.P., McCarthy, S.J., Baker, S.M., 2013. Chitosan dressing promotes healing in third degree burns in mice: Gene expression analysis shows biphasic effects for rapid tissue regeneration and decreased fibrotic signaling. J. Biomed. Mater. Res. Part A 101A, 340–348. https://doi.org/10.1002/jbm.a.34328

Beloqui, A., Solinís, M.Á., Rodríguez-Gascón, A., Almeida, A.J., Préat, V., 2016. Nanostructured lipid carriers: Promising drug delivery systems for future clinics. Nanomedicine Nanotechnology, Biol. Med. https://doi.org/10.1016/j.nano.2015.09.004

Bennison, L., Miller, C., Summers, R., Minnis, A., Sussman, G. and, McGuiness, W., 2017. The pH of wounds during healing and infection: A descriptive literature review, in: Wound Practice & Research.

Bouwman-Boer, Y., Fenton-May, V., Le Brun, P. (Eds.), 2015. Practical Pharmaceutics - An International Guideline for the Preparation, Care and Use of Medicinal Products. Springer International Publishing, Cham. https://doi.org/10.1007/978-3-319-15814-3

Braiman-Wiksman, L., Solomonik, I., Spira, R., Tennenbaum, T., 2007. Novel Insights into Wound Healing Sequence of Events. Toxicol. Pathol. 35, 767–779. https://doi.org/10.1080/01926230701584189

British Standards Institution, 2002. Moisture Vapour Transmission Rate (MVTR) of Vapour Permeable Film Dressings. BS EN 13726-2.

Bulbuller, N., Dogru, O., Yekeler, H., Cetinkaya, Z., Ilhan, N., Kirkil, C., 2005. Effect of melatonin on wound healing in normal and pinealectomized rats. J. Surg. Res. 123, 3–7. https://doi.org/10.1016/j.jss.2004.05.022

Calvo, J.R., González-Yanes, C., Maldonado, M.D., 2013. The role of melatonin in the cells of the innate immunity: a review. J. Pineal Res. 55, 103–120. https://doi.org/10.1111/jpi.12075

Calvo, P., Remuñan-López, C., Vila-Jato, J.L., Alonso, M.J., 1997. Chitosan and chitosan/ethylene oxide-propylene oxide block copolymer nanoparticles as novel carriers for proteins and vaccines. Pharm. Res. 14, 1431–1436. https://doi.org/10.1023/A:1012128907225

Chereddy, K.K., Vandermeulen, G., Préat, V., 2016. PLGA based drug delivery systems: Promising carriers for wound healing activity. Wound Repair Regen. 24, 223–236. https://doi.org/10.1111/wrr.12404

Chigurupati, S., Mughal, M.R., Okun, E., Das, S., Kumar, A., McCaffery, M., Seal, S., Mattson, M.P., 2013.

Effects of cerium oxide nanoparticles on the growth of keratinocytes, fibroblasts and vascular endothelial cells in cutaneous wound healing. Biomaterials 34, 2194–2201. https://doi.org/https://doi.org/10.1016/j.biomaterials.2012.11.061

Crooke, A., Guzman-Aranguez, A., Mediero, A., Alarma-Estrany, P., Carracedo, G., Pelaez, T., Peral, A., Pintor, J., 2015. Effect of Melatonin and Analogues on Corneal Wound Healing: Involvement of Mt $_2$ Melatonin Receptor. Curr. Eye Res. 40, 56–65. https://doi.org/10.3109/02713683.2014.914540

da Costa, A.O., de Assis, M.C., Marques, E. de A., Plotkowski, M.C., 1999. Comparative analysis of three methods to assess viability of mammalian cells in culture. Biocell 23, 65—72.

Dai, T., Tanaka, M., Huang, Y.-Y., Hamblin, M.R., 2011. NIH Public Access. Expert Rev Anti Infect Ther 9, 857–879. https://doi.org/10.1586/eri.11.59.Chitosan

Dash, M., Chiellini, F., Ottenbrite, R.M., Chiellini, E., 2011. Chitosan—A versatile semi-synthetic polymer in biomedical applications. Prog. Polym. Sci. 36, 981–1014. https://doi.org/10.1016/j.progpolymsci.2011.02.001

Davies, P., 2012. Exudate assessment and management. Br. J. Community Nurs. 17, S18–S24. https://doi.org/10.12968/bjcn.2012.17.Sup9.S18

Davis, M., Walker, G., 2018. Recent strategies in spray drying for the enhanced bioavailability of poorly water-soluble drugs. J. Control. Release 269, 110–127. https://doi.org/10.1016/j.jconrel.2017.11.005

De Cicco, F., Porta, A., Sansone, F., Aquino, R.P., Del Gaudio, P., 2014a. Nanospray technology for an in situ gelling nanoparticulate powder as a wound dressing. Int. J. Pharm. 473, 30–37. https://doi.org/10.1016/j.ijpharm.2014.06.049

De Cicco, F., Reverchon, E., Adami, R., Auriemma, G., Russo, P., Calabrese, E.C., Porta, A., Aquino, R.P., Del Gaudio, P., 2014b. In situ forming antibacterial dextran blend hydrogel for wound dressing: SAA technology vs. spray drying. Carbohydr. Polym. 101, 1216–1224. https://doi.org/10.1016/j.carbpol.2013.10.067

Demirci, S., Doğan, A., Karakuş, E., Halıcı, Z., Topçu, A., Demirci, E., Sahin, F., 2015. Boron and Poloxamer (F68 and F127) Containing Hydrogel Formulation for Burn Wound Healing. Biol. Trace Elem. Res. 168, 169–180. https://doi.org/10.1007/s12011-015-0338-z

Doktorovová, S., Kovačević, A.B., Garcia, M.L., Souto, E.B., 2016. Preclinical safety of solid lipid nanoparticles and nanostructured lipid carriers: Current evidence from in vitro and in vivo evaluation. Eur. J. Pharm. Biopharm. 108, 235–252. https://doi.org/10.1016/j.ejpb.2016.08.001

Dong, X., Xu, J., Wang, W., Luo, H., Liang, X., Zhang, L., Wang, H., Wang, P., Chang, J., 2008. Repair effect of diabetic ulcers with recombinant human epidermal growth factor loaded by sustained-release microspheres. Sci. China Ser. C Life Sci. 51, 1039–1044. https://doi.org/10.1007/s11427-008-0126-5

Drobnik, J., 2012. Wound healing and the effect of pineal gland and melatonin. J. Exp. Integr. Med. 2, 3. https://doi.org/10.5455/jeim.040112.ir.009

Drobnik, J., Owczarek, K., Piera, L., Tosik, D., Olczak, S., Ciosek, J., Hrabec, E., 2013. Melatonin-induced augmentation of collagen deposition in cultures of fibroblasts and myofibroblasts is blocked by luzindole – a melatonin membrane receptors inhibitor. Pharmacol. Reports 65, 642–649. https://doi.org/10.1016/S1734-1140(13)71041-7

Du, L., Feng, X., Jin, X.X. and Y., 2016. Wound Healing Effect of an in Situ Forming Hydrogel Loading Curcumin-Phospholipid Complex. Curr. Drug Deliv. https://doi.org/http://dx.doi.org/10.2174/1567201813666151202195437

Duvnjak, M., 2010. Optimization of spray-drying by factorial design for production of melatonin loaded chitosan microparticles. University of Zagreb, Faculty of Pharmacy and Biochemistry.

European Medicines Agency, 2000. Decision trees for the selection of sterilisation methods (CPMP/QWP/054/98).

Felipe, V., Breser, M.L., Bohl, L.P., Rodrigues da Silva, E., Morgante, C.A., Correa, S.G., Porporatto, C., 2019. Chitosan disrupts biofilm formation and promotes biofilm eradication in Staphylococcus species isolated from bovine mastitis. Int. J. Biol. Macromol. 126, 60–67. https://doi.org/https://doi.org/10.1016/j.ijbiomac.2018.12.159

Fischer, T.W., Slominski, A., Zmijewski, M.A., Reiter, R.J., Paus, R., 2008. Melatonin as a major skin protectant: from free radical scavenging to DNA damage repair. Exp. Dermatol. 17, 713–730. https://doi.org/10.1111/j.1600-0625.2008.00767.x

Food and Drug Administration Center for Drug Evaluation and Research, 2015. Draft Guidance: Investigational New Drug Applications Prepared and Submitted by Sponsor-Investigators.

Friedman, D.B., Stauff, D.L., Pishchany, G., Whitwell, C.W., Torres, V.J., Skaar, E.P., 2006. Staphylococcus aureus redirects central metabolism to increase iron availability. PLoS Pathog. 2, 0777–0789. https://doi.org/10.1371/journal.ppat.0020087

Fronza, M., Heinzmann, B., Hamburger, M., Laufer, S., Merfort, I., 2009. Determination of the wound healing effect of< i> Calendula</i> extracts using the scratch assay with 3T3 fibroblasts. J. Ethnopharmacol. 126, 463–467. https://doi.org/https://doi.org/10.1016/j.jep.2009.09.014

Fumakia, M., Ho, E.A., 2016. Nanoparticles Encapsulated with LL37 and Serpin A1 Promotes Wound Healing and Synergistically Enhances Antibacterial Activity. Mol. Pharm. 13, 2318–2331. https://doi.org/10.1021/acs.molpharmaceut.6b00099

Gad, H.A., Abd El-Rahman, F.A.A., Hamdy, G.M., 2019. Chamomile oil loaded solid lipid nanoparticles: A naturally formulated remedy to enhance the wound healing. J. Drug Deliv. Sci. Technol. 50, 329–338. https://doi.org/10.1016/j.jddst.2019.01.008

Gainza, G., Aguirre, J.J., Pedraz, J.L., Hernández, R.M., Igartua, M., 2013. rhEGF-loaded PLGA-Alginate microspheres enhance the healing of full-thickness excisional wounds in diabetised Wistar rats. Eur. J. Pharm. Sci. 50, 243–252. https://doi.org/10.1016/j.ejps.2013.07.003

Gainza, G., Pastor, M., Aguirre, J.J., Villullas, S., Pedraz, J.L., Hernandez, R.M., Igartua, M., 2014. A novel strategy for the treatment of chronic wounds based on the topical administration of rhEGF-loaded lipid nanoparticles: In vitro bioactivity and in vivo effectiveness in healing-impaired db/db mice. J. Control. Release 185, 51–61. https://doi.org/10.1016/j.jconrel.2014.04.032

Garcês, A., Amaral, M.H., Sousa Lobo, J.M., Silva, A.C., 2018. Formulations based on solid lipid nanoparticles (SLN) and nanostructured lipid carriers (NLC) for cutaneous use: A review. Eur. J. Pharm. Sci. 112, 159–167. https://doi.org/10.1016/j.ejps.2017.11.023

Garcia-Orue, I., Gainza, G., Garcia-Garcia, P., Gutierrez, F.B., Aguirre, J.J., Hernandez, R.M., Delgado, A., Igartua, M., 2019. Composite nanofibrous membranes of PLGA/Aloe vera containing lipid nanoparticles for wound dressing applications. Int. J. Pharm. 556, 320–329. https://doi.org/10.1016/j.ijpharm.2018.12.010

Garcia-Orue, I., Gainza, G., Girbau, C., Alonso, R., Aguirre, J.J., Pedraz, J.L., Igartua, M., Hernandez, R.M., 2016. LL37 loaded nanostructured lipid carriers (NLC): A new strategy for the topical treatment of chronic wounds. Eur. J. Pharm. Biopharm. 108, 310–316. https://doi.org/10.1016/j.ejpb.2016.04.006

George D. Winter, 1962. Formation of the scab and the rate of epithelization of superficial wounds in the skin of the young domestic pig. Nature 193, 293–294. https://doi.org/10.1038/193293a0

Ghodrati, M., Farahpour, M.R., Hamishehkar, H., 2019. Encapsulation of Peppermint essential oil in nanostructured lipid carriers: In-vitro antibacterial activity and accelerative effect on infected wound healing. Colloids Surfaces A Physicochem. Eng. Asp. 564, 161–169. https://doi.org/10.1016/j.colsurfa.2018.12.043

Goy, R.C., Britto, D. de, Assis, O.B.G., 2009. A review of the antimicrobial activity of chitosan. Polímeros 19, 241–247. https://doi.org/10.1590/S0104-14282009000300013

Gulcin, İ., Buyukokuroglu, M.E., Kufrevioglu, O.I., 2003. Metal chelating and hydrogen peroxide scavenging effects of melatonin. J. Pineal Res. 34, 278–281. https://doi.org/10.1034/j.1600-079X.2003.00042.x

Güneş, S., Tıhmınlıoğlu, F., 2017. Hypericum perforatum incorporated chitosan films as potential bioactive wound dressing material. Int. J. Biol. Macromol. 102, 933–943. https://doi.org/https://doi.org/10.1016/j.ijbiomac.2017.04.080

Gupta, A., Kowalczuk, M., Heaselgrave, W., Britland, S.T., Martin, C., Radecka, I., 2019. The production and application of hydrogels for wound management: A review. Eur. Polym. J. 111, 134–151. https://doi.org/https://doi.org/10.1016/j.eurpolymj.2018.12.019

Hamedi, H., Moradi, S., Hudson, S.M., Tonelli, A.E., 2018. Chitosan based hydrogels and their applications for drug delivery in wound dressings: A review. Carbohydr. Polym. 199, 445–460. https://doi.org/https://doi.org/10.1016/j.carbpol.2018.06.114

Hasatsri, S., Pitiratanaworanat, A., Swangwit, S., Boochakul, C., Tragoonsupachai, C., 2018. Comparison of the Morphological and Physical Properties of Different Absorbent Wound Dressings. Dermatol. Res. Pract. 2018, 1–6. https://doi.org/10.1155/2018/9367034

Jain, S., Patel, N., Shah, M.K., Khatri, P., Vora, N., 2017. Recent Advances in Lipid-Based Vesicles and Particulate Carriers for Topical and Transdermal Application. J. Pharm. Sci. 106, 423–445. https://doi.org/10.1016/j.xphs.2016.10.001

Jasim, T.M., Alabbassi, M.G., Almuqdadi, S.F.H., Kamel, J.K., 2010. Anti-bacterial Properties of Melatonin against Mycobacterium Tuberculosis in Vitro Introduction. Iraqi J Pharm Sci 19, 59–63.

Kant, V., Gopal, A., Kumar, Dhirendra, Gopalkrishnan, A., Pathak, N.N., Kurade, N.P., Tandan, S.K., Kumar, Dinesh, 2014. Topical pluronic F-127 gel application enhances cutaneous wound healing in rats. Acta Histochem. 116, 5–13. https://doi.org/10.1016/j.acthis.2013.04.010

Kaplani, K., Koutsi, S., Armenis, V., Skondra, F.G., Karantzelis, N., Champeris Tsaniras, S., Taraviras, S., 2018. Wound healing related agents: Ongoing research and perspectives. Adv. Drug Deliv. Rev. 129, 242–253. https://doi.org/10.1016/j.addr.2018.02.007

Khurana, S., Jain, N.K., Bedi, P.M.S., 2013. Development and characterization of a novel controlled release drug delivery system based on nanostructured lipid carriers gel for meloxicam. Life Sci. 93, 763–772. https://doi.org/10.1016/j.lfs.2013.09.027

Kim, H.S., Sun, X., Lee, J.-H., Kim, H.-W., Fu, X., Leong, K.W., 2018. Advanced drug delivery systems and artificial skin grafts for skin wound healing. Adv. Drug Deliv. Rev. https://doi.org/10.1016/j.addr.2018.12.014

Kim, I.Y., Yoo, M.K., Seo, J.H., Park, S.S., Na, H.S., Lee, H.C., Kim, S.K., Cho, C.S., 2007. Evaluation of semi-interpenetrating polymer networks composed of chitosan and poloxamer for wound dressing application. Int. J. Pharm. 341, 35–43. https://doi.org/10.1016/j.ijpharm.2007.03.042

Kirsner, R.S., 2016. The wound healing society chronic wound ulcer healing guidelines update of the 2006 guidelines—blending old with new. Wound Repair Regen. 24, 110–111. https://doi.org/10.1111/wrr.12393

Klančnik, A., Piskernik, S., Jeršek, B., Možina, S.S., 2010. Evaluation of diffusion and dilution methods to determine the antibacterial activity of plant extracts. J. Microbiol. Methods 81, 121–126. https://doi.org/10.1016/j.mimet.2010.02.004

Kouchak, M., Handali, S., Naseri Boroujeni, B., 2015. Evaluation of the Mechanical Properties and Drug Permeability of Chitosan/Eudragit RL Composite Film. Osong Public Heal. Res. Perspect. 6, 14–19. https://doi.org/https://doi.org/10.1016/j.phrp.2014.12.001

Leaper, D.J., Schultz, G., Carville, K., Fletcher, J., Swanson, T., Drake, R., 2012. Extending the TIME concept: what have we learned in the past 10 years? *. Int. Wound J. 9, 1–19. https://doi.org/10.1111/j.1742-481X.2012.01097.x

Lee, S.M., Park, I.K., Kim, Y.S., Kim, H.J., Moon, H., Mueller, S., Jeong, Y.-I., 2016. Physical, morphological, and wound healing properties of a polyurethane foam-film dressing. Biomater. Res. 20, 15. https://doi.org/10.1186/s40824-016-0063-5

Liang, C.C., Park, A.Y., Guan, J.L., 2007. In vitro scratch assay: A convenient and inexpensive method for analysis of cell migration in vitro. Nat. Protoc. 2, 329–333. https://doi.org/10.1038/nprot.2007.30

Linse, P., Malmsten, M., 1992. Temperature-dependent micellization in aqueous block copolymer solutions. Macromolecules 25, 5434–5439. https://doi.org/10.1021/ma00046a048

Liu, L., Gao, Q., Lu, X., Zhou, H., 2016. In situ forming hydrogels based on chitosan for drug delivery and tissue regeneration. Asian J. Pharm. Sci. 11, 673–683. https://doi.org/10.1016/j.ajps.2016.07.001

Liu, Q., Huang, Y., Lan, Y., Zuo, Q., Li, C., Zhang, Y., Guo, R., Xue, W., 2017. Acceleration of skin regeneration in full-thickness burns by incorporation of bFGF-loaded alginate microspheres into a CMCS-PVA hydrogel.

J. Tissue Eng. Regen. Med. 11, 1562–1573. https://doi.org/10.1002/term.2057

Liu, Y., Jiang, Y., Zhu, J., Huang, J., Zhang, H., 2019. Inhibition of bacterial adhesion and biofilm formation of sulfonated chitosan against Pseudomonas aeruginosa. Carbohydr. Polym. 206, 412–419. https://doi.org/10.1016/j.carbpol.2018.11.015

Lu, G., Ling, K., Zhao, P., Xu, Z., Deng, C., Zheng, H., Huang, J., Chen, J., 2010. A novel in situ-formed hydrogel wound dressing by the photocross-linking of a chitosan derivative. Wound Repair Regen. 18, 70–79. https://doi.org/10.1111/j.1524-475X.2009.00557.x

Ma, Z., Garrido-Maestu, A., Jeong, K.C., 2017. Application, mode of action, and in vivo activity of chitosan and its micro- and nanoparticles as antimicrobial agents: A review. Carbohydr. Polym. 176, 257–265. https://doi.org/10.1016/j.carbpol.2017.08.082

Madian, N.G., El-Hossainy, M., Khalil, W.A., 2018. Improvement of the physical properties of chitosan by γ-ray degradation for wound healing. Results Phys. 11, 951–955. https://doi.org/10.1016/j.rinp.2018.10.051

Majidinia, M., Sadeghpour, A., Mehrzadi, S., Reiter, R.J., Khatami, N., Yousefi, B., 2017. Melatonin: A pleiotropic molecule that modulates DNA damage response and repair pathways. J. Pineal Res. 63, e12416. https://doi.org/10.1111/jpi.12416

Morton, L.M., Phillips, T.J., 2016. Wound healing and treating wounds. J. Am. Acad. Dermatol. 74, 589–605. https://doi.org/10.1016/j.jaad.2015.08.068

Murali, R., Thanikaivelan, P., Cheirmadurai, K., 2016. Melatonin in functionalized biomimetic constructs promotes rapid tissue regeneration in Wistar albino rats. J. Mater. Chem. B 4, 5850–5862. https://doi.org/10.1039/C6TB01221C

Nema, S., Ludwig, J.D. (Eds.), 2019. Parenteral Medications. CRC Press. https://doi.org/10.1201/9780429201400

Notario-Pérez, F., Martín-Illana, A., Cazorla-Luna, R., Ruiz-Caro, R., Bedoya, L.-M., Tamayo, A., Rubio, J., Veiga, M.-D., 2017. Influence of Chitosan Swelling Behaviour on Controlled Release of Tenofovir from Mucoadhesive Vaginal Systems for Prevention of Sexual Transmission of HIV. Mar. Drugs 15, 50. https://doi.org/10.3390/md15020050

Nunthanid, J., Huanbutta, K., Luangtana-anan, M., Sriamornsak, P., Limmatvapirat, S., Puttipipatkhachorn, S., 2008. Development of time-, pH-, and enzyme-controlled colonic drug delivery using spray-dried chitosan acetate and hydroxypropyl methylcellulose. Eur. J. Pharm. Biopharm. 68, 253–259. https://doi.org/10.1016/j.ejpb.2007.05.017

Nursal, T.Z., Yakupoglu, H., Renda, N., Hamaloglu, E., Sayek, I., Onat, D., Palaoglu, S., Enünlü, T., 2002. Pinealectomy Does Not Affect the Healing of Experimental Colonic Anastomoses. J. Investig. Surg. 15, 61–68. https://doi.org/10.1080/08941930290085804

Pardeike, J., Hommoss, A., Müller, R.H., 2009. Lipid nanoparticles (SLN, NLC) in cosmetic and pharmaceutical dermal products. Int. J. Pharm. 366, 170–184. https://doi.org/10.1016/j.ijpharm.2008.10.003

Park, C.J., Clark, S.G., Lichtensteiger, C.A., Jamison, R.D., Johnson, A.J.W., 2009. Accelerated wound closure of pressure ulcers in aged mice by chitosan scaffolds with and without bFGF. Acta Biomater. 5, 1926–1936. https://doi.org/10.1016/j.actbio.2009.03.002

Patrulea, V., Ostafe, V., Borchard, G., Jordan, O., 2015. Chitosan as a starting material for wound healing applications. Eur. J. Pharm. Biopharm. 97, 417–426. https://doi.org/10.1016/j.ejpb.2015.08.004

Pechanova, O., Paulis, L., Simko, F., 2014. Peripheral and Central Effects of Melatonin on Blood Pressure Regulation. Int. J. Mol. Sci. 15, 17920–17937. https://doi.org/10.3390/ijms151017920

Pérez-Díaz, M., Alvarado-Gomez, E., Magaña-Aquino, M., Sánchez-Sánchez, R., Velasquillo, C., Gonzalez, C., Ganem-Rondero, A., Martínez-Castañon, G., Zavala-Alonso, N., Martinez-Gutierrez, F., 2016. Anti-biofilm activity of chitosan gels formulated with silver nanoparticles and their cytotoxic effect on human fibroblasts. Mater. Sci. Eng. C 60, 317–323. https://doi.org/10.1016/j.msec.2015.11.036

Perinelli, D.R., Fagioli, L., Campana, R., Lam, J.K.W., Baffone, W., Palmieri, G.F., Casettari, L., Bonacucina, G., 2018. Chitosan-based nanosystems and their exploited antimicrobial activity. Eur. J. Pharm. Sci. 117, 8–20. https://doi.org/https://doi.org/10.1016/j.ejps.2018.01.046

Phillips, C.J., Humphreys, I., Fletcher, J., Harding, K., Chamberlain, G., Macey, S., 2016. Estimating the costs associated with the management of patients with chronic wounds using linked routine data. Int. Wound J. 13, 1193–1197. https://doi.org/10.1111/iwj.12443

Pierre, E.J., Perez-Polo, J.R., Mitchell, A.T., Matin, S., Foyt, H.L., Herndon, D.N., 1997. Insulin-like Growth Factor-I Liposomal Gene Transfer and Systemic Growth Hormone Stimulate Wound Healing. J. Burn Care Rehabil. 18, 287–291. https://doi.org/10.1097/00004630-199707000-00002

Pilcer, G., Sebti, T., Amighi, K., 2006. Formulation and characterization of lipid-coated tobramycin particles for dry powder inhalation. Pharm. Res. 23, 931–940. https://doi.org/10.1007/s11095-006-9789-4

Porporato, P.E., Payen, V.L., De Saedeleer, C.J., Préat, V., Thissen, J.-P., Feron, O., Sonveaux, P., 2012. Lactate stimulates angiogenesis and accelerates the healing of superficial and ischemic wounds in mice. Angiogenesis 15, 581–592. https://doi.org/10.1007/s10456-012-9282-0

Powers, J.G., Higham, C., Broussard, K., Phillips, T.J., 2016. Wound healing and treating wounds. J. Am. Acad. Dermatol. 74, 607–625. https://doi.org/10.1016/j.jaad.2015.08.070

Premarathna, A.D., Ranahewa, T.H., Wijesekera, S.K., Wijesundara, R.R.M.K.K., Jayasooriya, A.P., Wijewardana, V., Rajapakse, R.P.V.J., 2019. Wound healing properties of aqueous extracts of Sargassum illicifolium: An in vitro assay. Wound Med. 24, 1–7. https://doi.org/https://doi.org/10.1016/j.wndm.2018.11.001

Pugazhenthi, K., Kapoor, M., Clarkson, A.N., Hall, I., Appleton, I., 2008. Melatonin accelerates the process of wound repair in full-thickness incisional wounds. J. Pineal Res. 44, 387–396. https://doi.org/10.1111/j.1600-079X.2007.00541.x

Queen, D., Gaylor, J.D.S., Evans, J.H., Courtney, J.M., Reid, W.H., 1987. The preclinical evaluation of the water vapour transmission rate through burn wound dressings. Biomaterials 5, 367–371.

Rai, M., Yadav, A., Gade, A., 2009. Silver nanoparticles as a new generation of antimicrobials. Biotechnol. Adv. 27, 76–83. https://doi.org/https://doi.org/10.1016/j.biotechadv.2008.09.002

Ranjan, S., Fontana, F., Ullah, H., Hirvonen, J., Santos, H.A., 2016. Microparticles to enhance delivery of drugs and growth factors into wound sites. Ther. Deliv. 7, 711–732. https://doi.org/10.4155/tde-2016-0039

Reiter, R., Rosales-Corral, S., Tan, D.-X., Acuna-Castroviejo, D., Qin, L., Yang, S.-F., Xu, K., 2017. Melatonin, a Full Service Anti-Cancer Agent: Inhibition of Initiation, Progression and Metastasis. Int. J. Mol. Sci. 18, 843. https://doi.org/10.3390/ijms18040843

Ribeiro, M.P., Espiga, A., Silva, D., Baptista, P., Henriques, J., Ferreira, C., Silva, J.C., Borges, J.P., Pires, E., Chaves, P., Correia, I.J., 2009. Development of a new chitosan hydrogel for wound dressing. Wound Repair Regen. 17, 817–824. https://doi.org/10.1111/j.1524-475X.2009.00538.x

Saghazadeh, S., Rinoldi, C., Schot, M., Kashaf, S.S., Sharifi, F., Jalilian, E., Nuutila, K., Giatsidis, G., Mostafalu, P., Derakhshandeh, H., Yue, K., Swieszkowski, W., Memic, A., Tamayol, A., Khademhosseini, A., 2018. Drug delivery systems and materials for wound healing applications. Adv. Drug Deliv. Rev. 127, 138–166. https://doi.org/10.1016/j.addr.2018.04.008

Sahib, A.S., Al-Jawad, F.H., Al-Kaisy, A.A., 2009. Burns, endothelial dysfunction, and oxidative stress: the role of antioxidants. Ann. Burns Fire Disasters 22, 6–11.

Salmerón-González, E., García-Vilariño, E., Ruiz-Cases, A., Sánchez-García, A., García-Sánchez, J., 2018. Absorption Capacity of Wound Dressings. Plast. Surg. Nurs. 38, 73–75. https://doi.org/10.1097/PSN.0000000000000218

Salvi, V.R., Pawar, P., 2019. Nanostructured lipid carriers (NLC) system: A novel drug targeting carrier. J. Drug Deliv. Sci. Technol. 51, 255–267. https://doi.org/10.1016/j.jddst.2019.02.017

Sanad, R.A.B., Abdel-Bar, H.M., 2017. Chitosan–hyaluronic acid composite sponge scaffold enriched with Andrographolide-loaded lipid nanoparticles for enhanced wound healing. Carbohydr. Polym. 173, 441–450. https://doi.org/10.1016/j.carbpol.2017.05.098

Santos, D., Maurício, A.C., Sencadas, V., Santos, J.D., Fernandes, M.H., Gomes, P.S., 2018. Spray Drying: An Overview, in: Maurício, A.C. (Ed.), Biomaterials - Physics and Chemistry - New Edition. InTech, Rijeka, p.

Ch. 2. https://doi.org/10.5772/intechopen.72247

Saporito, F., Sandri, G., Bonferoni, M.C., Rossi, S., Boselli, C., Icaro Cornaglia, A., Mannucci, B., Grisoli, P., Vigani, B., Ferrari, F., 2017. Essential oil-loaded lipid nanoparticles for wound healing. Int. J. Nanomedicine Volume 13, 175–186. https://doi.org/10.2147/IJN.S152529

Shah, R., Eldridge, D., Palombo, E., Harding, I., 2015. Lipid Nanoparticles: Production, Characterization and Stability. Springer, Cham, Switzerland. https://doi.org/10.1007/978-3-319-10711-0

Shrotriya, S.N., Vidhate, B. V., Shukla, M.S., 2017. Formulation and development of Silybin loaded solid lipid nanoparticle enriched gel for irritant contact dermatitis. J. Drug Deliv. Sci. Technol. 41, 164–173. https://doi.org/10.1016/j.jddst.2017.07.006

Simões, D., Miguel, S.P., Ribeiro, M.P., Coutinho, P., Mendonça, A.G., Correia, I.J., 2018. Recent advances on antimicrobial wound dressing: A review. Eur. J. Pharm. Biopharm. 127, 130–141. https://doi.org/10.1016/j.ejpb.2018.02.022

Singh, A., Van den Mooter, G., 2016. Spray drying formulation of amorphous solid dispersions. Adv. Drug Deliv. Rev. 100, 27–50. https://doi.org/10.1016/j.addr.2015.12.010

Sinha, V.., Singla, A.., Wadhawan, S., Kaushik, R., Kumria, R., Bansal, K., Dhawan, S., 2004. Chitosan microspheres as a potential carrier for drugs. Int. J. Pharm. 274, 1–33. https://doi.org/10.1016/j.ijpharm.2003.12.026

Skaar, E.P., 2010. The battle for iron between bacterial pathogens and their vertebrate hosts. PLoS Pathog. 6, 1–2. https://doi.org/10.1371/journal.ppat.1000949

Slominski, A.T., Hardeland, R., Zmijewski, M.A., Slominski, R.M., Reiter, R.J., Paus, R., 2018. Melatonin: A Cutaneous Perspective on its Production, Metabolism, and Functions. J. Invest. Dermatol. 138, 490–499. https://doi.org/10.1016/j.jid.2017.10.025

Slominski, A.T., Zmijewski, M.A., Jetten, A.M., 2016. RORα is not a receptor for melatonin. Bioessays 38, 1193–1194. https://doi.org/10.1002/bies.201600204

Song, R., Ren, L., Ma, H., Hu, R., Gao, H., Wang, L., Chen, X., Zhao, Z., Liu, J., H., G., L., W., X., C., Z., Z., 2016. Melatonin promotes diabetic wound healing in vitro by regulating keratinocyte activity. Am. J. Transl. Res. 8, 4682–4693.

Soybir, G., Topuzlu, C., Odabaş, Ö., Dolay, K., Bilir, A., Köksoy, F., 2003. The Effects of Melatonin on Angiogenesis and Wound Healing. Surg. Today 33, 896–901. https://doi.org/10.1007/s00595-003-2621-3

Srinivasan, V., Mohamed, M., Kato, H., 2012. Melatonin in Bacterial and Viral Infections with Focus on Sepsis: A Review. Recent Pat. Endocr. Metab. Immune Drug Discov. 6, 30–39. https://doi.org/10.2174/187221412799015317

Sung, J.H., Hwang, M.-R., Kim, J.O., Lee, J.H., Kim, Y. Il, Kim, J.H., Chang, S.W., Jin, S.G., Kim, J.A., Lyoo, W.S., Han, S.S., Ku, S.K., Yong, C.S., Choi, H.-G., 2010. Gel characterisation and in vivo evaluation of minocycline-loaded wound dressing with enhanced wound healing using polyvinyl alcohol and chitosan. Int. J. Pharm. 392, 232–240. https://doi.org/https://doi.org/10.1016/j.ijpharm.2010.03.024

Tekbas, O.F., Ogur, R., Korkmaz, A., Kilic, A., Reiter, R.J., 2008. Melatonin as an antibiotic: New insights into the actions of this ubiquitous molecule. J. Pineal Res. 44, 222–226. https://doi.org/10.1111/j.1600-079X.2007.00516.x

Teo, S.Y., Yew, M.Y., Lee, S.Y., Rathbone, M.J., Gan, S.N., Coombes, A.G.A., 2017. In Vitro Evaluation of Novel Phenytoin-Loaded Alkyd Nanoemulsions Designed for Application in Topical Wound Healing. J. Pharm. Sci. 106, 377–384. https://doi.org/10.1016/j.xphs.2016.06.028

Thiruvoth, F., Mohapatra, D., Sivakumar, D., Chittoria, R., Nandhagopal, V., 2015. Current concepts in the physiology of adult wound healing. Plast. Aesthetic Res. 2, 250. https://doi.org/10.4103/2347-9264.158851

Turner, C.T., Hasanzadeh Kafshgari, M., Melville, E., Delalat, B., Harding, F., Mäkilä, E., Salonen, J.J., Cowin, A.J., Voelcker, N.H., 2016. Delivery of Flightless I siRNA from Porous Silicon Nanoparticles Improves Wound Healing in Mice. ACS Biomater. Sci. Eng. 2, 2339–2346. https://doi.org/10.1021/acsbiomaterials.6b00550

Vowden, K., Vowden, P., 2017. Wound dressings: principles and practice. Surg. 35, 489–494. https://doi.org/10.1016/j.mpsur.2017.06.005

Wang, X., Sng, M.K., Foo, S., Chong, H.C., Lee, W.L., Tang, M.B.Y., Ng, K.W., Luo, B., Choong, C., Wong, M.T.C., Tong, B.M.K., Chiba, S., Loo, S.C.J., Zhu, P., Tan, N.S., 2015. Early controlled release of peroxisome proliferator-activated receptor β/δ agonist GW501516 improves diabetic wound healing through redox modulation of wound microenvironment. J. Control. Release 197, 138–147. https://doi.org/10.1016/j.jconrel.2014.11.001

Wiegand, C., Abel, M., Hipler, U.-C., Elsner, P., 2019. Effect of non-adhering dressings on promotion of fibroblast proliferation and wound healing in vitro. Sci. Rep. 9, 4320. https://doi.org/10.1038/s41598-019-40921-y

Wiegand, C., Hipler, U.-C., 2009. Evaluation of Biocompatibility and Cytotoxicity Using Keratinocyte and Fibroblast Cultures. Skin Pharmacol. Physiol. 22, 74–82. https://doi.org/10.1159/000178866

Wlaschek, M., Singh, K., Sindrilaru, A., Crisan, D., Scharffetter-Kochanek, K., 2019. Iron and iron-dependent reactive oxygen species in the regulation of macrophages and fibroblasts in non-healing chronic wounds. Free Radic. Biol. Med. 133, 262–275. https://doi.org/https://doi.org/10.1016/j.freeradbiomed.2018.09.036

Wu, Y.-K., Cheng, N.-C., Cheng, C.-M., 2019. Biofilms in Chronic Wounds: Pathogenesis and Diagnosis. Trends Biotechnol. 37, 505–517. https://doi.org/10.1016/j.tibtech.2018.10.011

Xiang, Q., Xiao, J., Zhang, Hongbo, Zhang, X., Lu, M., Zhang, Hui, Su, Z., Zhao, W., Lin, C., Huang, Y., Li, X., 2011. Preparation and characterisation of bFGF-encapsulated liposomes and evaluation of wound-healing activities in the rat. Burns 37, 886–895. https://doi.org/10.1016/j.burns.2011.01.018

Xu, R., Xia, H., He, W., Li, Z., Zhao, J., Liu, B., Wang, Y., Lei, Q., Kong, Y., Bai, Y., Yao, Z., Yan, R., Li, H., Zhan, R., Yang, S., Luo, G., Wu, J., 2016. Controlled water vapor transmission rate promotes wound-healing via wound re-epithelialization and contraction enhancement. Sci. Rep. 6, 24596. https://doi.org/10.1038/srep24596

Yari, A., Yeganeh, H., Bakhshi, H., Gharibi, R., 2014. Preparation and characterization of novel antibacterial castor oil-based polyurethane membranes for wound dressing application. J. Biomed. Mater. Res. Part A 102, 84–96. https://doi.org/10.1002/jbm.a.34672

Ying, H., Zhou, J., Wang, M., Su, D., Ma, Q., Lv, G., Chen, J., 2019. In situ formed collagen-hyaluronic acid hydrogel as biomimetic dressing for promoting spontaneous wound healing. Mater. Sci. Eng. C 101, 487–498. https://doi.org/10.1016/j.msec.2019.03.093

Yousuf, D.A., Afify, O.M., El Soudany, K.S., Ghoniem, S.M., 2013. The effect of local application of melatonin gel on the healing of periodontal osseous defects in experimentally induced diabetes in rabbits. Tanta Dent. J. 10, 48–57. https://doi.org/https://doi.org/10.1016/j.tdj.2013.08.003

Yu, X., Li, Z., Zheng, H., Ho, J., Chan, M.T.V., Wu, W.K.K., 2017. Protective roles of melatonin in central nervous system diseases by regulation of neural stem cells. Cell Prolif. 50, e12323. https://doi.org/10.1111/cpr.12323

Zetner, D., Andersen, L., Rosenberg, J., 2016. Melatonin as Protection Against Radiation Injury: A Systematic Review. Drug Res. (Stuttg). 66, 281–296. https://doi.org/10.1055/s-0035-1569358

Zhang, G., Li, X., Xu, X., Tang, K., Vu, V.H., Gao, P., Chen, H., Xiong, Y.L., Sun, Q., 2019. Antimicrobial activities of irradiation-degraded chitosan fragments. Food Biosci. 29, 94–101. https://doi.org/10.1016/j.fbio.2019.03.011

Ziaee, A., Albadarin, A.B., Padrela, L., Femmer, T., O'Reilly, E., Walker, G., 2019. Spray drying of pharmaceuticals and biopharmaceuticals: Critical parameters and experimental process optimization approaches. Eur. J. Pharm. Sci. 127, 300–318. https://doi.org/10.1016/j.ejps.2018.10.026

8. BIOGRAPHY

Marieta Duvnjak Romić was born on 27th of November 1987 in Nova Gradiška, Croatia. She finished elementary school and the General gymnasium in Nova Gradiška. She graduated from the Faculty of Pharmacy and Biochemistry, University of Zagreb, in 2011. During her studies she was awarded the Dean's Prize for scientific work "Optimization of spray-drying by factorial design for production of melatonin loaded chitosan microparticles".

From 2011. to 2012. she worked as a teaching assistant at the Department of Pharmaceutical Technology, Faculty of Pharmacy and Biochemistry, University of Zagreb.

In 2012. she started working for PLIVA Croatia Ltd. in Research and Development in Zagreb. From 2012. to 2015. she worked as a Researcher Analyst and from 2015. to 2018. as a Senior Researcher Analyst.

In 2013. she enrolled in postgraduate doctoral study "Pharmaceutical-Biochemical Sciences" at the Faculty of Pharmacy and Biochemistry, University of Zagreb. In 2014. she joined project "Development of *in vitro* and ex vivo models for permeability testing of new topical ophthalmic formulations" (Partnership in research: 04.01/56, Croatian science foundation and PLIVA Croatia Ltd.) and project "Melatonin-loaded chitosan (nano)systems" (industrial partner PLIVA Croatia Ltd.). Her doctoral thesis research was conducted as a part of this project. In 2015. she joined project "Emulsions pharmaceutical spray-drying process modeling in laboratory and pilot scales" (industrial partner PLIVA Croatia Ltd.).

Since 2018. she works as a Principal Scientist - Analytical Project Leader in Novartis Pharma AG.

She co-authored six peer-reviewed papers and participated in different international scientific workshops and conferences.

List of publications:

M. Duvnjak Romić, A. Sušac, J. Lovrić, B. Cetina-Čižmek, J. Filipović-Grčić and A. Hafner, Evaluation of stability and in vitro wound healing potential of melatonin loaded (lipid enriched) chitosan based microspheres**,** Acta Pharm. 69 (2019) 635-648.

M. Duvnjak Romić, D. Špoljarić, M. Šegvić Klarić, B. Cetina-Čižmek, J. Filipović-Grčić, A. Hafner, Melatonin loaded lipid enriched chitosan microspheres – Hybrid dressing for moderate exuding wounds, J. Drug Deliv. Sci. Technol. 52 (2019) 431–439.

A. Šutić, **M. Duvnjak Romić**, S. Miočić, B. Cetina-Čižmek, Development of Analytical Method for *In vitro* Release Testing of Dexamethasone Nanosuspensions, Dissolution Technol. 26 (2019) 40–46.

M. Duvnjak Romić, M.Š. Klarić, J. Lovrić, I. Pepić, B. Cetina-Čižmek, J. Filipović-Grčić, A. Hafner, Melatonin-loaded chitosan/Pluronic® F127 microspheres as *in situ* forming hydrogel: An innovative antimicrobial wound dressing, Eur. J. Pharm. Biopharm. 107 (2016) 67–79.

F. Blažević, T. Milekić, **M. Duvnjak Romić**, M. Juretić, I. Pepić, J. Filipović-Grčić, J. Lovrić, A. Hafner, Nanoparticle-mediated interplay of chitosan and melatonin for improved wound epithelialisation, Carbohydr. Polym. 146 (2016) 445–454.

A. Hafner, J. Lovrić, **M. Duvnjak Romić**, M. Juretić, I. Pepić, B. Cetina-Čižmek, J. Filipović-Grčić, Evaluation of cationic nanosystems with melatonin using an eye-related bioavailability prediction model, Eur. J. Pharm. Sci. 75 (2015) 142–150.

Temeljna dokumentacijska kartica

Sveučilište u Zagrebu **Doktorski rad**
Farmaceutsko-biokemijski fakultet
Zavod za farmaceutsku tehnologiju
A. Kovačića 1, 10000 Zagreb, Hrvatska

RAZVOJ FUNKCIONALNIH OBLOGA ZA RANE S TERAPIJSKIM (NANO)SUSTAVIMA KITOZANA I MELATONINA

Marieta Duvnjak Romić

SAŽETAK

Cijeljenje rana dinamičan je dobro koordiniran biološki proces koji uključuje interakcije stanica, izvanstaničnog matriksa i signalnih molekula. Proces cijeljenja obično se dijeli u četiri faze - hemostaza, upala, proliferacija i maturacija i remodeliranje. Mnogi unutarnji i vanjski čimbenici, s infekcijom kao najčešćom, mogu poremetiti kaskadu cijeljenja i potom dovesti do kroničnih stanja. Uz porast otporezistencije bakterija na amtibiotike, razvoj inovativnih, funkcionalnih obloga za rane koje pružaju odgovarajuće uvjete vlage, zaštitu od vanjskih faktora te omogućuju kontrolirano oslobađanje djelatne tvari u područje rane, jedan je od imperativa u istraživanju. U ovom je radu tehnologijom sušenja raspršivanjem razvijena inovativna obloga za rane na bazi kitozana u obliku suhog praha i karakterizirana i uspoređena s komplementarnim mikrosferama. Pripravljena su tri različita terapijska sustava: kitozanske mikrosfere, kitozansko-poloksamerske mikrosfere te kitozansko-poloksamerske mikrosfere s uklopljenim nanostrukturiranim lipidnim nosačima (NLC). Terapijski sustavi (obloge) su dizajnirani u obliku suhog praha koji bubri u kontaktu s eksudatom rane, tvoreći *in situ* hidrogel. Obloge su potom okarakterizirane u pogledu fizikalno-kemijskih svojstava, *in vitro* oslobađanja lijeka, svojstava koja se odnose na vlagu, antibakterijske učinkovitosti, *in vitro* biokompatibilnosti s staničnim linijama kože, *in vitro* potencijala za cijeljenje i dugoročne stabilnosti u suhom stanju. Kitozansko-poloksamerske mikrosfere s uklopljenim NLC optimizirane su primjenom definitivnog pretražnog dizajna. NLC obogaćene mikrosfere pokazale su poboljšana svojstva tečenja i produljeno oslobađanje lijeka pri izlaganju blago kiselim uvjetima, kao i niži kapacitet bubrenja, prijenosa vodene pare i brzinu isparavanja. Pokazalo se da su kitozansko-poloksamerske mikrosfere prikladne za primjenu kao obloga za rane koje stvaraju velike količine eksudata, dok su mikrosfere obogaćene NLC pogodnije za primjenu za rane s umjerenim lučenjem eksudata. Ispitivani sustavi pokazali su antimikrobnu aktivnost i potencijal inhibicije / iskorjenjivanja biofilma protiv sojeva *S. aureus* ATCC i *S. aureus* MRSA. Kitozansko-poloksamerske mikrosfere s uklopljenim nanostrukturiranim lipidnim nosačima pokazale su se kompatibilnima s dermalnim keratinocitima i fibroblastima *in vitro*, s respektabilnim potencijalom za promicanje procesa zacjeljivanja rana. Mikrosfere u suhom stanju pokazale su dobru dugotrajnu stabilnost. Konačno, predloženi *in situ* oblozi pokazali su komplementarni potencijal za poboljšanje cijeljenja različitih vrsta kroničnih rana, održavanjem povoljnog vlažnog okruženja, istovremeno pružajući antibakterijsko utočište.

Rad je pohranjen u Središnjoj knjižnici Sveučilišta u Zagrebu Farmaceutsko-biokemijskog fakulteta.

Rad sadrži: 90 stranica, 7 grafičkih prikaza, 1 tablicu i 138 literaturnih navoda. Izvornik je na engleskom jeziku.

Ključne riječi: melatonin, kitozan, mikrosfere, sušenje raspršivanjem, nanostrukturirani lipidni nosači, cijeljenje rana

Mentor: **Dr. sc. Anita Hafner**, *izvanredni profesor Sveučilišta u Zagrebu Farmaceutsko-biokemijskog fakulteta.*

Ocjenjivači: **Dr. sc. Mario Jug**, *izvanredni profesor Sveučilišta u Zagrebu Farmaceutsko-biokemijskog fakulteta.*
Dr. sc. Maja Šegvić Klarić, *redoviti profesor Sveučilišta u Zagrebu Farmaceutsko-biokemijskog fakulteta.*
Dr. sc. Marjana Dürrigl, *PLIVA Hrvatska d.o.o.*

Rad prihvaćen: 23. listopada 2019.

Basic documentation card

University of Zagreb
Faculty of Pharmacy and Biochemistry
Department of Pharmaceutical Technology
A. Kovačića 1, 10000 Zagreb, Croatia

Doctoral dissertation

DEVELOPMENT OF FUNCTIONAL WOUND-DRESSINGS WITH CHITOSAN AND MELATONIN THERAPEUTIC (NANO)SYSTEMS

Marieta Duvnjak Romić

SUMMARY

Wound healing is a dynamic well-coordinated biological process involving complex interactions among cells, extracellular matrix components and signalling compounds, resulting in wound closure. Healing process is usually divided into four overlapping phases – haemostasis, inflammation, proliferation and remodelling. Many internal and external factors, with infection being the most common one, can disrupt the healing cascade and subsequently lead to chronic and nonhealing states. Accompanied with growing bacterial resistance, design of functional wound dressings that provide adequate conditions for healing in terms moist environment, gas exchange, protection from external contamination and drug delivery, represents a great imperative and challenge. In this thesis, novel chitosan-based wound dressing in the form of dry powder was developed by spray drying technology and evaluated and compared with complementary microparticulate dressings. Three variants of melatonin loaded wound dressings were evaluated - chitosan, chitosan/Pluronic® F127 and NLC enriched chitosan/Pluronic® F127 microspheres. Dressings were designed in form of dry powder that swells in contact with wound exudate, forming an in situ hydrogel. Therefore, dressings were characterized in terms of physico-chemical properties, in vitro drug release, moisture related properties, antibacterial efficacy, in vitro biocompatibility with skin cell lines, in vitro healing potential and long-term stability in dry state. Melatonin loaded NLC enriched chitosan/Pluronic® F127 microspheres was optimized employing definitive screening design. NLC enriched microspheres showed improved flowability features and prolonged drug release when exposed to slightly acidic conditions, as well as lower fluid uptake capacity, water vapour transition and evaporation rate. Melatonin loaded chitosan/Pluronic® F127 microspheres were shown to be suitable for application as dressing for wounds that produce high amounts of exudate, while NLC enriched microspheres were more appropriate for application to moderately exuding wounds. Tested systems showed antimicrobial activity and biofilm inhibition/eradication potential against S. aureus ATCC and S. aureus MRSA strains. Melatonin loaded NLC enriched and NLC free chitosan/Pluronic® F127 microspheres were shown as biocompatible with dermal keratinocytes and fibroblasts in vitro, with respectable potential to promote wound healing process. Powders in dry state demonstrated good long-term stability. Conclusively, proposed in situ forming dressings showed the complementary potential to improve healing of different types of chronic wounds by maintaining favourable moist environment, while providing antibacterial shelter.

The dissertation is deposited in the Central Library of the University of Zagreb Faculty of Pharmacy and Biochemistry.

Dissertation includes: 90 pages, 7 figures, 1 table and 138 references. Original is in English language.

Keywords: melatonin, chitosan, microspheres, spray drying, NLC, wound healing

Mentor: **Anita Hafner**, **Ph.D.** *Associate Professor,* University of Zagreb Faculty of Pharmacy and Biochemistry

Reviewers: **Mario Jug**, **Ph.D.** *Associate Professor,* University of Zagreb Faculty of Pharmacy and Biochemistry
Maja Šegvić Klarić, **Ph.D.** *Full Professor,* University of Zagreb Faculty of Pharmacy and Biochemistry
Marjana Dürrigl, **Ph.D.** *PLIVA Croatia Ltd.*

The thesis was accepted: October 23rd, 2019.